DYNAMICAL ASPECTS IN THE SCHWARZSCHILD - DE SITTER GEOMETRY

A thesis sumitted

by

Tolu Biressa

to

The Physics Department

in partial fulfillment of the requirements

for the degree of

Doctor of Philosophy in

Physics

Addis Ababa University

College of Natural Sciences

Adds Ababa, Ethiopia

December 2020

Thesis Supervisor

Prof. J. A. de Freitas Pacheco (Professor Emeritus)

The Lagrange Laboratory of the Côte d'Azur Observatory (OCA),

France, Nice

Author

Tolu Biressa

Addis Ababa University

Physics Department

The undersigned hereby certify that they have read and recommend to the College of Natural Sciences for acceptance a thesis entitled "**DYNAMICAL ASPECTS IN THE SCHWARZSCHILD - DE SITTER GEOMETRY**" by **Tolu Biressa** in partial fulfillment of the requirements for the degree of **Doctor of Philosophy in Physics**.

Dated: December 2020

External Examiner: _____
Prof. Júlio César Fabris

Internal Examiner: _____
Dr. Seblu Humne

Research Supervisor: _____
Prof. J. A. de Freitas Pacheco (Professor Emeritus)

Examing Committee Chairperson: _____
Dr. Teshome Senbeta

Addis Ababa University

Date: **December 2020**

Author: **Tolu Biressa**

Title: **DYNAMICAL ASPECTS IN THE SCHWARZSCHILD - DE SITTER GEOMETRY**

Department: **Physics Department**

Degree: **Ph.D.**
Convocation: **December**
Year: **2020**

Permission is herewith granted to Addis Ababa University to circulate and to have copied for non-commercial purposes, at its discretion, the above title upon the request of individuals or institutions.

_____
Signature of Author

To those who have sacrificed their lives

for the welfare of the others

Table of Contents

List of Tables

List of Figures

Abstract

Within the ΛCDM model, we studied dynamical aspects of the universe in SdS spacetime background. Mainly, the precession of orbits from solar-planetary to binary galaxy, the effect of geometry in radially falling particles to massive compacts and the gravitational deflection of light by extended sources. Using Einstein field equations and conservation laws, equation of motion and the general effective potential in SdS were derived. The potential has used in the characterization of the orbits, where hypothetical potential sources ranging from small mass to critical black holes were used. The sample orbiters cover both massive and massless particles with and without angular momentum. Generally, SdS potential differs from the Schwarzschild potential. Moreover, the potential has used to derive important boundary conditions in the motion of the particles. Specially, it has used to derive photon orbit and radial solution of closed circular orbits of massive particles. Taking into account the positions of the source, lens and observer the photon orbit solution used to derive the gravitational bending angle; where it has in turn used in gravitational lensing to estimate the mass of the lensing where Λ effect was of order 2% relative to the Schwarzschild background. In the case of circular orbits, the radial deviation has studied, where the effect was insignificant at small-scale, within Milky-Way galaxy; but at binary galaxy level becomes viable, $k$pc to Mpc order. For the case of elliptical orbits, a two-body problem has developed to derive the precession. Λ effect was dominant over the Schwarzschild in open and wide systems like binary galaxy, but insignificant in others. Λ has significant effect compared to the Schwarzschild case on radiations from in falling particles to massive objects if appreciable distances are considered. Finally, we have reflected our views regarding the criticisms on Einstein modified field equations, attributed to the cosmological constant. A detailed review with some supplementary works presented to enrich the relevance of the cosmological constant as an intrinsic constant.

Keywords: ΛCDM model, SdS, cosmological constant, Orbit precession, light bending, lensing, GR

Acknowledgements

I would like to thank Prof. J. A. de Freitas Pacheco, my thesis supervisor for his professional supervision including designing of the project. I thank him much for his willingness to supervise me remotely and closely during the hard time when I was in much trouble. Certainly, I have learned a lot from him and got the sense of real physics. I would like to thank him also for his fatherly assistance in social affairs where I got many friends and supporters during my stay at Observatoire de la Côte d'Azur. I would also like to thank his family for their care to make my stay joyful at the observatory.

I would like to thank all the community at the laboratory who has supported me: the scholars, librarians, ICT people, administrators, and all the rest. They were all wonderful. Special thanks go to Chadia Kanaan, Matias Montesinos, Severine Neveu, Jean-Christophe Mauduit and Professor Bertrand Chauvineau for their friendly assistances.

I would like to thank the Observatoire de la Côte d'Azur for its hospitality and facilities during my stay at the observatory to enjoy my work.

I would like to thank Dr. Menberu Mengesha for his proof reading and suggestions.

I would like to thank Dr. Solomon Belay, my colleague for his encouragements and mutual assistant we had while we were PhD students at Addis Ababa University. We have also shared some of the hardships but have used to train ourselves.

I would like to thank Addis Ababa University for the learning opportunity, facilities and all the supports it has provided me. Thanks to the officials, administrators, librarians supporting staffs and all the communities for their assistances during my stay at the university. Special thanks go to the Physics department for its close assistance. I sincerely thank all the staff members of the department. They were all amazing to me to share the joy of my success. Thanks to the heads of the department for their unfold help during my stay at the department and afar to wind the thesis.

The late Dr. Legesse Wetro (deceased) was a fortune to Ethiopia in pulling such large number of youths towards astronomy and space science. Among which I was one of his early MSc. students and primer entry for PhD notwithstanding to separate. I thank him for the service he had given to develop the science of astronomy and space science in Ethiopia.

I thank Jimma University for the sponsorship.

My thanks go to all friends, whom I cannot mention all, for their encouragements to complete the dissertation.

Finally, my especial thanks go to my brothers Belay Biressa and Yadessa Biressa, and my sister Tarike Biressa. They have sacrificed their joy in all my troubles. I thank my wife Juwara Muse for her patience, courage and help to wind the thesis.

Part I

General introduction

In general the work is structured into three parts including this part as follows:

Part I - General introduction: In this introductory part we provide the background of the work including, motivation, literature reviews/issues thereof, objectives and methods. More detailed cosmological constant history, issue and progress in relation to the full theory of general relativity is addressed. In addition, the background physics, General Relativity (GR) theory is previewed where the current standard Cosmological Constant & Cold Dark Matter (ΛCDM) model has considered in the work.

Part II - Motion in SdS geometry, precession of orbits, light bending and radiation

Covers the study of motion of particles in SdS geometry, the effect of cosmological constant in the precession of orbits of astrophysical systems that includes: solar-planetary system, binary stars, binary-discs around the Milky-Way galaxy center and binary galaxies all performed in the SdS spacetime background. The photon trajectory in SdS spacetime and the effect of Λ in gravitational bending of light and lensing will also covered. Finally, this part includes the study of radiation from in falling particles into BHs/AGNs and other massive systems.

Part III - Future perspective and summary

This part includes the future perspective chapter, in which some views and complementary works be given and covers the summary chapter.

Chapter 1

Background and Literature reviews

1.1 Motivation

The motivation for the choice of the title was basically instigated from the then recent and active issue concerning the discovery of the accelerated universe. It was very fresh where the standard theory was questioned for alternative theories to replace. Actually, before this thesis I was working on another thesis issued on “Pulsars’ timing noise model” under the supervision of Dr. Legesse (Addis Ababa University) and co-supervision of Prof. Okkie de Jager (Timing pulsar group, SKA) where the project was also well received for collaboration at ICTP for three years grant. But due to later modeling issue arguments among ourselves I was forced to identify a new supervisor from abroad to continue. Thus, though, identifying a potential supervisor was not so easy, it was fortunate to me to have my current supervisor with such rich scientific career and fatherly helpful scientist with this presented and different issue. So this thesis is accompanied with a lot of background own interesting history including motivation and development background setup.

Initially, this thesis was focused to calculate i) planetary orbits to estimate the effects of periastron precession, ii) the orbit described by two neutron stars, iii) the orbits of relativistic and non-relativistic particles around a very massive black holes using Schwarzschild - de

Sitter (SdS) metric and then to compare the results with that of the classical Schwarzschild background. However, as mentioned earlier due to complicated situations related to my home institutes Jimma University (the sponsor of my PhD work) and Addis Ababa university (for my affiliation), unexpected period has elapsed where I could not had regular communication for close assistance and focus from my supervisor. So, with this real situation the thesis shaped in the present view with much extended issues as addressed in the coming sections, the background rationale - methodology design to bear the recent update issues including the original design of the thesis too.

1.2 Background rationale

The pioneering work in both observational and theoretical developments during the period 1920-1930 [1, 2, 3, 4, 5, 6, 7, 8, 9, 10, 11, 12, 13, 14] in astronomy and physics has rewarded the discovery of expanding universe where its inaugural discovery is recognized mainly by [9]. Until 1998, the expanding universe had considered as a decelerating one, where gravity has purely considered ever as attractive with two future fate scenarios. i) If the mass density of the universe were greater than the critical density, then the universe would reach a maximum expansion to halt for a while and then begin to collapse to the Big-Bang state (a Big Crunch); then the dynamics recycles. ii) If the density in the universe were equal to or below the critical density, the expansion slows down but never stops so that the average temperature of the universe would gradually and asymptotically approaches to the absolute zero a Big-Freeze leading to a scenario known as heat death. For detailed reviews, see for example the literatures by [15, 16, 17]. However, the late discovery of the accelerated expansion of the universe [18, 19] has come up with more complication problem in the study of the cosmos. It has raised the issue that whether gravity can act

repulsively at large scale bringing more new concerns about the nature of gravity and the content of the universe. Is the acceleration being driven by dark energy? Or is general relativity itself in error, requiring a modification to account for the late acceleration?

Consequently, there is a lot of effort in progress both (1) in further developing the existing General Relativity (GR) based cosmological model where the dark energy & dark matter scenario is being entertained and (2) in the construction of modified gravity models as alternatives to dark energy. Also, in connection to the theoretical progress there are interesting developments in the mechanisms of cosmological tests of gravity.

The GR based and extensions model that can explain the accelerated expansion of the universe if, besides baryonic and dark matter, another component is present in the universe. Such a component, dubbed dark energy, would represent approximately 70% of the total matter-energy content of the universe today and is characterized by a "negative" pressure. Then the idea is constructing an extension of GR with unified, continuous description of the early inflationary era and the late-time cosmic acceleration epoch of the universe. Various Scalar field models with generic features have been introduced into the Einstein-Hilbert action (See the literatures: [16, 20, 21, 22, 23] and the references therein.). The simplest isotropic and homogeneous scalar field ϕ introduced, is constructed from a self-interaction(slowly rolling) potential $V(\phi)$ with associated energy density ρ_ϕ and pressure p_ϕ given by

$$\begin{aligned} \rho_\phi &= \frac{\dot{\phi}^2}{2} + V(\phi) \\ p_\phi &= \frac{\dot{\phi}^2}{2} - V(\phi) \end{aligned} \tag{1.2.1}$$

The corresponding equation of state is given by

$$\omega = \frac{p_\phi}{\rho_\phi} = \frac{\frac{\dot{\phi}^2}{2} - V(\phi)}{\frac{\dot{\phi}^2}{2} + V(\phi)}. \tag{1.2.2}$$

A dot on ϕ means derivative with respect to the cosmic time.

A negative pressure can be obtained if the potential term dominates the kinetic one. Two situations are possible: a) The equation of state can be dynamical, with slightly time-varying scalar field ϕ which is referred as “quintessence"; b) the kinetic term is null, corresponding to the constant equation of state, $\omega = -1$. In this case the dark energy component is a vacuum energy density, the “cosmological constant” case. To this end, a near $\omega = -1$ equation of state is favoured by the present epoch of the universe as the recent observational data analysis indicate. This means that, either a “quintessence” case with dynamic energy density whose present equation of state $\omega \approx -1$ or the cosmological constant case whose equation of state remains constant ($\omega = -1$) will be considered.

The newly constructed modified gravity model theories include f(R) gravity, braneworld gravity, Horndeski theory and massive/bigravity theory. As the review works indicate that, in general, the modification scenarios commonly share the need of additional degrees of freedom into the gravity sector with extra fields which couple non-minimally to gravity that ultimately lead to new fifth forces, for example see the recent reviews by [24, 25, 26] and the references therein.

However, the modified gravity theories need time to pass all the local and large scale structure evolutionary tests within the available mechanisms or that come to support. Presently, there are challenges from both small and large scale structures. For example [27, 28] and the references therein well discuss the challenges to self-acceleration in modified gravity from gravitational waves and large-scale structure. Moreover, the detection of the first gravitational wave signal in 2015 from binary black hole mergers [29] and the first direct observation of a binary neutron star inspiral gravity wave (GW170817) [30], from the joint gravitational and electromagnetic observation by the Advanced LIGO and Advanced Virgo

gravitational-wave detectors provides the success of General Relativity Theory. Supplementary analysis and review works of the observations, for example [31, 32] rule out the structure of (non -)viable gravitational actions, and some current popular modified gravity models. In effect, this encourages researches for further development of General Relativity and extensions.

1.3 Research Proposal/Statement of the problem

As current reviews indicate that the modified gravity theories for cosmological models are interesting and in progress (see 1.2). Probably, these theories will be amongst the future standard theories that will solve the current unresolved cosmological problems awaiting observational tests. However, though they are viable candidate theories, they need to pass the present observational constraints and featured observational tests. On the other hand, the standard ΛCDM base cosmology seems successfully explaining cosmological issues from small scale to large scale structures. It is consistent with a wide range of cosmological data. It is successfully explaining temperature and polarization anisotropies of the cosmic microwave background (CMB) radiation spectra, lensing, dark matter & dark energy sector, neutrino sector, the standard big bang nucleosynthesis predictions, Baryon acoustic oscillation (BAO), the Early-Universe inflationary scenario, structures and formations of systems in small and large scale systems [24, 30, 31, 32, 33, 34, 35, 36, 37, 38, 39, 40, 41, 42, 43]. Even the effect of the positive cosmological constant on the radial velocity profile of galaxy groups in the Local Universe studied by [44] corresponding to scales of 1-2 Mpc were shown to fit with actual data in preference over the bare cosmological constant.

Here, questions aroused by reviews related to the models and their developments are unissued in our case. We are relaxed to accept that they are not yet finished and so believed

to be open to research. With this belief, we are interested to address some issues within the current standard ΛCDM base model where the cosmological constant is considered as an intrinsic geometric quantity as originally proposed by Einstein. Then, the background metric is a de Sitter spacetime; while locally around a point mass object the SdS metric is used for the description of dynamical aspects. Concerning the model issue, we will provide some comments and our supplementary works under the future perspective chapter. Thus, we have designed the following research questions to work.

Research questions

i. Questions related to origin of ΛCDM and astrophysical implications:

1. Is Λ a real geometrical entity or a "hand craft" constant as "concordance" as it is called or other else?

ii. Questions related to light bending and its application (gravitational lensing):

1. How does Λ affect bending of light around a massive compact object?
2. Is there a way that Λ effect will be explicitly determined in gravitational lensing?

iii. Questions related to precession of orbits of various systems:

1. To what extent does the cosmological constant affect the precession of planets in solar system? Is cosmological constant locally measurable?
2. Is the effect of cosmological constant significant on the precession of binary stars: including pulsars and binary supermassive black holes?
3. Does cosmological constant affect the precession of motion of binary-discs around the nucleus of the Milky-Way galaxy?

4. Is the effect of cosmological constant on the precession of orbits of satellite galaxies being observable?

iv. Miscellaneous questions

1. What is the effect of cosmological constant on the radiation of radially falling particles to massive objects like BHs/AGNs?

1.4 Objectives

General objective

To study dynamical aspects in the Schwarzschild-de Sitter geometry.

Specific objectives

1. To derive photon trajectory in SdS spacetime and then study the effect of Λ in gravitational bending of light and lensing.

2. To study the effect of cosmological constant in precession of orbits of systems that includes solar-planetary system, binary stars, binary-discs around the Milky Way galaxy and binary galaxies in the SdS spacetime background.

3. To derive radiation from in falling particles to BHs/AGNs and other massive compact systems in the SdS background and describe the effect of Λ.

4. To comment and supply additional notes on issues raised concerning the modification of EFE, the case of cosmological constant.

1.5 Methodology

The current standard ΛCDM base model where GR is considered as the fundamental physics of the model is being assumed. The observed accelerated universe is caused by a "dark component" is taken into account where the repulsive force is associated with the cosmological constant is considered.

The local effect of cosmological constant near a point mass M can be included, if the Schwarzschild-de Sitter (SdS) metric [45] is considered, which is given as

$$ds^2 = -\left(1 - \frac{2MG}{r} - \frac{\Lambda}{3}r^2\right)dt^2 + \left(1 - \frac{2MG}{r} - \frac{\Lambda}{3}r^2\right)^{-1}dr^2 + r^2 d\Omega^2. \quad (1.5.1)$$

Note that, in the absence of material source, $M = 0$, the SdS metric goes to the de Sitter metric given by [46]:

$$ds^2 = -\left(1 - \frac{\Lambda}{3}r^2\right)dt^2 + \left(1 - \frac{\Lambda}{3}r^2\right)^{-1}dr^2 + r^2 d\Omega^2. \quad (1.5.2)$$

Here, we notice that the SdS metric is asymptotically a de Sitter metric where the background spacetime curves. Therefore, geometrically it differs from the flat Minkowski spacetime background.

On the other hand, at a relatively small distance where the contribution from the cosmological constant is negligible, the SdS metric describes the Schwarzschild geometry given by [47]

$$ds^2 = -\left(1 - \frac{2GM}{c^2 r}\right)dt^2 + \left(1 - \frac{2GM}{c^2 r}\right)^{-1}dr^2 + r^2 d\Omega^2. \quad (1.5.3)$$

So, all the problems raised here by the research questions related to studying the local effects of Λ near astrophysical systems are all calculated by the SdS metric. The remaining projects raised by the research problems will considered as complementary to GR.

More additional supplementary methods such as the detailed boundary conditions are being

introduced in view of literatures and physical assumptions under the respective specific researches.

Finally, we underscore that the historical overview of cosmological constant together with the preview of GR theory (the background physics for the research) would be considered as an enriching background of the methodologies.

Chapter 2

Expanding universe and cosmological constant historical background

2.1 An overview of the beginning of modern cosmology

Historically, the observational evidence of an expanding universe is dated back to the development of Einstein's General Relativity (GR) theory during the 1910's. Coincidentally, during this period there was also an interesting observational activities both in data extraction and developing physical mechanisms to calculate distances at different observatories. Specially the data extraction carried out by V.M. Slipher at Lowell Observatory [1, 2] is considered as the first step towards discovery. The spectral data that Slipher had collected (summarized as in table 2.1 of the book by [48], page 162) and the spectroscopic work of light from other several spiral nebulae (later re-christened galaxies) were red-shifted with only few of them were blue-shifted (for example see the remarks by [49]). For historical remarks, for example see the history by [50, 51].

From observational viewpoint the 1910's period is considered as the beginning of the modern cosmology towards the expanding universe discovery. Slipher is considered as one of the main pioneer contributor both in providing data and inspiring for the later developments

Table 2.1: Slipher 1910's observational data from spiral nebula as it appears in the book by [48, page 162]

RADIAL VELOCITIES OF SPIRAL NEBULAE

+ indicates receding, − approaching

N.G.C.	R.A. h m	Dec. ° ′	Rad. Vel. km. per sec.	N.G.C.	R.A. h m	Dec. ° ′	Rad. Vel. km. per sec
221	0 38	+40 26	− 300	4151*	12 6	+39 51	+ 980
224*	0 38	+40 50	− 300	4214	12 12	+36 46	+ 300
278†	0 47	+47 7	+ 650	4258	12 15	+47 45	+ 500
404	1 5	+35 17	− 25	4382†	12 21	+18 38	+ 500
584†	1 27	− 7 17	+1800	4449	12 24	+44 32	+ 200
598*	1 29	+30 15	− 260	4472	12 25	+ 8 27	+ 850
936	2 24	− 1 31	+1300	4486†	12 27	+12 50	+ 800
1023	2 35	+38 43	+ 300	4526	12 30	+ 8 9	+ 580
1068*	2 39	− 0 21	+1120	4565†	12 32	+26 26	+1100
2683	8 48	+33 43	+ 400	4594*	12 36	−11 11	+1100
2841†	9 16	+51 19	+ 600	4649	12 40	+12 0	+1090
3031	9 49	+69 27	− 30	4736	12 47	+41 33	+ 290
3034	9 49	+70 5	+ 290	4826	12 53	+22 7	+ 150
3115†	10 1	− 7 20	+ 600	5005	13 7	+37 29	+ 900
3368	10 42	+12 14	+ 940	5055	13 12	+42 37	+ 450
3379*	10 43	+13 0	+ 780	5194	13 26	+47 36	+ 270
3489†	10 56	+14 20	+ 600	5195†	13 27	+47 41	+ 240
3521	11 2	+ 0 24	+ 730	5236†	13 32	−29 27	+ 500
3623	11 15	+13 32	+ 800	5866	15 4	+56 4	+ 650
3627	11 16	+13 26	+ 650	7331	22 33	+33 23	+ 500
4111†	12 3	+43 31	+ 800				

of the expanding universe. While other contributors including the development of physical mechanisms to astronomical distances are acknowledged today. For example [52] strongly acclaim that Slipher's data were very necessary for the formulation of the expansion law both by Hubble and Lemaître discovered in the 1920's. On the other hand, [53] and many more scholars emphasize for better acknowledgment of others contributions during this time including the 1920's work for the discovery.

On the theoretical grounds, the expanding unverse was already embedded in GR and would have celebrated as discovery. Einstein had already noticed the dynamism of the solutions to his field equations. But immediately reacted to modify it. He was in a tug of contrary ideas between the implication of his original theory, which was with dynamic solutions and his philosophical perception to establish a static universe seeking Mach's principle. In fact, the notion for the theoretical development of the modern cosmology has started during the time where de Sitter and Albert Einstein were in scientific debates over the "dynamic" and

"static" forms of Einstein's field equations in the period 1916 - 1918 where the two have formulated their own mathematical expressions for the metric of the universe as a whole. For details see the review by [54] and the forthcoming section 2.2 for how this initiated the present day cosmological models.

Notably, the second decade of the beginning of the 20th century era was one of the scientific revolutionary events where the theoretical GR was developed and further initiated cosmological models while looking to proceed for observational tests and, on the other hand, the observational side has independently entered and further lured up for new cosmological outlooks. A theoretical model that incorporates the interpretations to such observational nebulae redshifts was needed. Further observational investigations, improved spectroscopic work and more data were required for firm observational conclusions .

The 1920's and 1930's are the magnificent decades where the current cosmology foundation has been shaped when theory and observation converged to develop the current model of the expanding universe. Theory and observation have been converged to confirm the Island Universe hypothesis (today known as extra-galaxies outside the Milky-Way galaxy), the classification of extragalactic nebulae, the discovery of a linear relationship between distance and velocity for extragalactic nebulae, providing the first evidence for the expanding universe, the brightness profile of galaxies. In fact the new attempt mechanisms including to use novae as standard candles to measure the distances to spiral nebulae during the 1910's were materialized to derive expressions for radial distance in terms of the linear velocity where internal evolutionary scenarios were also entertained. Mainly, the methods developed by Hubble were considered as confirmation of the discovery of the extragalactic nature of the spirals and its exploited extension in the discovery of the expanding universe,

for detail reviews see [50, 51, 52, 53] and the references therein. In the case of the expanding universe, Hubble had selected a set of extra galactic nebulae data mainly from Slipher data and some from others including his own to measure the shift of spectral lines. Interpreting the observed shift he derived that the velocities v were correlated linearly to the apparent distance of the nebulae r as:

$$v = H_0 r \tag{2.1.1}$$

where H_0 is the proportionality constant now called the present Hubble-Lemaître constant.

On theoretical grounds, [13, 14] and [10] are considered to have discovered an expanding universe. Because in these seminal papers both Friedmann and Lemaître independently derived dynamic solutions to Einstein's GR equations that describe an expanding universe. In particular Lemaître also derives that the expansion of the universe implies the spectra of distant galaxies are redshifted by an amount proportional to their distances. Furthermore, he used published data on the velocities and photometric distances of galaxies to derive the rate of expansion of the universe (assuming the linear relation) [55] and for more details refer the forthcoming section 2.2.

The 1930's period which has even extended until the end of 1940's is more of philosophical debates over methodological approaches where mathematical physics came into play. In particular, the philosophy initiated by [56] purely based on kinematical considerations was drawn attention. In subsequent works Milne developed "kinematic theory of relativity" where he had reworked and summarized it in his book [57]. On the other hand, some of his contemporaries with different viewpoints adopted his operational method [58, 59, 60, 61, 62, 63] to develop a paring of non-observational concepts, then embed the

resulting minimalist concept set in an axiomatic hypothetical-deductive structure, for detail reviews see [64, 65] and the references therein. Where then the expanding metric known as the Robertson-Walker (RW) metric was introduced. On the other hand, the contrary views and other supplementary works by others were directly and as well indirectly contributed in enriching this new theory. Consequently, this philosophical debate later in 1948 was emerged with the steady-state theory of the universe developed by [66, 67] (For details, refer the popular books by [65, 68, 69]).

On the contrary, Gamow and collaborators were persistent with the expanding universe developed from GR that has led to the development of the hot "big bang" theory of the expanding universe. Gamow was the earliest to employ the non-static solutions of Einstein field equations (EFE) derived by Friedmann and Lemaître describing a universe that would have evolved from a primordial quantum as Lemaître suggested in the 1920's. His idea that the early universe was dominated by radiation rather than by matter is the founding evolutionary scenario in creation of chemical elements (cosmic nucleosynthesis) and to the subsequent formation of galaxies. Gamow, contemporaries and collaborators ([70, 71, 72, 73, 74] and the supporting reference therein) exploited this new idea in developing radiation and matter density ratio mechanism to determine the density of the relict background radiation of the "big-bang," which had supported by the discovery of the cosmic background radiation (CMBR) by Penzias and Wilson in 1965, [75] (Which was already observed in 1941 before such theoretical prior established [76]).

Then subsequently more new observational discoveries during the late 1960's and the beginning of the 1970's like quasars, active galaxies, gravitational lensing, Sunyaev-Zeldovich effect, etc including new technical abilities favored the "hot big-bang " model over the steady-state-cosmology. Thus, GR theory and extensions were taken seriously for further

research to test and apply. While others begin to look for modifications and alternative theories. It is during this period that, on one side clear distinction between models being made and on the other side the current candidate models have being seriously taken in advance, for modification and seek for alternatives. As a result, the field of cosmology has evolved to the current understanding in two pictures of expanding scenario, the decelerating and accelerating pictures. In the next section we try to overview these development issues.

2.2 Current cosmological models development overview

Certainly, the period 1910's to the mid of 1960's was marked by the exploration of new revolutionary physical philosophies that are in effect today. These new modern physical philosophies (particle, quantum, GR, etc) are implemented to develop model theories for empirical discoveries, develop new mechanisms and techniques to test theories, unison of fields, etc. In essence, modern cosmology has benefited this trend where mainly GR is considered as successful. Some bright ideas like evolutionary scenarios including synthesis and structure, mathematical model equations to determine geometry were introduced in cosmology. Accordingly, in the case of cosmology, GR base cosmological equations developed by Friedmann, Lemaître, Robertson, Walker commonly acknowledged as Friedmann-Lemaître-Robertson-Walker (FLRW) cosmology is one of such products. However, it is important to recognize that generally the status of our today science is a built up through generations that cannot be addressed in any single file but shall be acknowledged back. For comprehensive reviews see the classical books by [65, 69], and review articles by [16, 21, 23, 54, 77].

As briefly introduced in earlier section 2.1, the observational capabilities and advance during the late 1960's and the beginning of the 1970's has already favored the "hot big-bang" model over the steady-state-cosmology. Then, the majority of pioneering cosmologists lost further research interest towards the steady-state models. Yet, Hoyle and Narlikar including little followers maintained their views on the viability of steady-state model with modified versions (where the current one is called Quasi-steady state cosmology(QSSC)) [78, 79, 80, 81, 82]. Now by then, the favored hot big-bang theory is both being to challenge and to be challenged by more cosmological tests ahead of it.

Accordingly, the main ingredient of the model that the overall mass-energy system perceived as gravitationally attractive so that the rate of expansion expected to be slowing down is a crucial challenge to ascertain. Because, the related fundamental question whether this decrease in the rate of expansion is sufficiently enough that at some point the expansion would stop and reverse (a "Big-Crunch" and then recycle to the bang, a closed universe) or insufficient to stop to expand forever (an open universe) was decisive to establish. Secondly, the theory was also constrained to explain the following observed problems by then.

a) The missed mass problem: The majority of the observed structures, distributions and evolutionary scenario of astrophysical systems show that the baryonic matter we know now is too small to account by the hot big-bang model. Approximately about 95% of the universe by mass is non-baryonic whose nature is not well known. For brief reviews and reports see [83, 84, 85, 86].

b) The horizon problem: Observationally, the universe appears homogenous and isotropic in large scale structure but with small primordial anisotropies of cosmic background such as: CMBR, gravity, etc. [30, 39, 69, 87].

c) The flatness problem: The total energy density of the universe is closer to its critical value where the spacetime curvature is flat. [54, 69, 87]

d) The magnetic monopole problem: From the Grand Unified Theories (GUTs) of particle physics, the hot big-bang model is expected to predict huge number of magnetic monopoles at the Planck scale. Then, as the GUTs explain these seed frozen in monopoles are expected to exist in abundant relicts of cosmic background at least one per baryonic nucleon relict surviving phase transitions. But observationally, there exist no noticeable number of monopoles except in small anisotropies. See for details

[69, 88, 89].

Interestingly, the problems of the second issue were successfully addressed through subsequent developments in the 1980's within the GR theory where the hot big-bang model is modified to an inflation driven Cold Dark Matter (CDM) big-bang model. The CDM in the first place is modeled to account the missed mass, by postulating a massive particle whose nature is yet unknown(non-baryonic) called Dark Matter (DM). In the second place, the DM is considered to be free of interaction with known baryonic matter physics except that of gravitation where its presence is proclaimed by; that it is an electrically neutral and pressureless matter fluid (cold fluid) [90, 91, 92]. For detailed review and supplementary comments see [69] and the references therein.

On top of this, the introduction of theory of inflation has offered a solution to the problems with provisional mechanisms of testing the origin of large-scale structure, by observations of anisotropies in the cosmic microwave background [93, 94, 95, 96, 97]. Today the inflationary theories are satisfactorily describing the observed CMB anisotropies including gravitational waves and the large scale structures [30, 39].

The first issue related to the fate of the universe has observationally surprised the scientific community with an acceleration rate contrary to the expected deceleration rate [18, 19]. This new scenario, on one hand has solved the problem of the big crunch but on the other hand has brought more puzzles about the nature of the universe. To incorporate this acceleration a new hypothetical energy (Dark Energy, DE) with negative pressure was proposed. Within the GR theory, the simplest solution came as in the form of the cosmological constant and was significantly able to explain the observations. Consequently, further enhancing and testing mechanisms of GR in the realm of standard particle physics were being progressively envisioned and developed. Besides the GR base cosmologies, a number of

new theories were began to develop.

Historically, the emergence of new theories of gravity will probably be longer. Regardless of this, the emergence of the current developments is just not far from the completion of GR theory when Weyl [98, 99] and others soon developed an alternative theory of gravitation in higher order differential field equations than the GR. The appearance of the majority of these alternatives or new theories are linked to the observations of dark sectors (DM & DE) of the universe [23, 25, 26, 41, 54]. However, while the GR base is found to be consistent with all current data sets, the constraints are still too large to exclude some of the new possible theories [95, 96, 100]. Nonetheless, some others need sometimes to proceed for viability, or succeed to overtake the GR or being invalidated to terminate.

In general, the current modern cosmology has developed enormously less than a century ago mainly conceived with the birth of GR together with the advancement of fundamental physical sciences including particle physics, mathematical methods, etc. Also, new technological innovations, capabilities in modeling observational mechanisms and tools for data extraction and analysis have played significant role. Moreover, whatsoever philosophical and physical views therein for the emergence of the various current viable theories, undeniably their emergence is directly or indirectly linked to this historical startup either for comprehensive theory to explain fully both observations and future predictions or philosophical and physical framework issues.

Finally, irrespective of the ongoing progresses for better and more comprehensive theory to establish, cosmological theories framed within the harmony of GR and the standard theory of particle physics seem favorable. In particular, the DE-CDM along with inflation theories developed during the 1980's and 1990's came up as viable theories. Where, today the simplest of which the ΛCDM model is the standard cosmology that has successfully

explained most of the observations like large scale structure and distributions, the big bang nucleosynthesis together with Baryonic Acoustic Oscillations (BAO) with little tension [18, 19, 30, 38, 40]. It is also taken as the standard used to test new features, constrain other theories and considered as a buildup for further progress to develop its extensions for more success or other alternative theories.

2.3 Origin, role and inspirations of Λ in cosmology

As addressed in the preceding sections including the background chapter, the history of modern cosmology is directly or indirectly associated to Einstein GR theory. Especially, the entertainment of the cosmological constant has played a great role both in observational and theoretical advances. So, in this section we highlight some relevant historical issues of the cosmological constant in modern cosmology and physics. Thus, first we try to address the introduction of Λ as Einstein's cosmic background perception. Then, next we see the implications of the modified equations. And finally, we look at a glance the role of Λ and its inspirations in modern cosmology. Moreover, chapter two will be consulted in case detail GR technical and mathematical explanations are required.

2.3.1 Einstein field equations and cosmic interest: Introduction of Λ

Einstein original GR field equations [3, 4, 5, 6] are given as 2.3.1:

$$R_{\mu\nu} - \frac{1}{2} g_{\mu\nu} R = \frac{8\pi G}{c^4} T_{\mu\nu} \tag{2.3.1}$$

Where the signature (-,+,+,+) for the metrics is adopted from the book by Misner, Thorne, and Wheeler (MTW) [101] for sign convention. The quantities appearing in the equations are: $R_{\mu\nu}$ is the Ricci curvature tensor, R is the scalar curvature, $g_{\mu\nu}$ is the metric tensor, G is Newton's gravitational constant, c is the speed of light in vacuum, and $T_{\mu\nu}$ is the stress-energy tensor. Note also that throughout this work the Greek indices like $\mu, \nu, ...$ run from 0 to 3, while Latin indices like $i, j, ...$ run from 1 to 3.

Then, in 1916 Einstein was interested to apply his theory to cosmology [7] with the idea of incorporating Mach's principle (universe with a finite average density of matter) provided that he finds a static solution of the field equations. But soon noticed that his field equations

yield a non-static solution, a dynamic universe that will expand or contract. As the consequence, Einstein himself introduced a positive cosmological constant Λ with the belief of constructing a static solution [8]. The idea is that, the constant introduces a repulsive force which can counterbalance the attractive force of gravity leading to the "static Einstein universe."

The modified Einstein's 1917 field equations with the cosmological constant is

$$R_{\mu\nu} - \frac{1}{2} g_{\mu\nu} R + \Lambda g_{\mu\nu} = \frac{8\pi G}{c^4} T_{\mu\nu} \tag{2.3.2}$$

Einstein's model considers a universe filled with matter in a uniform manner, which de Sitter called it as "Material postulate of relativity of inertia." The metrics in his field equations has to exhibit a finite spherically static universe where then the $g_{\mu\nu}$'s shall be zero at infinity, which de Sitter called this mathematical framework "Mathematical postulate of relativity of inertia." However, [12] did derive spherically static solutions to Einstein's modified equations by proposing another expression of the metric. By using spherical polar coordinates (r, θ, ϕ), he represented the Einstein universe (system A), i.e. as 3-dimensional hyper-spheres embedded in a 4-dimensional Euclidean space while he proposes an elliptical geometry (in preference to Einstein's model) for simpler imagination of the "physical world" and models it as a hyperboloid universe (system B) embedded in a 4-dimensional Euclidean space:

$$ds^2_{_A} = -c^2 dt^2 + dr^2 + \mathcal{R}^2 \sin^2\left(\frac{r}{\mathcal{R}}\right) d\Omega^2 \tag{2.3.3}$$

$$ds^2_{_B} = -c^2 \cos^2\left(\frac{r}{\mathcal{R}}\right) dt^2 + dr^2 + \mathcal{R}^2 \sin^2\left(\frac{r}{\mathcal{R}}\right) d\Omega^2 \tag{2.3.4}$$

where $d\Omega^2 = d\theta^2 + \sin^2\theta d\phi^2$. $\mathcal{R}$ is the radius of the universe.

Assuming pressureless and internal forces free and supposing all matter at rest, the only

non vanishing stress-tensor is:

$$T_{00} = \rho g_{00} \tag{2.3.5}$$

where ρ is decomposed into ρ_0, the average uniform density of the "world matter" and ρ_1, the density of local matter that attributes to the local inhomogeneity.

Neglecting the local effect, "gravitation", the global solution of Einstein universe "world matter" according to de Sitter [12] is strictly connected to the cosmological constant Λ through the uniform density ρ_0 and the radius of the universe $\mathcal{R}$ as:

$$\Lambda = \frac{4\pi G\rho_0}{c^4} = \frac{1}{\mathcal{R}^2} \tag{2.3.6}$$

de Sitter model considers an empty universe that contains no matter but somehow be adjusted to describe the real universe, provided the density of matter is close enough to zero.

Historically, it therefore seems that the introduction of Λ by Einstein himself with his cosmic background interest and de Sitter's supplementary work and genuine scientific debates during 1916 - 1918 to Einstein's discovery has laid the foundation of the modern cosmology both as model framework and progress, where the two did formulate their own mathematical expressions for the metric of the universe as a whole. In fact in 1916 Einstein [7] was providing the meanings and contents of his summarized works of the principles of general relativity. While de Sitter [12] was working on further interpretations and liabilities of this new theory by providing supplementary interpretations and some additional elegant mathematical frameworks. In that he was verifying the theory with supplementary examples of astronomical consequences. de Sitter was observed to acknowledge Einstein's theory of gravitation as a powerful instrument of discovery that Einstein had laid intimate

connections between various science disciplines which before were entirely considered independent of each other * and thus considered Einstein's new theory as the first step towards the unity of nature. However, on the other side, de Sitter was raising question on the origin of inertia. He called the world - matter concept of Einstein the "Machian concept of inertia" and further strengthen his view calling it "absolute space under another name."† in the other next year.

These initiatives and motives in effect have brought forth the 1920's preeminent progress for the present modern cosmological foundation [52, 53] while the Einstein's field equations in its "dynamic" and "static" forms remained with debates and speculations of model formalisms.

2.3.2 Implications of Einstein modified equations

It is obvious that the modified EFEs due to the presence of Λ have different philosophical and physical consequences on space, time and gravitation. Philosophically, it has primarily blurred Einstein himself again and again from its conception to dropout. While on the way to publish his modified field equations in the presence of Λ, Einstein was suspicious of the future consequence of his work. Actually, as explained in the previous subsection 2.3.1, Einstein was able to establish a field equation that avoids collapsing universe. But the problem is that, Einstein was unaware of its state of expansion where de Sitter had soon recognized. This was uncomfortable to Einstein, while de Sitter was glad with the modified equation. Here, some of the philosophical logics requested by de Sitter in the original

*In an Astronomical Monthly Review of November 1912, entitled as "Absorption of Gravitation,"de Sitter remarks that there was no satisfactory physical explanation for law of gravitation and gravitation was not interconnected to other physical theories. On the other hand, in his 1916 work the newly discovered theory of gravitation by Einstein has answered it and thus declares the theory to be approved at once.

†de Sitter in his 1917 work calls Einstein's concept of world - matter "The material postulate of relativity of inertia"

equation (where de Sitter was questioning the logic why Einstein was pleading for a matter filled universe) apparently had delivered viable logic in the modified one.

On the other hand, the modified equation has received criticism since from its birth that the introduction of Λ is a simple hand set constant without proper logical explanation. Yet, there is no concrete reasoning that challenges to invalidate the modification*. To the contrary, the complementary and supplementary works of distinguished scholars signify it as the more general field equations that can be constructed from Riemannian invariants in four dimensional spacetime geometry. Furthermore, the scholars also show that the fundamental metric $g_{\mu\nu}$ itself, its first and second derivatives are the only possible ones being used for the construction of such Riemannian invariants to establish the more general field equations in four dimension. For comprehensive description, refer [12, 48, 69, 102, 103].

Besides the principles of mathematical competence and implications, the astrophysical consequences were also crucial issues. As pointed out earlier, the formalism had already gone beyond Einstein's goal of establishing a static universe. However, though it was unpleasant to Einstein, its astrophysical consequences had immediately attracted a number of both observational and theoretical pioneering scholars. On the observation side, in its early development stage it was considered to explain the observed receding nebulae [10, 48, 49]. However, the unanimous empirical confirmation of the expanding universe at the end of 1920's had cast shadow on the inclusion of Λ for three decades, until 1960's mainly for two reasons: 1) Einstein himself and others lost interest in Λ assuming that the original field equations (without Λ) can explain the expansion.; 2) The conception and birth of Steady-state-universe cosmology as an alternative with attractive theoretical philosophy. Yet, few had maintained EFE in the presence of Λ to explain observational discrepancies

*We argue that Einstein was reasonable enough in his own style. We supply our arguments under the supplementary chapter, ch. 8.

faced by the other theories. Especially, the discrepancy between astronomical and geological age estimates of astrophysical systems including our own galaxy, the universe, nucleosynthesis and abundances were all preferably explained by EFE with Λ. Furthermore, the earlier mechanisms developed to predict cosmic radiations associated to the Big Bang were succeeded by its discovery in the mid of 1960's as discussed earlier.

2.3.3 Cosmological constant as a paradigm shift

A demanding considerate and success of GR theory with Λ came in the 1960's when the steady-state cosmology failed to explain new observations like excess quasi-stellar objects (QSOs) near the redshift $z \simeq 1.95$. Therefrom, GR had gained success to its early theoretical predictions where Λ was invoked on several occasions as a tool to address diverse empirical puzzles such as the time span of cosmic expansion, the formation of galaxies and the redshifts of quasars. Thus, interests begun to develop on the revaluation of the cosmological constant in the mid of 1960s where [104, 105] took the initiative for the possible unification of gravity and quantum, where the observed vacuum energy fluctuation in quantum field theory is considered as the possible association to Λ. Since then, the involvement of pioneering field theoreticians and cosmologists including Zeldo'vich in the unification effort successfully and cumulatively have shown that the form of the vacuum energy density associated with the inflation of the universe shall consider a scalar field that takes the form of a cosmological constant. Conversely, the cosmological constant is that scalar field that plays the role of vacuum energy fluctuation in quantum field and the form of negative/dark energy in the case of cosmology, so that it is either a pure fundamental scalar constant or a varying scalar with time where its present value should coincide with the present observations. However, the calculated energy density at the Planck's ultraviolet cutoff is more than 120 orders of magnitude larger than is allowed by observation,

[54, 106, 107]. Moreover, its coincidence in order of magnitude as that of matter in present universe has remained an open puzzle. Irrespective of these puzzles, current observations has favoured the unrevealed dark energy sector in the form of cosmological constant 2.3.1.

The standard ΛCDM model has so far successful apart from its limitation in explaining the nature of the dark sectors that mainly constitute the universe and the unresolved unification of gravity and quantum; where Λ is used to decide the vacuum constant as dark energy in the large scale structure while it is considered as the quantum vacuum fluctuation energy in the small scale case. On the other hand, several modified gravity models introduced have not yet resolved the problem either. However, most of these new theories mimic the ΛCDM model in the late cosmic acceleration as viable models either with fine tune or be challenged by observational constraints in other astrophysical applications. Among, the modified gravity theories, the $f(R)$ are successful as the ΛCDM model in weak-field region but in trouble in the strong-field region.

In general, the cosmological constant has played a great role as interplay between theoretical physics and astronomical observation. Since from its birth, conceived with philosophical believe of static universe has got attention with outstanding scientific debates both on philosophical and observational estates. A century has passed without common agreement to the nature of this term whether it is a temporal integration or pure physical constant related to some fundamental nature of force or geometry. However, the cosmological constant has overcome the challenges to abandon it and so succeeded on many occasions in subsequent decadal programmed testing issues. Some of such outstanding specific observational puzzles addressed by the cosmological constant include: the timespan of cosmic expansion, the formation of large-scale structure, the redshifts of quasars, the cosmic

microwave background fluctuations, gravitational lensing and galaxy clustering (see for example [108, 109, 110, 111] and references therein). On the theoretical ground, it has caught attention from its birth as necessity for the completeness of the Riemann tensor being constructed and the field equations being established under GR; though it is occasionally criticized as a handcraft extension for the then Einstein philosophical perception towards universe. However, since the beginning 1980's it has received physical attention in the context of the hypothesis of cosmic inflation of a universe with an inflationary phase in early times and an accelerated expansion at late times, indicative of a positive cosmological constant dominant at both epochs [93, 94, 112]; an ingredient of the current standard ΛCDM model.

Apart from the standard ΛCDM model, the cosmological constant found a theoretical motivation in steady-state cosmology [66, 113], and found physical attachment in other recently introduced modified computing alternative gravity theories with wide range of views including: gravity with extra fields like Brans-Dicke gravity (eg. [114]), vector theory of gravity (eg. [115, 116]), higher derivative and non-local theories of gravity like f(R) gravity (eg. [117]) & [118] and higher dimensional theories of gravity such as for example [119]; Also more advocating traceable facts can be deduced from more detailed reports like [25, 100] and others.

Finally, the vast number of exact solutions so far derived for EFE exhibits the richness and mathematical beauty of the field, where those physically interpreted ones have successfully passed all observations they have being tested. On the other hand, the remaining majorities and others that will possibly be derived in the future leave open research for its completeness where the cosmological constant therein inherits issues both explicitly and implicitly. Also, most viable modified gravity theories claim the cosmological constant in

some form as discussed earlier. Thus, the recent attention towards the cosmological constant in modern cosmology seems a compelling paradigm shift, considered to be stipulated as supplementary and complementary fundamental physics problem to be discovered.

Chapter 3

Introduction to general relativity and its basic principles in cosmology

3.1 General relativity fundamental principles and basics

Albert Einstein's theory of general relativity is a modified theory of gravity that describes gravity as a cause of spacetime curvature and feedback effect due to distribution of matter and energy over the entire spacetime in continuum. The principle of covariance - that is the laws of physics must be independent of any coordinate system is the foundation of the theory. So, the mathematical objects being used to construct the field equations must be tensors or other coordinate independent entities. Locally, the theory is expected to be consistent with special relativity and must inherit its principles including the equivalence of local inertial frames of reference, the universal constancy of the speed of light in vacuum, and the Lorentz-invariance of the theory.

Past surveys of leading expertise opinions consider the theory either as i) the geometrization of gravity as the reduction of spacetime geometry or as ii) the advancement of the unification program of all physics in direct continuation of special relativity to the general theory of inertia and gravity or iii) both. Nevertheless (regardless of these sentiments), the

guiding principles of general covariance and unification of all physics is implicitly concealed in all outlooks of the formalisms. Moreover, irrespective of lack of understanding in some astrophysical situations, all the approaches of GR theory development are being motivated to accommodate matching observables in all astrophysical applications.

Here we introduce the fundamentals of GR and related basic concepts based on the general coordinate transformation approach. Its aim is to provide the background physics being implemented in the main work of the thesis. It is also true that, conversely the thesis is there to develop extensions of the theory and also provides complementary and supplementary issues to the theory as outlined in the background objectives. Whenever a deep understanding of GR theory is required, the standard books and review works like [23, 48, 54, 65, 100, 101, 120, 121, 122, 123] will be consulted.

3.1.1 Spacetime geometry of gravitation

In general relativity the geometry is a curved pseudo-Riemannian space, having locally the structure of 4-dimensional Euclidean space, and to lowest order have the structure of Minkowski space with its light cones.

Distances on these intrinsic surfaces are defined by the line element called metric given as

$$ds^2 = g_{\mu\nu} dx^\mu dx^\nu \tag{3.1.1}$$

Where $g_{\mu\nu}$ is called the metric tensor. It is symmetric and intrinsic to the structure of the Riemannian space. The signature (-,+,+,+) is used for the metrics as in [101] for sign convention.

The inverse of $g_{\mu\nu}$ is denoted as $g^{\mu\nu}$ so that

$$g^{\mu\sigma} g_{\sigma\nu} = \delta^\mu_\nu \tag{3.1.2}$$

Moreover, the geometries have geodesics defined as lines of stationary length,

$$\delta \int ds = 0 \tag{3.1.3}$$

which can be minimal, or maximal.

3.1.2 Tensor: Mathematical language of General Relativity

A non-Euclidean geometry called Riemannian geometry, is the key mathematical framework which Einstein found it to fit his conception of gravity to develop general relativity. It was identified meanwhile Einstein was in search for relativistic theory of gravity as an extension of Special relativity(SR) that eventually has modified Newtonian gravity. The development of this new physics was recalled as a fortunate for Einstein to consult great mathematicians like Marcel Grossmann and others including physicists. Even, it is considered by many that the very foundations of GR theory and its field equations were besought the language of tensors for assertion. Thus, the mathematics used in Einstein GR is the tensor algebra developed for the Riemannian geometry.

3.1.3 The metric tensor and Affine connection

The metric tensor is a fundamental object in Einstein's general relativity that describes the geometry of spacetime and its effects in the dynamics of physical systems on it. It plays great roles in the generation of other field tensor both in the construction and solutions of Einstein field equations. On the other hand, the so called affine connection is a non-tensorial object that plays great roles in the construction of other tensor fields and transformations.

The metric tensor

In GR the spacetime structure of SR is generalized on the basis of the principle of equivalence, where gravitation is locally a freely falling system. That means, on infinitesimal

scale related locally inertial system, special relativity remains valid. So, the transformation from the locally inertial system where the metric is Minkowskian $\eta_{\mu\nu}$ to the general metric $g_{\mu\nu}$ is carried out from the locally inertial coordinate ξ^{α} to the general coordinate system x^{μ} as

$$g_{\mu\nu}(x) = \frac{\partial \xi^{\alpha}}{\partial x^{\mu}} \frac{\partial \xi^{\beta}}{\partial x^{\nu}} \eta_{\alpha\beta} \tag{3.1.4}$$

Affine Connection

Affine connection is an additional important geometrical structure of the manifold associated to differential transformation of the tensor fields owned by the geometry. It is considered as an operator that defines a covariant derivative which transforms tensor fields into other tensor fields, such as parallel transport of vectors on tangent planes along a smooth curve, and geodesics. Furthermore, an affine connection fully characterizes the curvature and torsion of a manifold.

To gain an insight of the affine connection, here the equivalence principle is being implemented to see how the motion of a particle from a free fall coordinate ξ^{α} system is transformed to that of an arbitrary (general) coordinate system x^{μ}. Thus, in the free fall coordinate the equation of the particle is

$$\frac{d^2 \xi^{\alpha}}{d\tau^2} = 0 \tag{3.1.5}$$

where $d\tau$ is the proper time in this free fall coordinate given as

$$d\tau^2 = \eta_{\alpha\beta} d\xi^{\alpha} d\xi^{\beta} \tag{3.1.6}$$

Since the free fall coordinates ξ^{α} are functions of the general coordinates x^{μ}, then with little algebra the transformation of the free fall particle equation 3.1.5 to the general coordinate

system takes the form

$$\frac{d^2x^\lambda}{d\tau^2} + \Gamma^\lambda_{\mu\nu}\frac{dx^\mu}{d\tau}\frac{dx^\nu}{d\tau} = 0 \tag{3.1.7}$$

where now the proper time $d\tau$ is just the infinitesimal line element given as by eq. 3.1.2,

$$d\tau^2 = g_{\mu\nu}dx^\mu dx^\nu$$

The mathematical symbol $\Gamma^\lambda_{\mu\nu}$ used in 3.1.7, also known as the Christoffel symbol of second kind which is denoted as $\{\mu\nu, \lambda\}$ or $\{^\lambda_{\mu\nu}\}$, is apparently recognized as the affine connection between the two set of coordinate systems in the transformation expressed as

$$\Gamma^\lambda_{\mu\nu} \equiv \frac{\partial x^\lambda}{\partial \xi^\alpha}\frac{\partial^2 \xi^\alpha}{\partial x^\mu \partial x^\nu} \tag{3.1.8}$$

By virtue of eq. 3.1.7 the affine connection acts as the field that determines the gravitational force. In fact, for slowly moving particle in a week stationary gravitational field we may neglect $\frac{d\mathbf{x}}{d\tau}$ in comparison to $\frac{dt}{d\tau} \simeq 1$, so that eq. 3.1.7 will yield

$$\frac{d^2x^i}{dt^2} \simeq -\Gamma^i_{00} = \nabla\Phi \tag{3.1.9}$$

Equation 3.1.9 indicates the equivalence between the local gravitational force Γ^i_{00} and the Newtonian force as the Newtonian limit in the weak-gravity approximation for a slowly moving particle. sub

3.1.4 Relationships between the metric tensor and affine connection

As discussed earlier, physically the affine connection determines the gravitational force in the Riemannian spacetime geometry. On the other hand, by mathematical intuition the forms of equations 3.1.4 & 3.1.8 suggest that the affine connection is a derivative form of the metric tensor, so that the metric tensor is thought of as representing the gravitational potential. Thus, both have field of gravitation in common to relate.

There are various approaches in deriving the relationships between the two, where one of them is using equations 3.1.4 & 3.1.8, see for example [120]. Here, we use the variational technique in the extremization of the invariant line element eq. 3.1.1.

From the variational principle along a curve $x^\mu(\sigma)$ parameterized by the parameter σ the extremum condition of equation 3.1.3, is

$$\int ds = \int \sqrt{g_{\mu\nu}\frac{dx^\mu}{d\sigma}\frac{dx^\nu}{d\sigma}}d\sigma = \int \mathcal{L}d\sigma = 0 \tag{3.1.10}$$

The Euler-Lagrange equation for the extremum associated with the integral is

$$\frac{d}{d\sigma}\left(\frac{\partial\mathcal{L}}{\partial\dot{x}^\mu}\right) - \frac{\partial\mathcal{L}}{\partial x^\mu} = 0 \tag{3.1.11}$$

where dot over the vector indicates derivative with respect to the parameter σ: $\dot{x}^\mu = \frac{dx^\mu}{d\sigma}$
Then using the symmetric property of the metric and applying contraction properties, we obtain

$$\ddot{x}^\mu + \frac{1}{2}g^{\mu\rho}\left(\frac{\partial g_{\rho\nu}}{\partial x^\lambda} + \frac{\partial g_{\rho\lambda}}{\partial x^\nu} - \frac{\partial g_{\lambda\nu}}{\partial x^\rho}\right)d\dot{x}^\lambda d\dot{x}^\nu = 0$$

Or

$$\frac{d^2x^\mu}{d\sigma^2} + \frac{1}{2}g^{\mu\rho}\left(\frac{\partial g_{\rho\nu}}{\partial x^\lambda} + \frac{\partial g_{\rho\lambda}}{\partial x^\nu} - \frac{\partial g_{\lambda\nu}}{\partial x^\rho}\right)\frac{dx^\lambda}{dx^\sigma}\frac{dx^\nu}{dx^\sigma} = 0 \tag{3.1.12}$$

Now comparing eq. 3.1.7 & eq. 3.1.12 the relationship between the affine connection and the metric tensor is given by

$$\Gamma^\sigma_{\lambda\mu} = \frac{1}{2}g^{\nu\sigma}\left(\frac{\partial g_{\mu\nu}}{\partial x^\lambda} + \frac{\partial g_{\lambda\nu}}{\partial x^\mu} - \frac{\partial g_{\mu\lambda}}{\partial x^\nu}\right) \tag{3.1.13}$$

Considering once again the stationary weak-field gravity approximation for a slowly moving particle with the metric

$$g_{\mu\nu} \approx \eta_{\mu\nu} + h_{\mu\nu}(\mathbf{x}) \tag{3.1.14}$$

so that all time derivatives of the metric tensors are zero and the relevant force Γ^i_{00} to the significant terms in the particle motion 3.1.7 to first order in $h(\mathbf{x})$ by equation 3.1.13 is

$$\Gamma^i_{00} = -\frac{1}{2}\frac{\partial h_{00}(\mathbf{x})}{\partial x^i} = -\frac{1}{2}\nabla h_{00}(\mathbf{x}) \equiv -\nabla\Phi(\mathbf{x}) \tag{3.1.15}$$

just the Newtonian force. On other hand, the metric tensor $g_{00}(\mathbf{x})$ acts as gravitational potential that modifies the Minkowski metric component by $2\Phi(\mathbf{x})$.

$$g_{00}(\mathbf{x}) = -1 + 2\Phi(\mathbf{x}) \tag{3.1.16}$$

3.1.5 Curvature & the curvature tensor

In GR gravity is described as the relative acceleration of particles resulted from the curvature of spacetime in which the particles are moving, but not gravitational forces. Riemann and others generalized the concept of curvature to a number of intrinsic and extrinsic groups. In the Riemannian geometry it is quantified by an invariant Riemann tensor, which is derived from the affine connection. This Riemann tensor arises as the measure of curvature of geometry when the tensor fields are being transformed by the affine connection covariantly. In other ways, it arises when any of the properties of locally flatness geometry alter during transformations including parallel transport of vectors around a closed loop, covariant derivatives of tensors, and so on.

Einstein GR is developed to provide the exact mathematical foundation for applying this new idea of gravitation as the manifestation curvature of the manifold they are moving in, the curvature of the given surface. Thus, the field equations are constructed from the curvature tensor as the measure of spacetime geometry where this tensor is also used to construct other important lower rank curvature tensors, such as the Ricci and scalar curvature tensors used in the equations. In metric approach of GR theory development especially

the Riemann curvature tensor is the only tensor that can be constructed from the metric tensor itself and its first and second derivatives.

Here, we provide some key relations and equations of these important tensors that can be used later in the construction of EFEs (without detailed derivations).

a) Riemann curvature tensor

$$R^{\lambda}_{\mu\kappa\nu} = \frac{\partial \Gamma^{\lambda}_{\mu\nu}}{\partial x^{\kappa}} - \frac{\partial \Gamma^{\lambda}_{\mu\kappa}}{\partial x^{\nu}} + \Gamma^{\lambda}_{\eta\kappa}\Gamma^{\eta}_{\mu\nu} - \Gamma^{\lambda}_{\eta\nu}\Gamma^{\eta}_{\mu\kappa} \tag{3.1.17}$$

The Riemann curvature tensor in its full covariant form can be constructed as,

$$R_{\sigma\mu\kappa\nu} = g_{\sigma\lambda}R^{\lambda}_{\mu\kappa\nu} \tag{3.1.18}$$

Upon expansion this can also be written directly in terms of the space-time metric and product of the affine connections as,

$$\begin{aligned} R_{\sigma\mu\kappa\nu} &= \frac{1}{2}\left(\frac{\partial^2 g_{\sigma\nu}}{\partial x^{\mu}\partial x^{\kappa}} + \frac{\partial^2 g_{\mu\kappa}}{\partial x^{\sigma}\partial x^{\nu}} - \frac{\partial^2 g_{\sigma\kappa}}{\partial x^{\mu}\partial x^{\nu}} - \frac{\partial^2 g_{\mu\nu}}{\partial x^{\sigma}\partial x^{\kappa}}\right) \\ &\quad + g_{\eta\rho}\left(\Gamma^{\eta}{}_{\mu\kappa}\Gamma^{\rho}{}_{\sigma\nu} - \Gamma^{\eta}{}_{\mu\nu}\Gamma^{\rho}{}_{\sigma\kappa}\right) \end{aligned} \tag{3.1.19}$$

Using the symmetric properties of both the metric tensor and the affine connection, other important algebraic properties of the curvature tensor can be deduced including symmetry, antisymmetry and cyclicity properties. As such, eq. 3.1.19 will be used to deduce these properties.

1. Symmetry

$$R_{\lambda\mu\nu\kappa} = R_{\nu\kappa\lambda\mu} \tag{3.1.20}$$

2. Antisymmetry

$$R_{\lambda\mu\nu\kappa} = -R_{\mu\lambda\nu\kappa} = -R_{\lambda\mu\kappa\nu} = R_{\nu\kappa\lambda\mu} \tag{3.1.21}$$

3. Cyclicity

$$R_{\lambda\mu\nu\kappa} + R_{\mu\kappa\lambda\nu} + R_{\lambda\kappa\mu\nu} = 0 \tag{3.1.22}$$

Note that spacetime is considered flat if the Riemann tensor vanishes everywhere.

b) Ricci tensor

Applying the symmetric and anitsymmetric properties of the Riemann tensor a unique two rank important symmetric tensor can be constructed by contraction of the Riemann tensor as

$$R_{\mu\nu} \equiv R^{\gamma}_{\mu\gamma\nu} = g_{\lambda\sigma} g^{\sigma\kappa} R^{\lambda}_{\mu\kappa\nu} \tag{3.1.23}$$

c) The scalar curvature tensor

Another important invariant scalar tensor constructed by further contraction of the Riemann tensor equivalent to the construction of Ricci tensor given as

$$R \equiv R^{\mu}_{\mu} = g^{\mu\kappa} R_{\mu\kappa} = g^{\lambda\nu} g^{\mu\kappa} R_{\lambda\mu\nu\kappa} \tag{3.1.24}$$

The antisymmetric and cyclicity properties of the Riemann tensor determine that R is unique.

3.1.6 The Bianchi identities & Einstein tensor

By Equivalence principle it is always possible to define a locally inertial coordinate system so that the torsion (affine connection) vanishes. So at any point in locally inertial coordinate system the covariant derivative of eq. 3.1.19 yields

$$R_{\sigma\mu\kappa\nu\,;\,\lambda} = \frac{1}{2}\frac{\partial}{\partial x^{\lambda}}\left(\frac{\partial^2 g_{\sigma\nu}}{\partial x^{\mu}\partial x^{\kappa}} + \frac{\partial^2 g_{\mu\kappa}}{\partial x^{\sigma}\partial x^{\nu}} - \frac{\partial^2 g_{\sigma\kappa}}{\partial x^{\mu}\partial x^{\nu}} - \frac{\partial^2 g_{\mu\nu}}{\partial x^{\sigma}\partial x^{\kappa}}\right) \tag{3.1.25}$$

By permuting κ, ν and λ cyclically, we obtain the Bianchi identities,

$$R_{\sigma\mu\kappa\nu\,;\,\lambda} + R_{\sigma\mu\nu\lambda\,;\,\kappa} + R_{\sigma\mu\lambda\kappa\,;\,\nu} = 0 \tag{3.1.26}$$

Recall that, the metric tensor is an invariant tensor so that its covariant derivative vanishes (also possible to show). Thus, the double contraction of eq. 3.1.26 by $g^{\sigma\kappa}g^{\mu\nu}$ implies

$$(R^{\mu}_{\lambda} - \frac{1}{2}\delta^{\mu}_{\lambda}R)_{;\mu} = 0 \tag{3.1.27}$$

$$(R^{\mu\nu} - \frac{1}{2}g^{\mu\nu}R)_{;\mu} = 0 \tag{3.1.28}$$

Equation 3.1.28 suggests the existence of a divergence free tensor which was actually identified by Einstein in the derivation of his field equations. Thus, it is called Einstein tensor given as

$$G_{\mu\nu} = R_{\mu\nu} - \frac{1}{2}g_{\mu\nu}R \tag{3.1.29}$$

3.1.7 Energy-Momentum Tensor

The energy-momentum tensor is the source of the gravitational field in Einstein field equations attributed from matter, radiation, and other force fields. It describes the density and flux of energy and momentum in the given spacetime. From a geometric point of view the stress-energy-momentum tensor is a very much debated issue that still stands. However, its flow in the given spacetime geometry is commonly understood as a two rank tensor that describes the projection of the flux of a momentum vector across a surface with a constant coordinate. That means if $T^{\mu\nu}$ is considered to represent this two rank symmetric tensor, then it is described as the flux of the μ^{th} component of the momentum vector across the surface with constant x^{ν} coordinate.

$$T_{\mu\nu} = pg_{\mu\nu} + (\rho + p)u_{\mu}u_{\nu} + q_{\mu}u_{\nu} + u_{\mu}q_{\nu} + \pi_{\mu\nu} \tag{3.1.30}$$

where u^{μ} is the tangent velocity 4-vector normalized by $u_{\mu}u^{\mu} = -1$, ρ is the relativistic mass-energy density, p is the isotropic pressure, q^{μ} the energy flux, and $\pi_{\mu\nu}$ is the trace-free

anisotropic pressure or stress, all relative to u^{μ}. The quantities ρ, p, q^{ν}, and $\mu\nu_{\pi}$ are functions of time and space.

In the standard (ΛCDM) cosmology, it is assumed that the cosmic fluid is well-described by a perfect fluid (i.e., $q_{\mu} = 0$ and $\pi_{\mu\nu} = 0$) at the cosmic background level which accounts for baryons, dark matter, radiation and a cosmological constant or another dark energy component. Then the energy-momentum tensor reduces to

$$T_{\mu\nu} = pg_{\mu\nu} + (\rho + p)u_{\mu}u_{\nu} \tag{3.1.31}$$

3.1.8 Einstein Field Equation

Einstein field equations assume equivalence of geometry that determines the behavior of the sources of fields t hat exist in it, and conversely the sources of the fields pronounce the underlying geometry they exist in and also further alter the geometry to other fields. Accordingly, any Energy-momentum tensor being constructed must be a covariantly divergence free that fits to describe the densities and fluxes of energy and momentum flows in this geometry.

Thus, Einstein derived his field equations with this assumption where the geometrical part is contained by his geometrical tensor (eq. 3.1.29) while the energy-momentum tensor is considered as the sources of gravitation. That means a divergence free energy-momentum tensor that informs such evolution and distribution shall be equated with the geometrical counterpart as the totality of stable universe for coexistence. Moreover, in the week-field gravity approximation the field equations must be reduced to that of Newtonian physics Poisson equation via Equivalence principle that well accurately describes experimental results of such weak fields.

So Einstein original field equation was constructed by equating the geometrical tensor

with that of the source tensor which is given as

$$G_{\mu\nu} = kT_{\mu\nu} \tag{3.1.32}$$

where the matching constant k is identified from Poisson equation as the limiting case of Newtonian physics, as discussed earlier.

Assuming a pressureless fluid in the weak-field approximation, the time-time component of the stress-tensor & the field equation are respectively given as

$$T_{00} = \rho u^0 u^0 \simeq \rho c^2 \tag{3.1.33}$$

$$R_{00} \simeq \frac{1}{2} k\rho \tag{3.1.34}$$

Using eqs. 3.1.16 & 3.1.17 in eq. 3.1.34 to first order in h we obtain

$$\nabla^2 h_{00}(\mathbf{x}) \simeq -k\rho c^2 \tag{3.1.35}$$

Using eqs. 3.1.16 & 3.1.35, we obtain the familiar Poisson equation given by

$$\nabla^2 \Phi(\mathbf{x}) \simeq -\frac{k}{2}\rho c^2 = -\frac{4\pi G}{c^2}\rho \tag{3.1.36}$$

Then follows the matching constant given by

$$k = \frac{8\pi G}{c^4} \tag{3.1.37}$$

Later, Einstein modified his equation with the idea of establishing a static universe given by

$$G_{\mu\nu} + \Lambda g_{\mu\nu} = kT_{\mu\nu} \tag{3.1.38}$$

The modification was controversial in several ways since from its birth that include philosophy, mathematical framework and physical interpretations. However, currently it is considered as the major field equation being used in the theory of gravitation and cosmological applications as discussed in the historical background chapter.

3.2 Solutions of Einstein field equation

As literatures point out that EFEs have over 1300 exact solutions that have been derived over the last century, see for example [100] and the references therein. Regardless of such large rich number of solutions a number of these solutions still lack any physical interpretation.

Some solutions that have found direct applications in astrophysical systems include:

1) spherically symmetric static vacuum solutions to model spacetime around concentric masses like the sun, static black holes and so on, for example Schwarzschild solution

2) solutions to axially symmetric rotating compact objects, for example Kerr solution

3) solutions used to model interior of stellar system, for example Tolman solution

4) solutions used to model gravitational waves where linearization of EFEs is used

5) solutions used in cosmological models like the homogenous cosmological models, for example the Friedmann-Lemaître-Robertson-Walker (FLRW) solution and the inhomogeneous cosmological models, such as the Lemaître-Tolman-Bondi solutions.

Here we focus only on 1) the spherically symmetric static vacuum solution around a concentric mass that yields the Schwarzschild-de Sitter (SdS) solution and 2) the standard FLRW cosmological solution that we use in our work. Moreover, the linearization of the fields will be discussed under the topic it is intended to apply.

3.2.1 The Schwarzschild-de Sitter solution

Looking for a symmetrically static and isotropic solution, the metric given by eq. 3.1.1 takes the form (see, for instance [120])

$$ds^2 = -B(r)dt^2 + A(r)dr^2 + r^2 d\Omega^2 \tag{3.2.1}$$

where

$$d\Omega^2 = r^2(d\theta^2 + \sin^2\theta d\varphi^2) \tag{3.2.2}$$

Now the components of the metric tensor $g_{\mu\nu}$ are

$$\begin{aligned} g_{rr} = (g^{rr})^{-1} = A(r);\ \ g_{\theta\theta} = (g^{\theta\theta})^{-1} = r^2;\ \ g_{\varphi\varphi} = (g^{\varphi\varphi})^{-1} = r^2\sin^2\theta; \\ g_{tt} = (g^{tt})^{-1} = -B(r);\ \ g_{\mu\nu} = g^{\mu\nu} = 0, \text{ for } \mu \neq \nu \end{aligned} \tag{3.2.3}$$

The forms of $A(r)$ and $B(r)$ are determined from the field equations by allowing the source to vanish.

$$G_{\mu\nu} = R_{\mu\nu} + \Lambda g_{\mu\nu} = 0 \tag{3.2.4}$$

Using the metric components given by eq. 3.2.3 in eq. 3.2.4 we obtain the following set of equations corresponding to the coordinate components:

$$R_{rr} + \Lambda g_{rr} = 0 \Rightarrow \frac{B''}{2B} - \frac{B'}{4B}\left(\frac{A'}{A} + \frac{B'}{B}\right) - \frac{1}{r}\left(\frac{A'}{A}\right) = -\Lambda A \tag{3.2.5}$$

$$R_{\theta\theta} + \Lambda g_{\theta\theta} = 0 \Rightarrow -1 + \frac{r}{2A}\left(-\frac{A'}{A} + \frac{B'}{B}\right) + \frac{1}{A} = -\Lambda r^2 \tag{3.2.6}$$

$$R_{\varphi\varphi} = \sin^2\theta R_{\theta\theta} \tag{3.2.7}$$

$$R_{tt} + \Lambda g_{tt} = 0 \Rightarrow -\frac{B''}{2A} + \frac{B'}{4A}\left(\frac{A'}{A} + \frac{B'}{B}\right) - \frac{1}{r}\left(\frac{B'}{A}\right) = \Lambda B \tag{3.2.8}$$

$$R_{\mu\nu} = 0, \text{ for } \mu \neq \nu \tag{3.2.9}$$

Primes on A & B imply differentiation with respect to r.

Using eqs. 3.2.5 & 3.2.8 with a little algebra we obtain

$$\frac{A'}{A} + \frac{B'}{B} = 0 \tag{3.2.10}$$

Integrating this we get

$$A(r)B(r) \equiv \text{constant} \tag{3.2.11}$$

Using equations 3.2.6 & 3.2.10 we get

$$\frac{d}{dr}\left(\frac{r}{A}\right) = -\Lambda r^2 \tag{3.2.12}$$

Equation 3.2.12 is integrated to yield

$$A(r)^{-1} = 1 - \frac{\Lambda}{3}r^2 + \frac{\mathrm{C}}{r} \tag{3.2.13}$$

Where the constant of integration C is determined inquiring the Newtonian limit. This condition identifies the constant of integration in eq.3.2.11 as unity, so that

$$A(r)B(r) = 1 \Rightarrow A(r)^{-1} = B(r) \tag{3.2.14}$$

On the other hand, the equivalence of the metrics under this limiting case, by eqs. 3.1.14, 3.1.16 3.2.13 & 3.2.14 implies that

$$A_{NL}(r)^{-1} = B_{NL}(r) = -g_{tt_{NL}}(r) \approx 1 + \frac{2\Phi(r)}{c^2} = 1 - \frac{2GM/c^2}{r} \tag{3.2.15}$$

where the subscript $_{NL}$ stands for the Newtonian limit.

In view of eqs. 3.2.13 & 3.2.15, we recognize that the constant of integration C is given by

$$C = \frac{2GM}{c^2} \tag{3.2.16}$$

This constant is after all called the Schwarzschild radius denoted as r_S for historical honor of Schwarzschild who had first derived the exact solution of EFEs in the absence of the cosmological constant, as we see soon. Also for historical reasons it is called gravitational radius denoted as r_g. Here after, we represent this constant as:

$$r_S \equiv r_g = \frac{2GM}{c^2} \tag{3.2.17}$$

Note also that this constant of integration constrains the cosmological constant value at most of the order of $10^{-52}m^{-2}$ in order to fit with present astronomical observations. Regarding constraining of the cosmological constant value case, we raise it again in our main work issued under comments in the development of GR. There, we provide a new alternative approach to rediscover the value theoretically.

Now using eqs. 3.2.13, 3.2.14 & 3.2.16 , A(r) and B(r) are given by

$$A(r)^{-1} = B(r) = 1 - \frac{\Lambda}{3}r^2 - \frac{2GM}{c^2 r} \tag{3.2.18}$$

Finally, the required spherically static, homogenous and isotropic metric derived from Einstein field equations with Λ that describes the geometry around a point mass is

$$ds^2 = -\left(1 - \frac{2GM}{c^2 r} - \frac{\Lambda}{3}r^2\right)dt^2 + \left(1 - \frac{2GM}{c^2 r} - \frac{\Lambda}{3}r^2\right)^{-1} dr^2 + r^2 d\Omega^2 \tag{3.2.19}$$

This metric is known as the Schwarzschild-de Sitter metric since in the limiting cases, it yields the Schwarzschild metric in one way and the de Sitter metric in the other way, as we see soon. It is also known as the Kottler metric since first derived in its general form [45].

Limiting case

i) At sufficiently large distance from a concentrated mass, i.e., as $\frac{1}{r} \to 0$ or equivalently in the absence of material source $M = 0$, the metric describes the de Sitter universe given by [46]:

$$ds^2 = -\left(1 - \frac{\Lambda}{3}r^2\right) dt^2 + \left(1 - \frac{\Lambda}{3}r^2\right)^{-1} dr^2 + r^2 d\Omega^2 \tag{3.2.20}$$

Notice that, eq. 3.2.20 is the "static" form of the de Sitter spacetime. Its dynamic version can be obtained by a suitable coordinate transformation provided as in section 3.2.3.

ii) At a relatively small distance where the contribution from the cosmological constant is negligible, it describes the Schwarzschild geometry given by [47]

$$ds^2 = -\left(1 - \frac{2GM}{c^2 r}\right) dt^2 + \left(1 - \frac{2GM}{c^2 r}\right)^{-1} dr^2 + r^2 d\Omega^2 \tag{3.2.21}$$

The event horizon at the Schwarzschild radius $r = r_g$ leads to gravitational collapse. All radii smaller than this, describe what we call black hole interior. The surface at the Schwarzschild radius acts as an event horizon in a non-rotating body where no particle can escape through this surface from the region inside, hence the name “black hole”.

3.2.2 The Friedmann-Lemaître-Robertson-Walker (FLRW) solution

Universe modeling was among the important essences of GR theory by Einstein where originally he thought of it as a static universe. In fact, the solutions were later determined to be rather dynamic. Moreover, Einstein proposed a spatially isotropic and homogenous universe in the form of fluid at large scale. This principle is often known as the Cosmological principle.

The mathematical solution derived by [12] de Sitter for an empty universe was considered as the first theoretical prediction of an expanding universe. Later, a detailed theoretical solution was provided by [14] that covers all the possible cases and later independently worked out by [10] where observational data was also taken into account. From observational stand point GR theory gained attention after the discovery of expanding universe from observational data analysis by [9, 124] during the latter years of 1920's. Actually, the observational data used both by Lemaître and Hubble were mainly extracted by [1] and hence today the discovery is acknowledged as Hubble-Lemaître-Slipher (HLS) discovery. Furthermore, [59, 60, 61] and [62, 125] subsequently showed that the Friedmann-Lemaître solution was the only solution to Einstein field equations consistent with spatial homogeneity and isotropy expanding universe. Thus, the dynamical universe described by GR theory is known as the Friedmann-Lemaître-Robertson-Walker (FLRW) model.

The standard FLRW metric that describes the geometry of the universe is given by

$$ds^2 = -dt^2 + a^2(t)\left(\frac{dr^2}{1-kr^2} + r^2 d\Omega^2\right) \tag{3.2.22}$$

where $a(t)$ is the expansion scale factor representing the time-dependent evolution of the spatial part of the metric with constant surfaces of time and $k\,\epsilon\,\{-1, 0, 1\}$ is the signature of curvature that determines the geometry of the spatial sections; negatively curved, flat, or positively curved spaces, respectively.

The EFEs 3.1.38 for the FLRW metric 3.2.22 and a perfect fluid source energy-momentum tensor eq. 3.1.31 yield the two set of Friedmann dynamical differential equations as follows:

i) The time-time components of EFEs yield

$$H^2 = \frac{8\pi G}{3}\rho - \frac{k}{a^2} + \frac{\Lambda}{3} \tag{3.2.23}$$

where H is defined as the Hubble parameter

$$H = \frac{\dot{a}}{a} \tag{3.2.24}$$

the overdot indicates derivative with respect to time: $\dot{} = d/dt$

ii) The spatial-spatial components of EFEs

$$\frac{\ddot{a}}{a} = -\frac{k}{2a^2} - \frac{1}{2}\left(\frac{\dot{a}}{a}\right)^2 - 4\pi G p + \frac{\Lambda}{2} \tag{3.2.25}$$

Now using eqs. 3.2.23, 3.2.24 & 3.2.25 we obtain the second Friedmann equation given by:

$$\frac{\ddot{a}}{a} = -\frac{4\pi G}{3}(3p + \rho) + \frac{\Lambda}{3} \tag{3.2.26}$$

3.2.3 Relationship between FLRW and SdS metrics

The FLRW metric uses the co-moving coordinates (r, t). In order to obtain the FLRW metric, in "static"(T, R) coordinates, the following transformation of variables will be performed:

$$R = ra(t);\ \ T = t - F(R) \tag{3.2.27}$$

where $f(R)$ is only a function of R. Using eq. 3.2.27 in eq. 3.2.22 and applying Friedmann equations with appropriate reasonings we obtain the equivalent static metric given by:

$$ds^2 = -f(R,T)dT^2 \frac{dT^2}{1 - \frac{kR^2}{a^2(R,T)}} + f^{-1}(R,T)dR^2 + R^2 d\Omega^2 \tag{3.2.28}$$

where

$$f(R,T) = 1 - \frac{2GM}{R} - \left(\frac{\Lambda}{3} + \frac{2k}{a^2(R,T)}\right) R^2 \tag{3.2.29}$$

For flat universe, where $k = 0$, this metric is exactly the SdS metric given by eq. 3.2.19.

For the derivation of eqs. 3.2.28 & 3.2.29 we come back under thermodynamic radiation of SdS black holes in our development. Moreover, the detail connections can be inferred from literatures like [126, 127, 128] and others.

In the case of flat empty universe, the de Sitter universe, eq. 3.2.23 gives the scale factor $a(t) = e^{t/\ell}$, where $\ell = \sqrt{3/\Lambda}$. Then, the de Sitter metric in expanding coordinates is given by

$$ds^2 = -dt^2 + e^{2t/l}\left(dr^2 + d\Omega^2\right) \tag{3.2.30}$$

In order to obtain the static isotropic metric form of eq, 3.2.30 we can apply the transformation eq. 3.2.27 where the transformations be given by:

$$r = \frac{e^{-T/\ell}R}{\sqrt{1-(R/\ell)^2}}\,; \qquad t = T + \frac{l}{2}\ln\left(1 - \frac{R^2}{l^2}\right) \tag{3.2.31}$$

Then, the transformed expanding metric in its static isotropic form is given by

$$ds^2 = -\left(1 - \frac{R^2}{l^2}\right)d\tau^2 + \frac{dR^2}{\left(1 - \frac{R^2}{l^2}\right)} + R^2 d\Omega^2 \tag{3.2.32}$$

This is exactly the same as the SdS solution in the absence of source or equivalently at larger distance as in equation 3.2.20.

In summary, the SdS field goes over asymptotically to the de Sitter universe with increasing distance from generating mass. Moreover, its background metric to describe the cosmological phenomenon is the FLRW metric. On the other hand, the Schwarzschild field goes over asymptotically to the Minkowskian static flat space, which contradicts the observational evidence that the universe is expanding at an accelerating rate. And thus for reasonable distances, where the contribution of the cosmological constant be comparable at least with the second correction to the Schwarzschild effect, then the local effect of Λ will be analyzed by the SdS metric.

3.3 GR application and basic concepts in cosmology

3.3.1 Cosmic mass-energy budget and cosmic acceleration

Cosmic mass-energy budget

Conservation laws are among the important techniques used to derive dynamical equations in physics generally. This technique in GR is equivalent to the vanishing of covariant derivative of invariant tensors.

Consequently, an important dynamical equation that can determine the content and expansion rate of the universe will be derived from the conservation law of the energy-momentum tensor given by:

$$T^{\mu}_{\nu}\,;_{\,\mu} = 0 \tag{3.3.1}$$

Now, assuming the perfect fluid energy-momentum tensor given by eq. 3.1.31 and the FLRW metric given by eq. 3.2.22 in eq. 3.3.1 we obtain the fluid continuity equation

$$\dot{\rho} + 3\frac{\dot{a}}{a}(\rho + p) = 0 = \dot{\rho} + 3\frac{\dot{a}}{a}\rho(1 + w) \tag{3.3.2}$$

In the last step of eq. 3.3.2, w is defined as the fluid equation of state variable given by

$$p = w\rho \tag{3.3.3}$$

The general solution of eq. 3.3.2 is

$$\rho(t) = \rho^{o}\left(\frac{a_o}{a}\right)^{3(1+w)} \tag{3.3.4}$$

where the subscripts & superscripts denoted by o, are indicating that the parameters they stand for are being evaluated at t_o, and $a \equiv a(t)$.

Note that the total density $\rho(t)$ is the sum of all fluid contents of the universe contributions from matter, radiation, curvature, and other energy sources(often called dark energy)

including the cosmological constant.

So the total density of the universe is given by

$$\rho(t) = \sum_i \rho_i(t) \tag{3.3.5}$$

where the subscript $i \in \{m, r, k, de\}$ corresponding to matter, radiation, curvature & dark energy contributions respectively. So after all $\rho_m(t),\ \rho_r(t),\ \rho_k(t)$ & $\rho_{de}(t)$ are respectively defined as density of matter, radiation, curvature and dark energy (including the cosmological constant) respectively. The limiting cases are:

$$\begin{cases} w = 0, \text{ matter or “dust” EoS :} & \rho_m \propto a^{-3} \text{ ;} \\ w = \frac{1}{3}, \text{ radiation EoS :} & \rho_r \propto a^{-4} \text{ ;} \\ w < 0, \text{ quintessence - accelerated} & \\ w < -\frac{1}{3} : & \rho_{de} \propto a^{-3(1+w)} \text{ ;} \\ w = -1, \text{ Cosmological constant :} & \rho_{de} \equiv \rho_\Lambda = \frac{\Lambda}{8\pi G} \text{ ;} \\ w = -\frac{1}{3}, \text{ curvature EoS :} & \rho_k \propto a^{-2} \text{ .} \end{cases} \tag{3.3.6}$$

Eqs. 3.2.23, 3.3.4 & 3.3.5 are used to give

$$H^2 = \frac{8\pi G}{3}\rho(t) = \frac{8\pi G}{3}\sum_i \rho_i^o \left(\frac{a_0}{a}\right)^{3(1+w_i)} \tag{3.3.7}$$

In order to describe the energy budget of the universe, the simplest initial boundary conditions are to consider present measured observations. Thus, the reference density being evaluated today, often considered as the critical density ρ^o_{crit}. By eq. 3.3.7 this density is given by

$$\rho^o_{crit} = \frac{3H_o^2}{8\pi G} = \sum_i \rho_i^o \tag{3.3.8}$$

where the subscript & superscript represented by o are indicating present measurements.

Eq. 3.3.8 can be conveniently given by

$$1 = \Omega_o = \sum_i \Omega_i^o \tag{3.3.9}$$

where Ω is the density parameter defined as the ratio of the densities with respect to ρ^o_{crit}:

$$\Omega^o_i = \frac{\rho^o_i}{\rho^o_{crit}} \tag{3.3.10}$$

Now using eqs. 3.3.6, 3.3.7, 3.3.8 & 3.3.10 the general equation of Hubble parameter as a function of the expansion scale, the density parameters and the state parameters is give by

$$H^2(a;\Omega^o_i;w_i) = H^2_o \sum_i \Omega^o_i \left(\frac{a_0}{a}\right)^{3(1+w_i)} \tag{3.3.11}$$

where the curvature and the cosmological constant case density parameters are given by

$$\Omega^o_k = -\frac{k}{H^2_o a^2_o}; \quad w_{de} = -1 \Rightarrow \ \Omega^o_{de} \equiv \Omega^o_\Lambda = \frac{\Lambda}{3H^2_o} \tag{3.3.12}$$

Cosmic acceleration

The acceleration equation of the universe is described by the evolution of the scale factor with time given by the Friedmann eq. 3.2.25. This equation can be recast as

$$\frac{\ddot{a}}{a} = -\frac{4\pi G}{3}(3\tilde{p} + \tilde{\rho}) \tag{3.3.13}$$

where the density and pressure are redefined to contain the cosmological constant contribution in both forms as

$$\begin{aligned} \tilde{\rho} &= \rho + \rho_\Lambda \\ \tilde{p} &= p + p_\Lambda \\ \rho_\Lambda &= -p_\Lambda = \frac{\Lambda}{8\pi G} \end{aligned} \tag{3.3.14}$$

As we see eq. 3.3.13 is generally true including all forms of densities of the universe. Thus dropping the tildes and using eqs. 3.3.3 & 3.3.13 we obtain

$$\frac{\ddot{a}}{a} = -\frac{4\pi G}{3}\rho(t)\,(1+3w) \tag{3.3.15}$$

Upon using eqs. 3.3.7 & 3.3.11 in eq. 3.3.15, the acceleration equation will be expressed in more directly measurable parameters given as

$$\frac{\ddot{a}}{a} = -\frac{H_o^2}{2}\sum_i \Omega_i^o\,(1+3w_i)\left(\frac{a_0}{a}\right)^{3(1+w_i)} \tag{3.3.16}$$

Note that, eq. 3.3.15 can also be given in terms of the Newtonian acceleration as

$$\ddot{a} = -\frac{GM}{a^2}(1+3w) \tag{3.3.17}$$

where $M(t) = \frac{4\pi}{3}\rho(t)a^3(t)$.

Equation 3.3.17 looks like the classical equation of motion of a point particle moving on the surface of a sphere, where (in this case) the scale factor a is recognized as the radius of the sphere.

In general, the FLRW universe has the following three cases:

$$\begin{cases} \ddot{a} = 0 \Rightarrow w = -\frac{1}{3}, & \text{expanding universe at a constant rate whose age is equal to the Hubble time;} \\ \ddot{a} < 0 \Rightarrow w > -\frac{1}{3}, & \text{decelerated universe;} \\ \ddot{a} > 0 \Rightarrow w < -\frac{1}{3}, & \text{accelerated universe.} \end{cases} \tag{3.3.18}$$

The accelerated universe is dominated by negative pressure which causes the acceleration. The nature of this energy is yet undetermined, and so called dark energy. The particular case where $w = -1$ is equivalent to the cosmological constant energy content. Today, observations favor the dark energy in the form of cosmological constant.

For nearby objects the scale factor may be approximated by series expansion about the present time t_0 as

$$a(t) = a_o\left(1 + H_o(t-t_o) - \frac{q_o}{2}{H_o}^2(t-t_o)^2 + ...\right) \tag{3.3.19}$$

where the Hubble parameter H_o and the deceleration parameter q_o at t_o are respectively defined by

$$H_o = \frac{\dot{a}(t_o)}{a(t_o)};\ \ q_o = -\frac{a_o(t_o)\ddot{a}_o(t_o)}{\dot{a_o}^2(t_o)} = -\frac{1}{H_o^2}\frac{\ddot{a}_o(t_o)}{a_o(t_o)} \tag{3.3.20}$$

These present values of the Hubble parameter H_o and the deceleration parameter q_o are among the fundamental numerical constants that define observations in cosmology. Predominantly, in early developments of the modern standard cosmology these parameters were the major parameters used to constrain cosmological models.

Generally, the expansion scale factor $a(t)$ plays important roles in all cosmologies. It is used to derive and define key observational parameters and quantities that can explain the physical universe.

3.3.2 Cosmical redshift

Application of general relativity to cosmic observations is a subject of extracting information from the source to the observer. This information is primarily derived from the waves/particles that go out from the sources to the observers along their geodesies. Accordingly, for electromagnetic waves as the source of information propagating along radial direction, the photon null geodesy $ds^2 = 0$ is used. So, in this case eq. 3.2.22 yields

$$\frac{dt}{a(t)} = \pm\frac{dr}{\sqrt{1-kr^2}} \tag{3.3.21}$$

Moreover, if the propagation is considered along the radial coordinate where a photon in the position of $r = r_e$ at cosmic time, t_e, from the source propagates inward to reach an observer located at the origin r_o at the cosmic time t_o. In this approach r decreases as t

increases, so that the minus sign must be used in 3.3.21. Then, it is integrated to yield

$$\int_{t_e}^{t_o} \frac{dt}{a(t)} = \int_{r_o}^{r_e} \frac{dr}{\sqrt{1-kr^2}} = \begin{cases} \frac{\sin^{-1}\left(\sqrt{k}\, r_e\right) - \sin^{-1}\left(\sqrt{k}\, r_o\right)}{\sqrt{k}}, & k > 0; \\ r_e - r_o, & k = 0; \\ \frac{\sinh^{-1}\left(\sqrt{-k}\, r_e\right) - \sinh^{-1}\left(\sqrt{-k}\, r_o\right)}{\sqrt{-k}}, & k < 0. \end{cases} \tag{3.3.22}$$

Taking the origin at $r_o = 0$ and assuming the particular universes with curvatures $k = 1$, $k = 0$ & $k = -1$ eq. 3.3.22 is simplified to be given as

$$\int_{t_e}^{t_o} \frac{dt}{a(t)} = \int_{0}^{r_e} \frac{dr}{\sqrt{1-kr^2}} = \chi = \begin{cases} \sin^{-1}\left(r_e\right), & k = 1; \\ r_e, & k = 0; \\ \sinh^{-1}\left(r_e\right), & k = -1. \end{cases} \tag{3.3.23}$$

Consequently, eq. 3.3.23 is used to define an instantaneous radial comving distance given by

$$d(r_e; t) = a(t) \times r_e = a(t) \times \text{sinn}(\chi) \tag{3.3.24}$$

where $\text{sinn}(\chi)$ is defined as

$$\text{sinn}(\chi) = \begin{cases} \sin(\chi), & k > 0; \\ \chi, & k = 0; \\ \sinh(\chi), & k < 0. \end{cases} \tag{3.3.25}$$

Taking the differential of 3.3.23, and recalling that the radial coordinate r_e of co-moving sources is time-independent, we see that the interval δt_e between departure of subsequent light signals is related to the interval δt_o between arrivals of these light signals by (See for eg. [69])

$$\frac{\delta t_e}{a(t_e)} = \frac{\delta t_o}{a(t_o)} \tag{3.3.26}$$

The signal time intervals can be expressed in terms of their corresponding frequencies as:

$$\nu_o = \frac{1}{\delta t_o}; \;\; \nu_e = \frac{1}{\delta t_e} \tag{3.3.27}$$

For an increasing scale factor $a(t)$ with time,

$$\frac{a(t_o)}{a(t_e)} = \frac{\delta t_o}{\delta t_e} = \frac{\nu_e}{\nu_o} \geq 1 \tag{3.3.28}$$

so that the frequency received by the observer is smaller than the frequency emitted by the source as the two expand away from each other, a redshift to the observer.

Often the ratio of the excess frequency $\Delta\nu$ in ν_e with respect to the frequency received by the observer is defined as the redshift z given by

$$z = \frac{\Delta\nu}{\nu_o} \tag{3.3.29}$$

$$\frac{a(t_o)}{a(t)} = 1 + z \tag{3.3.30}$$

where $a(t)$ is the general scale factor at any emission time.

3.3.3 Cosmic distances

Distances are important in astronomy to calculate various parameters of astronomical objects including energy release, mass, physical size, age and other quantities. Distances are important in astronomy to calculate various parameters of astronomical objects including energy release, mass, physical size, age and other quantities. However, since the universe is expanding; measuring distances to distant objects like galaxies is not the same as measuring distances locally as in the Euclidean flat geometry. Therefore, it is important to describe distances both in comoving coordinates and static coordinates for genuine physical observations. So, here we derive some convenient operational cosmic distances used in cosmic observations.

a) The physical distance

The physical distance d_{phys}, also known as the proper distance, is the instantaneous co-moving distance defined along the radial direction of motion of the object. Actually, it was already derived in sec. 3.3.2 which is given by eq. 3.3.24 for universes with curvatures $k = 1$, $k = 0$ & $k = -1$. So for these universes at present $a(t) = a(t_o)$, the physical distance is given by

$$d_{phys} = a(t_o)\, r_e \tag{3.3.31}$$

b) The luminosity distance

The absolute luminosity (intrinsic luminosity) $\mathcal{L}$ of an object is the energy emitted per time by the source to the surrounding environment. While the apparent luminosity also called the apparent brightness or the energy flux $\mathcal{F}$ is the energy received per unit time per unit receiving area at the observer. Then, imagining the luminous object to be surrounded with a sphere whose radius is equal to the distance d_L between the luminous object and the observer, the apparent luminosity and the intrinsic luminosity are related by

$$\mathcal{F} = \frac{\mathcal{L}}{4\pi {d_L}^2} \tag{3.3.32}$$

The intrinsic luminosity at the source for n photons being emitted with frequency ν_e of each photon during an interval of time δt_e is given by

$$\mathcal{L} = n\frac{h\nu_e}{\delta t_e} \tag{3.3.33}$$

Using eqs. 3.3.28 & 3.3.29 in eq. 3.3.33 we obtain

$$\mathcal{L} = (1+z)^2\, n\frac{h\nu_o}{\delta t_o} = (1+z)^2\, \mathcal{L}_o \tag{3.3.34}$$

or

$$\mathcal{L}_o = \frac{\mathcal{L}}{(1+z)^2} \tag{3.3.35}$$

where $\mathcal{L}_o$ is considered to be the intrinsic luminosity at the observer.

Here the intrinsic luminosity is redshifted by $(1+z)^{-2}$ due to the expansion of the universe. On the other hand, the area of the physical sphere to which the photons being distributed during the expansion is equal to $4\pi d_{phys}^2$. Thus, the apparent luminosity is the ratio of the intrinsic luminosity at the observation to the physical sphere area to which the photons being distributed at the physical distance of the observer, which is given by

$$\mathcal{F} = \frac{\mathcal{L}_o}{4\pi d_{phys}^2} \tag{3.3.36}$$

Then, using eqs. 3.3.31, 3.3.34 & 3.3.36 the apparent luminosity is given by

$$\mathcal{F} = \frac{\mathcal{L}}{4\pi(1+z)^2\, a^2(t_o)\, r_e^2} \tag{3.3.37}$$

Finally, by eqs. 3.3.32 & 3.3.37 the luminosity distance is given by

$$d_L = (1+z)\, a(t_o)\, r_e = (1+z)\, d_{phys}; \quad \textbf{or} \quad d_{phys} = \frac{d_L}{1+z} \tag{3.3.38}$$

c) The angular diameter distance

If D is the physical extension of distant object, and θ is its angle subtended, then the angular diameter distance d_A is defined as usual in the Euclidean geometry given by

$$d_A = \frac{D}{\theta} \tag{3.3.39}$$

Conversely, if the object is imagined to be extended along the zenith, θ, coordinate over a physical sphere of radius equal to the angular distance d_A , then the differential of D defined at the emission time t_e is the line element given by eq. 3.2.22, where $dr = d\varphi = dt = 0$, so that

$$dD = a(t_e)\, r_e\, d\theta \tag{3.3.40}$$

Using eqs. 3.3.39 & 3.3.40 d_A is given as

$$d_A = a(t_e)\, r_e = \frac{a(t_e)}{a(t_o)}\, a(t_o)\, r_e \tag{3.3.41}$$

Finally, using eqs. 3.3.30, 3.3.38, & 3.3.41, the angular diameter distance is given by

$$d_A = \frac{d_{phys}}{1+z} = \frac{d_L}{(1+z)^2} \tag{3.3.42}$$

3.3.4 Expansion dynamics in terms of measurable parameters

So far, GR is used to develop theoretical models and equations of the expanding universe in a more general way. These theoretical models and equations must be expressed in terms of measurable parameters that can explain observable cosmic expansions. In standard cosmology, the universe content budget parameters (the Ω's), the Hubble parameter H_o and the cosmic acceleration parameter q_o are the major measurable parameters used to together with the cosmic redshift to calculate distances, ages, sizes and other cosmic observables. Here, some of these expansion observables be derived

Hubble and deceleration parameters

The Hubble parameter and deceleration parameter have long history in modern cosmological observations. They are continuing to serve as the main ingredients of measurable parameters to define observations.

a) The Hubble parameter

Using eqs. 3.3.11 & 3.3.30, the Hubble parameter in terms of the measurable quantities: the Hubble constant H_o, the redshift z, the density parameters Ω_i^o's and the equation of state parameter w_{de} is given as

$$H(z) = H_o E(z; \Omega_i^o; w_{de}) \tag{3.3.43}$$

where

$$E(z;\Omega_i^o;w_i) = \sqrt{\sum_i \Omega_i^o\,(1+z)^{3(1+w_i)}} \tag{3.3.44}$$

b) The deceleration parameter

In view of eq. 3.3.20, the deceleration parameter is given by

$$q = -\frac{1}{H^2}\frac{\ddot{a}}{a} \tag{3.3.45}$$

Using eqs. 3.3.11, 3.3.16 & 3.3.45 we get

$$q = \frac{\frac{1}{2}\sum_i \Omega_i^o\,(1+3w_i)\left(\frac{a_0}{a}\right)^{3(1+w_i)}}{\sum_i \Omega_i^o\,\left(\frac{a_0}{a}\right)^{3(1+w_i)}} \tag{3.3.46}$$

At present epoch: $a = a_0$ so that eq. 3.3.46 will be reduced to give the present deceleration

$$\begin{aligned} q_o &= \frac{1}{2}\sum_i \Omega_i^o\,(1+3w_i) \\ &= \frac{1}{2}(\Omega_m^o + 2\Omega_r^o + (1+3w_{de})\Omega_{de}^o) \end{aligned} \tag{3.3.47}$$

Ages

Using the Hubble parameter eq. 3.2.24 & the redshift eq. 3.3.30 we obtain

$$dt = \frac{-dz}{(1+z)H(z)} \tag{3.3.48}$$

Integrating this from the emission time to observation time we obtain

$$t_o - t_e = \frac{1}{H_o}\int_{t_e}^{t_o} \frac{dz}{(1+z)E(z';\Omega_i^o;w_{de})} \tag{3.3.49}$$

The time interval $t_o - t_e$ is called the lookback time used to measure ages during the interval between emission to observation events.

Distances

a) The physical distance

With the aid of eqs. 3.3.23, 3.3.24 & 3.3.31 the physical distance can be recast as

$$d_{phys} = a(t_o)r_e = a(t_o) \times \text{sinn}\left(\int_{t_e}^{t_o} \frac{dt}{a(t)}\right) \tag{3.3.50}$$

Eqs. 3.3.30, 3.3.48 & 3.3.44 are being used to recast eq. 3.3.50 as

$$d_{phys} = a(t_o)r(z) = \frac{H_o\, a(t_o)}{H_o}\text{sinn}\left[\int_o^z \frac{dz'}{H_o a(t_o) E(z'; \Omega_i^o; w_{de})}\right] \tag{3.3.51}$$

Finally, using eq. 3.3.12,where $H_o a(t_o) = \left(-\frac{k}{\Omega_k^o}\right)^{1/2}$, for all k the physical distance is given by

$$d_{phys} = \frac{1}{H_o\sqrt{\Omega_k^o}} \sinh\left[\sqrt{\Omega_k^o}\int_o^z \frac{dz'}{E(z'; \Omega_i^o; w_{de})}\right] \tag{3.3.52}$$

b) The Luminosity distance

Using eqs. 3.3.38 & 3.3.52, the luminosity distance is given by

$$d_L = \frac{1+z}{H_o\sqrt{\Omega_k^o}} \sinh\left[\sqrt{\Omega_k^o}\int_o^z \frac{dz'}{E(z'; \Omega_i^o; w_{de})}\right] \tag{3.3.53}$$

c) The angular distance

Using eqs. 3.3.42 & 3.3.52 or 3.3.53, the luminosity distance is given by

$$d_A = \frac{1}{(1+z)H_o\sqrt{\Omega_k^o}} \sinh\left[\sqrt{\Omega_k^o}\int_o^z \frac{dz'}{E(z'; \Omega_i^o; w_{de})}\right] \tag{3.3.54}$$

3.4 The flat ΛCDM model expansion dynamic equations

Since, in our work, we are going to apply the flat ΛCDM model in the large scale dynamics of the universe, so the general field equations developed in the previous sections are used

to derive simpler and reduced useful equations that consider the model .

Accordingly, a pressureless universe with zero curvature and dark energy content in the form of Λ is considered to derive the simpler and reduced equations.

Then, in the flat ΛCDM model the primary boundary equations are:

$$\begin{aligned} & k = 0 \Rightarrow \Omega_k = 0; \;\; w_{de} = -1 \Rightarrow \Omega_{de} = \Omega_\Lambda; \\ & w_m = 0 \Rightarrow \Omega_m = \Omega_m^o \left(\frac{a_o}{a}\right)^3; \;\; \rho_r \approx 0 \Rightarrow \Omega_r \approx 0. \end{aligned} \tag{3.4.1}$$

3.4.1 The scale factor, the Hubble and deceleration parameters

Using eqs. 3.3.11, 3.3.30 & 3.4.1 the Hubble parameter in terms of the scale factor and the redshift can be recast respectively as

$$H(a) = \frac{\dot{a}}{a} = H_o \sqrt{\Omega_\Lambda + \Omega_m^o \left(\frac{a_o}{a}\right)^3} \tag{3.4.2}$$

$$H(z) = H_o E(z; \Omega_i^o; w_{de}) = H_o \sqrt{\Omega_\Lambda + \Omega_m^o (1+z)^3}) \tag{3.4.3}$$

In order to obtain the scale factor $a(t)$, eq. 3.4.2 is used to establish the differential equation

$$\frac{da}{a\sqrt{1 + \left(\frac{\Omega_m^o}{\Omega_\Lambda} a_o^3\right) a^{-3}}} = \sqrt{\Omega_\Lambda} H_o \, dt \tag{3.4.4}$$

Eq. 3.4.4 is integrated to yield

$$a(t) = a(t_o) \left(\Omega_m^o / \Omega_\Lambda\right)^{1/3} \sinh^{2/3}\left(\frac{t_{_L}}{t_{_H}}\right) \tag{3.4.5}$$

where t_L and t_H are respectively defined as the lookback and the Hubble times given by

$$t_{_L} = t - t_e; \;\; t_{_H} = \frac{2}{3H_o\sqrt{\Omega_\Lambda}}. \tag{3.4.6}$$

Evaluating at $t = t_o$, the lookback time gives the age of the universe given by:

$$t_{univ} = \frac{2}{3H_0\sqrt{\Omega_\Lambda}} \sinh^{-1}\sqrt{\frac{\Omega_\Lambda}{\Omega_m^o}} \tag{3.4.7}$$

$$\begin{cases} \text{matter dominated universe}, & \frac{t_L}{t_H} \ll 1, \text{ then series expansion of eq. 3.4.5} \\ & \Rightarrow \sinh^{2/3}\left(\frac{t_L}{t_H}\right) \simeq \left(\frac{t_L}{t_H}\right)^3 + ... \\ & \Rightarrow a(t) \propto t^{2/3}\ ; \\ \Lambda \text{ dominated universe}, & \frac{t_L}{t_H} \gg 1 \\ & \Rightarrow \sinh^{2/3}\left(\frac{2t_L}{3t_H}\right) \simeq e^{\left(\frac{t_L}{t_H}\right)} \\ & \Rightarrow a(t) \propto e^{(H_o\sqrt{\Omega_\Lambda}\, t)} \end{cases} \tag{3.4.8}$$

The deceleration eq. 3.3.46 for the flat ΛCDM model with pressureless fluid is reduced to be given as

$$q = \frac{\frac{\Omega_m^o}{2}\left(\frac{a_0}{a}\right)^3 - \Omega_\Lambda}{\Omega_m^o\left(\frac{a_0}{a}\right)^3 + \Omega_\Lambda} = \frac{\frac{\Omega_m^o}{2}(1+z)^3 - \Omega_\Lambda}{\Omega_m^o(1+z)^3 + \Omega_\Lambda} \tag{3.4.9}$$

The condition where the universe goes from deceleration phase to the acceleration phase is acquired at $q = 0$ given as

$$a = a_o\left(\frac{\Omega_m^o}{2\Omega_\Lambda}\right)^{1/3} \tag{3.4.10}$$

In terms of the redshift, this transition phase is acquired at

$$z = \left(\frac{2\Omega_\Lambda}{\Omega_m^o}\right)^{1/3} - 1; \quad \Omega_\Lambda + \Omega_m^o = 1. \tag{3.4.11}$$

Since for source recession, the redshift is always greater than or equal to zero, then by eq. 3.4.11 Ω_m^o is limited by 2/3 as its upper boundary value.

Finally, using equation 3.4.9 the deceleration parameter at the present is given by

$$q_o = \frac{\Omega_m^o}{2} - \Omega_\Lambda \tag{3.4.12}$$

3.4.2 Distances and age

a) Distances

Notice that for the flat universe case, $k = 0$. Then using eq. 3.3.51 & 3.4.3 the physical distance is given by

$$d_{phys} = \frac{1}{H_0}\int_0^z \frac{dz}{\sqrt{\Omega_\Lambda^o + \Omega_m^o(1+z)^3}} \tag{3.4.13}$$

And the other distances by eqs. 3.3.38 & 3.3.42 immediately follow to be given by

$$d_L = (1+z)d_{phys} = \frac{1+z}{H_0}\int_0^z \frac{dz}{\sqrt{\Omega_\Lambda + \Omega_m^o(1+z)^3}} \tag{3.4.14}$$

$$d_A = \frac{d_{phys}}{1+z} = \frac{1}{H_0(1+z)}\int_0^z \frac{dz}{\sqrt{\Omega_\Lambda + \Omega_m^o(1+z)^3}} \tag{3.4.15}$$

b) Age

Using eqs. 3.3.49 & 3.4.3 age in terms of the lookback time is given by

$$t_{_L} = t_o - t_e = \frac{1}{H_o}\int_0^z \frac{dz'}{(1+z')\sqrt{\Omega_\Lambda + \Omega_m^o(1+z')^3}} \tag{3.4.16}$$

Eq. 3.4.16 is integrated to be given by

$$t_o - t_e = \frac{2}{3H_o\sqrt{\Omega_\Lambda}} \ln\left[\frac{(z+1)^{3/2}\left(1+\frac{1}{\sqrt{\Omega_\Lambda}}\right)}{1+\sqrt{1+\left(\frac{\Omega_m^o}{\Omega_\Lambda}\right)(z+1)^3}}\right] \tag{3.4.17}$$

The age of the universe is determined at very large redshift where z » 1. So eq. 3.4.17 will be used by the limiting case $z \to \infty$ to give

$$t_{univ}^o = \frac{2}{3H_o\sqrt{\Omega_\Lambda}} \ln\left[\frac{1+\sqrt{\Omega_\Lambda}}{\sqrt{\Omega_m^o}}\right] \tag{3.4.18}$$

For matter or Λ - dominated cases, the present age of these liming universes by eq. 3.4.7 are respectively given by:

$$\begin{cases} \text{matter dominated universe}, & t_{univ}^o = \frac{2}{3H_o}\left(1 - \frac{1}{(z_{univ}^o+1)^{3/2}}\right) \le \frac{2}{3H_o}; \\ \Lambda \text{ dominated universe}, & t_{univ}^o = \frac{1}{H_o}\ln(z_{univ}^o + 1) \end{cases} \tag{3.4.19}$$

For the matter dominated universe with the favored Hubble constant$H_0 \in [55, 75]$ km/s Mpc^{-1}, the maximum age of the present universe by eq. 3.4.19 is ~ 10 Gyr which is too small to fit present observations reporting ~ 14 Gyr. On the other hand, the Λ dominated universe to meet this age needs to be at redshift $z^o_{univ} \sim 2$ for the Big-bang observation which is even too small to meet the age of fainter galaxies observed with higher redshifts.

Consequently, in order to describe present observations the universe would exist in the form of different fluid admixtures. So in the simplest standard flat ΛCDM model both matter and Λ components expected to coexist in dynamism where observable parameters are used to measure them. The particular case of present age of the universe estimated to be 13.82Gyr is used to generate some fitting theoretical data for the present Hubble constant H_0, the matter and Λ density parameters is shown as in table 1 in the expected range of H_0. For the most likely measured value of $H_0 = 70$ the theoretical best fitting is corresponding to $\Omega_m = 0.27$ & $\Omega_\Lambda = 0.73$ that accurately in agreement with observations so far made. Whereas, in the general case, the contours in fig.3.1 indicate the possible present theoretical age of the universe in terms of the three parameters to be constrained by observations. As can be inferred from the general appearance of the contours relatively higher H_0's assume lower ages with more matter domination while lower H_0's assume higher ages with more Λ domination.

Table 3.1: ΛCDM model theoretical fitting data corresponding toH_0 & the density parameters Ω_m & Ω_Λ to the present age of the universe estimated to 13.82Gyr as of current observations.

H_0	55	56	57	58	59	60	61	62	63	64	65
Ω_m	0.62	0.59	0.55	0.52	0.49	0.47	0.44	0.42	0.40	0.38	0.36
Ω_Λ	0.38	0.41	0.45	0.48	0.51	0.53	0.56	0.58	0.60	0.62	0.64
H_0	66	67	68	69	70	71	72	73	74	75	
Ω_m	0.34	0.32	0.30	0.29	0.27	0.26	0.25	0.23	0.22	0.21	
Ω_Λ	0.66	0.68	0.70	0.71	0.73	0.74	0.75	0.77	0.78	0.79	

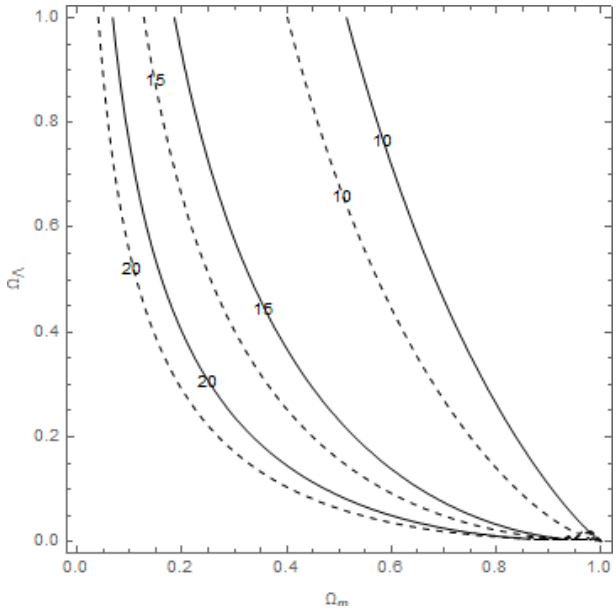

Figure 3.1: Present age of the universe in billion years where the solid & dashed contours are respectively corresponding to $H_0 = 67$ & $75\ km/s\, Mpc^{-1}$.

Part II

Motion in SdS, precession of orbits, light bending and radiation

Chapter 4

Motion of particles in SdS Geometry

4.1 The general equation of motion and horizon solutions

In this section, we derive the general conserved equations of motion in SdS geometry where the resulting equation is being used to further derive the event horizon solutions in the geometry. Then using the results, we discuss on the boundary conditions where the SdS metric be applied.

4.1.1 The general equation of motion

The equations of motion can be derived from the particle motion provided as in ch.3, eq. 3.1.7, recalled to be given as

$$\frac{d^2x^\mu}{d\rho^2} + \Gamma^\mu_{\nu\lambda}\frac{dx^\nu}{d\rho}\frac{dx^\lambda}{d\rho} = 0. \tag{4.1.1}$$

Where ρ is a parameter describing the trajectory in which the proper time $d\tau$ is generally expected to be proportional to it. Furthermore, for a material particle we could normalize ρ so that $\rho = \tau$.

In order to integrate these equation of motion, we use the non-vanishing components of the affine connection as in equation 3.1.13 and consider the orbit of particles confined to an

equatorial plane, i.e., $\theta = \frac{\pi}{2}$ so that we omit equations involving the zenith angle θ. Then the radial, azimuthal and time components of equation 4.1.1 are respectively given by

$$\frac{d^2r}{d\rho^2} + \frac{A'}{2A}\left(\frac{dr}{d\rho}\right)^2 - \frac{r}{A}\left(\frac{d\phi}{d\rho}\right)^2 + \frac{B'}{2A}\left(\frac{dt}{d\rho}\right)^2 = 0, \tag{4.1.2}$$

$$\frac{d^2\phi}{d\rho^2} + \frac{2}{r}\frac{d\phi}{d\rho}\frac{dr}{d\rho} = 0, \tag{4.1.3}$$

$$\frac{d^2t}{d\rho^2} + \frac{B'}{B}\frac{dt}{d\rho}\frac{dr}{d\rho} = 0. \tag{4.1.4}$$

The 'prime' on A and B shows derivative with respect to r.

Equation 4.1.3 is integrated to give one constant of motion

$$r^2\frac{d\phi}{d\rho} = J, \tag{4.1.5}$$

where J plays the role of angular momentum per unit mass per unit time.

The integral of equation 4.1.4 gives another constant of motion $\mathcal{E}$, which is a form of energy given as

$$\frac{dt}{d\rho} = \frac{\mathcal{E}}{B}. \tag{4.1.6}$$

Now using equations 4.1.5 & 4.1.6, equation 4.1.2 can be recast as:

$$\frac{d^2r}{d\rho^2} + \frac{A'}{2A}\left(\frac{dr}{d\rho}\right)^2 - \frac{J^2}{Ar^3} + \frac{B'}{2A}\frac{\mathcal{E}^2}{B^2} = 0. \tag{4.1.7}$$

Multiplying equation 4.1.7 by $2A$ and involving little algebra we obtain

$$\frac{d}{d\rho}\left[A\left(\frac{dr}{d\rho}\right)^2 + \left(\frac{J^2}{r^2} - \frac{\mathcal{E}^2}{B}\right)\right] = 0. \tag{4.1.8}$$

The integral of eq, 4.1.8 gives another constant of motion ϵ given as:

$$A\left(\frac{dr}{d\rho}\right)^2 + \frac{J^2}{r^2} - \frac{\mathcal{E}^2}{B} = -\epsilon. \tag{4.1.9}$$

Using the conservation of the four vector energy momentum one can easily verify that ϵ is equal to 1 for massive particles, and is equal to 0 for massless particles.

Using the relations $A = B^{-1}$, equation 4.1.9 can be recast as:

$$\mathcal{E}^2 = \left(\frac{dr}{d\rho}\right)^2 + \left(\epsilon + \frac{J^2}{r^2}\right) B, \tag{4.1.10}$$

$$B(r) = 1 - \frac{r_g}{r} - \frac{r^2}{\ell^2}, \tag{4.1.11}$$

where $r_g = 2GM$ is the Schwarzschild radius and $\ell = \sqrt{3/\Lambda}$ is the cosmological length.

Since $\mathcal{E}$ plays the role of the total energy per unit mass, consequently the first term on the right hand side of eq. 4.1.10 plays the role of the effective kinetic energy per unit mass, while the second term expression plays the role of the effective potential per unit mass. Then, in Schwarzschild - de Sitter spacetime the effective potential is defined as,

$$V_{_{eff}}(r) = \sqrt{\left(\epsilon + \frac{J^2}{r^2}\right) B(r)}\,. \tag{4.1.12}$$

Now introducing the value of ϵ for massive particles $\epsilon = 1$ and for massless particles $\epsilon = 0$, the effective potential is

$$\begin{cases} V_{_{eff}}(r) = \sqrt{\left(1 + \frac{J^2}{r^2}\right) B(r)}, & \epsilon = 1; \\ V_{_{eff}}(r) = \frac{J}{r}\sqrt{B(r)}, & \epsilon = 0. \end{cases} \tag{4.1.13}$$

It is advantageous to represent the potential in terms of dimensionless parameters defined as:

$$\alpha = \frac{J}{r_g};\ \ \beta = \frac{r_g}{\ell};\ \ x = \frac{r}{\ell}, \tag{4.1.14}$$

so that eq. the effective potential in terms of these parameters be given as

$$\begin{cases} V_{_{eff}}(x) = \sqrt{\left(1 + \frac{\alpha^2}{x^2}\right) B(x)}, & \epsilon = 1; \\ V_{_{eff}}(x) = \frac{\alpha\beta}{x}\sqrt{B(x)}, & \epsilon = 0. \end{cases} \tag{4.1.15}$$

Where,

$$B(x) = 1 - \frac{\beta}{x} - x^2. \tag{4.1.16}$$

4.1.2 SdS horizon and its region of application

The location of event horizons is given by the condition $B(x) = 0$, corresponding to

$$1 - \frac{\beta}{x} - x^2 = 0. \tag{4.1.17}$$

Eq. 4.1.17 is expect to provide three possible solutions for x, real or complex. However, being constrained by the beta parameter, only two physically meaningful positive real solutions are allowed. In view of eq. 4.1.17, the beta parameter constraining equation will be given by:

$$\beta(x) = x(1 - x^2). \tag{4.1.18}$$

For physical black holes the parameter β takes values ranging from 0 (at $x = 0$ or at $x = 1$) to $\beta_{max} = 2\sqrt{3}/9$ (at $x = \sqrt{3}/3$). This condition imposes on the solutions of the event horizon that there exist two distinct solutions between $x = 0$ and $x = 1$ corresponding to a single β except for the β_{max}, where the two degenerate to a single solution. The solutions are:

$$x_h = \frac{2}{\sqrt{3}} \sin\left(\frac{1}{3}\arcsin\Big(\frac{3\sqrt{3}}{2}\beta\Big)\right), \tag{4.1.19}$$

$$x_c = \frac{2}{\sqrt{3}} \cos\left(\frac{1}{3}\arccos\Big(-\frac{3\sqrt{3}}{2}\beta\Big)\right). \tag{4.1.20}$$

Here we notice that a Schwarzschild de Sitter black hole is characterized by two horizons, the black hole horizon x_h and the cosmological horizon x_c (See Fig. 4.1.2), where $x_h \leq x_c$. On the other hand, in the case of Schwarzschild spacetime, only the black hole horizon solution exists.

At the maximum value of β the black hole and the cosmological horizons coincide at $x_h = x_c = \frac{\sqrt{3}}{3}$. This point also predicts the maximum limiting mass of black holes, the

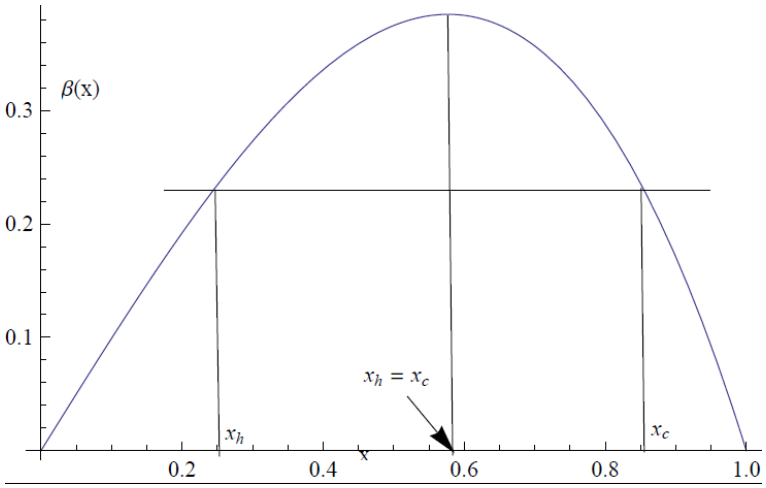

Figure 4.1: Graphical representation of the event horizons around SdS black hole. The intersections of the horizontal line determine the two horizons.

critical black hole to be $c^2/(3G\Lambda^{1/2})$. Conversely, this limiting condition will also impose observational constraints on the value of the cosmological constant if such black holes are observationally detectable. For example, if a giant galaxy of the order of $M = 10^{15}M_{\odot}$ is collapsed to form the critical black hole, the cosmological constant is considered to have value of $\sim 10^{-27}m^{-2}$. In case, if all the galaxies in our universe with such mean mass are merged to form a single black hole, where the mass of the ordinary matter of the universe is $\sim 10^{53}km$ (as of [40] data), then $\Lambda \sim 10^{-53}m^{-2}$. This particular case seems likely to fit the present observational value of the cosmological constant. Accordingly, the critical black hole is just an equivalent of the big-bang if the whole universe will be considered to collapse again. Subsequently, it is impossible to find any critical black hole in the universe to observe today.

Irrespective of the constraints on the exact value of the cosmological constant or else, the horizon solution extends in the region between $x = 0$ to $x = 1$, respectively corresponding to $r_h = r_g$ and $r_c = \ell$. In fact, a light star whose gravitational radius is less than

the surface radius r_s of the star cannot have the horizon $r_h = r_g$. In the rest of the cases, that is, for $r_g \geq r_s$ the two horizons exist where the horizons get very much closer to each other for black holes of mass near the critical black hole. On the other hand, the horizons are separated by $\ell - r_g$ for stars whose gravitational radii are approximately equal to their surface radii.

Where does the SdS metric be effective?

The region around where the gravitational attraction and the cosmological repulse in balance will be reasonably described by the SdS metric. By eq. 4.1.17 the balance occurs at

$$x_b = \beta^{1/3} \quad or \quad r_b = (\ell^2 r_g)^{1/3}. \tag{4.1.21}$$

In general the SdS metric is effective in the region from x_b to x_{out} outwards away from the hole; and x_b to x_{in} towards the hole to the extent of accuracy required by observation. Actually, in view of eqs. 4.1.19 & 4.1.20 the near field may also consider further closer regions to the hole as far as x_s (at the surface of the star) beyond the defined limits depending on the value of the angular momentum J.

4.2 Planetary motion and orbit solutions

4.2.1 General characteristics of the orbit

In this subsection, we examine the general characteristics of the SdS potential for both massive and massless particles in some general cases.

Case 1: The free fall case, $J = 0$.

In this case, the effective potential given by eq. 4.1.15 is reduced to

$$\begin{aligned} V(x) &= \sqrt{1 - \frac{\beta}{x} - x^2};\ \epsilon = 1, \\ V(x) &= 0\ ;\ \epsilon = 0 \end{aligned} \tag{4.2.1}$$

for massive and massless particles respectively.

From the reduced potential, we see that there is no effective potential on the massless particles. There is no difference between the Newtonian motion and the general relativistic cases. So a particle being in fall towards the potential source continuous to fall into it.

However, in the case of massive particles there are important characteristic features with significant differences and similarities among the three potentials corresponding to the Newtonian, Sch and SdS geometries.

The general qualitative behavior of the SdS potential (See Fig. 4.2) is characterized by developing a centrifugal barrier starting from $x = \left(\frac{\beta}{2}\right)^{1/3}$ outwards, away from the black hole. However, the potential turns out to be attractive from this point inwards in a similar fashion as that of the classical Schwarzschild potential does. Interestingly, this turning point nearly coincides with the balance point where the gravitational attraction and the cosmological repulse cancel each other, as discussed in subsection 4.1.1. Thus, there are

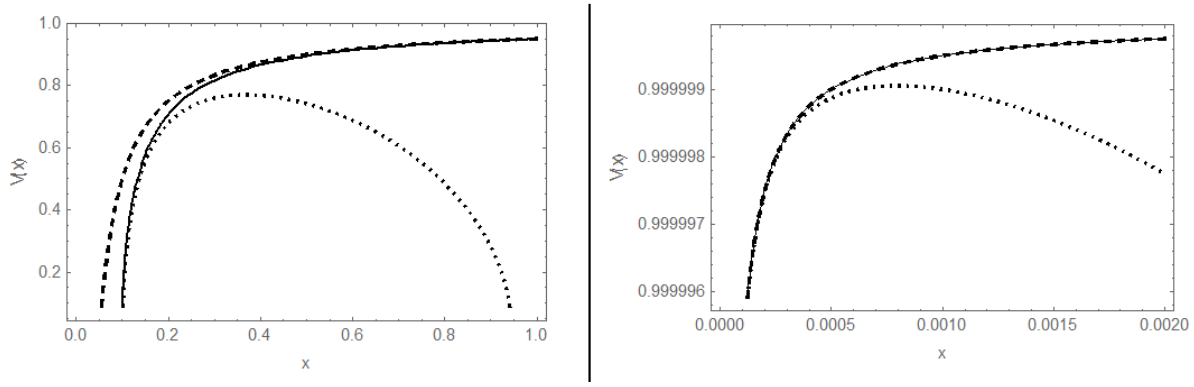

Figure 4.2: The free fall potential of a massive particle: The dashed, solid & dotted curves representing the Newtonian, Schwarzschild & SdS potentials respectively where $\beta = 0.1$ for the left panel while $\beta = 10^{-9}$ for the right panel.

basic differences between the SdS and that of the classical Schwarzschild potentials where the latter is ever attractive.

Case 2: Particle with sufficient angular momentum, $J \neq 0$

I. Massless Particles

Upon exploiting eq. 4.1.15, we observe that in wider range of the SdS horizon region, the potential is generally characterized by repulsion, towards the cosmological horizon. But, near the black hole horizon over a small region around $\chi = \frac{3}{2}\beta$ (where it attains the maximum potential, $V_{max} = \frac{2\sqrt{3}}{9}\alpha\sqrt{1 - 27\beta^2/4}$) the potential turns out to be attractive.

The plots of the potential (See Fig. 4.3) indicate that the orbits of motion of particles in the SdS potential are generally unbounded. These unbound orbits can be classified to three groups described as:

a) An ongoing particle with insufficient total energy, E, less than the maximum barrier potential (see the plots), upon colliding with the potential bounces back and will never return back to the potential source.

b) An ongoing particle with sufficient energy, E, greater than the barrier potential jumps into the massive object is trapped and never escape away.

c) An ongoing particle with energy, E, equal to the barrier potential will undergo an unstable circular orbit with probabilistic final destiny (being trapped or run away).

Moreover, there is no significant difference between the SdS and the Sch potentials near the black hole horizon. But, both deviate significantly from the Newtonian potential in this near zone. However, the SdS potential widely deviates from the Sch potential at far away from the black hole horizon where the Sch potential goes to that of the classical Newtonian potential.

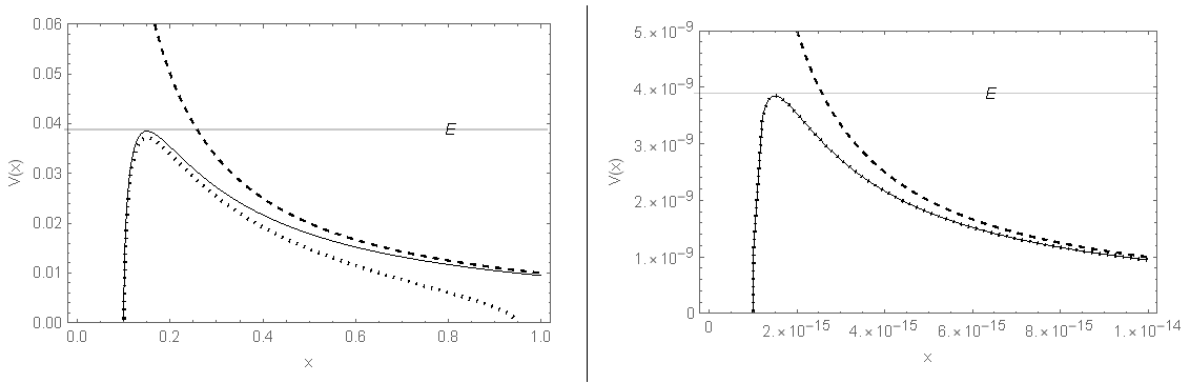

Figure 4.3: Potentials of massive black holes in the vicinity of massless particles with sufficient angular momentum. Left panel: $\alpha = 0.1$ and $\beta = 0.1$. Right panel: $\alpha = 10^{-8}$ and $\beta = 10^{-15}$. The dashed, solid & dotted curves representing the Newtonian, Schwarzschild & SdS potentials respectively.

II. Massive particles

Fig. 4.4 is the plot of the potential for supermassive black hole in the vicinity of motion of a massive particle possessing sufficient angular momentum. The considered black hole is

extremely massive but much less than the critical black hole. Hypothetically, it is supposed to represent the general characteristics of the SdS potential for all massive compact system. The details of the orbit solutions and their implications are addressed in the forthcoming section 4.2.2.

As we learn from the plot, the general potentials in the SdS region of application significantly differ among the Newtonian, Schwarzschild (Sch) and SdS geometries. In the case of the SdS, the general potential is characterized by three turning points where the particles velocities vanish, as usual. These turning points are attained either at locally minimum or maximum value of the potential.

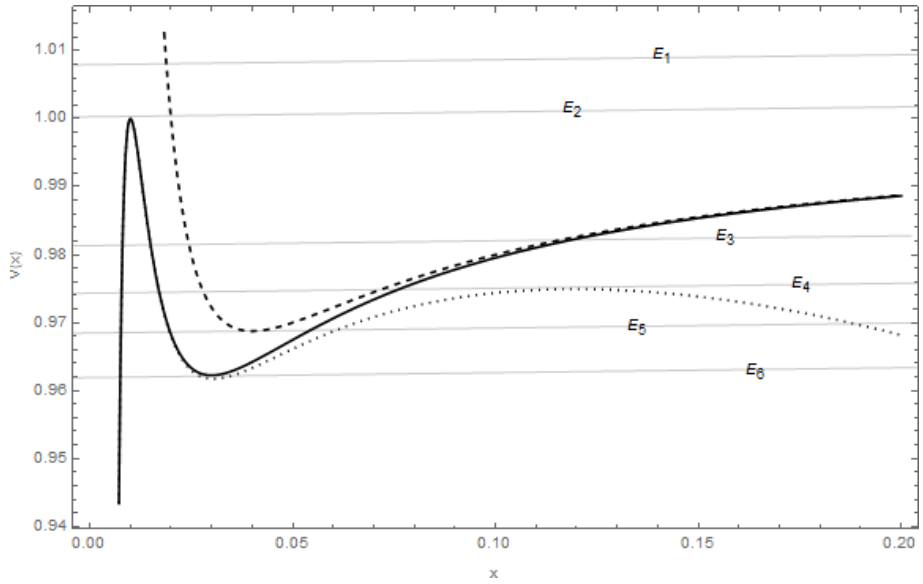

Figure 4.4: Potential of a massive black hole with $\beta = 10^{-3}$ in the vicinity of a particle with sufficient angular momentum, $\alpha = 2$. Dashed, solid & dotted curves respectively representing the Newtonian, Sch and SdS potentials.

Generally, the orbits are characterized as follows;

a) Bound orbits: An ongoing particle with energy, E, less than the potential well barrier surrounding the local minimum point of the potential exhibits a bound orbit. Thus,

in the SdS geometry ongoing particles with energy like E_5 & E_6 trapped by the potential well undergo bound orbits and never escape the barrier. Furthermore, the orbits of particles with E_5 are generally elliptical classes. While the special case of particles with E_6 are characterized by circular orbits. Note also that, all bound orbits in SdS potential are also bound in Sch potential. However, the orbits differ in their ellipticities where the SdS case posses relatively higher ellipticity.

b) Unbound orbits: An ongoing particle with sufficient energy, E, greater than the barrier potential well but less than the maximum potential energy like E_3 upon colliding with the potential bounces back and will never return back to the potential source. However, these same classes of particles, under the Sch and as well as Newtonian potentials will undergo bound orbits where the Sch case possesses relatively higher ellipticity. On the other hand, ongoing particles with energy, E, greater than the maximum potential energy of the SdS (which is also approximately equal to the Sch) like E_1 jump into the massive object are trapped and never escape away.

c) Unstable circular orbits: An ongoing particle with energy, E_2, equal to the maximum barrier potential will undergo an unstable circular orbit with probabilistic final destiny (being trapped or run away) both in SdS & Sch cases. Also ongoing particles with E_4 equal to the local maxima of the SdS potential will undergo an unstable circular orbit in the SdS geometry while the particles will undergo bound elliptical orbits in the Newtonian and Sch cases.

4.2.2 Orbit analytical solutions

In the previous subsection mainly the plots of the general equation of motion were used to describe the general characteristics of orbits in the SdS potential. In this section we

derive the analytical solutions of the orbits and discuss their implications in relation to the exploited plots in earlier section.

At the turning points, where the particles velocities vanish, the potential locally attains either its minimum or maximum values. The minima locations grant the presence of bound orbits depending on the potential developed around it and the magnitude of the energy of the particles passing through it. The locations of the exterima are determined by the condition,

$$\frac{dV(x)}{dx} = 0. \tag{4.2.2}$$

Using eqs. 4.1.15 & 4.2.2 we get a principal quintic radial equation given by;

$$x^2 - 2\beta\alpha^2 x + 3\alpha^2\beta^2 - \frac{2}{\beta}x^5 = 0. \tag{4.2.3}$$

By re-scaling this equation through the transformations:

$$\begin{aligned} x &= -\frac{3\beta}{2}y\ , \\ A &= \frac{3}{4\alpha^2}\ , \\ B &= \frac{81\beta^2}{16\alpha^2}\ , \end{aligned} \tag{4.2.4}$$

we obtain the principal quintic equation

$$By^5 + Ay^2 + y + 1 = 0. \tag{4.2.5}$$

One of the roots of this principal quintic equation, say y_1, is given as a series expansion:

$$y_1 = -\sum_{j,k\geqslant 0}(-1)^k \frac{(2j+5k)!}{j!k!(j+4k+1)!}A^j B^k. \tag{4.2.6}$$

Where the domain of convergence of this series is given by the condition:

$$3125|B|^2 - 256|B| + 108|A|^5 - 27|A|^4 + 1600|A||B| - 2250|A|^2|B| < 0. \tag{4.2.7}$$

By re-expressing B in terms of the parameters A and β, eq. 4.2.7 can be recast as

$$27A^3(-1+4A) - \frac{27}{16}\beta^2\left(1024 - 6400A + 9000A^2 - 84375A\beta^2\right) < 0. \tag{4.2.8}$$

This condition is readily satisfied for all practical black holes with $A < 1/4$. This condition in the case of Schwarzschild black holes leads to elliptical bound orbits. However, for theoretically giant black holes comparable to the critical black holes, the upper bound value of $A \lessapprox 0.0556557$ is required to fulfil the condition.

The other four roots of the principal quintic, different from y_1 can be obtained by constructing a quartic equation using Viete's relations. Accordingly, we construct this quartic equation of the following form:

$$y^4 - y_1 y^3 + y_1^2 y^2 + \left(A/B + y_1^3\right) y + \left(1/B + A/B\, y_1 + y_1^4\right) = 0. \tag{4.2.9}$$

The method of radicals is used to obtain algebraic expressions of the solutions of Eq. 4.2.9 in terms of the set of parameters used. The obtained expressions possess very large and complex terms. However, compact form expressions can be provided by defining U, V and W as:

$$\begin{aligned} U &= \frac{2^{1/3}}{81\beta^2}\left(32\alpha^2 + 60y_1 + 567\beta^2 y_1^4\right), \\ V &= \frac{16}{27\beta^4} - \frac{y_1^2}{9\beta^2}\left(80\alpha^2 - 24y_1 + 63\beta^2 y_1^4\right), \\ W &= \left(V + \sqrt{V^2 - 4U^3}\right)^{1/3}. \end{aligned} \tag{4.2.10}$$

Then the other four remaining solutions of y, generally complex conjugates, are given by:

$$y_{2,3} = \frac{y_1}{4} - Q \pm D_+, \tag{4.2.11}$$

$$y_{4,5} = \frac{y_1}{4} + Q \pm D_-. \tag{4.2.12}$$

Where Q and $D_{\pm}$ are given by:

$$\begin{aligned} Q &= \frac{1}{2}\sqrt{-\frac{5}{12}y_1^2 + \frac{\sqrt[3]{2}U}{3W} + \frac{W}{3\sqrt[3]{2}}}, \\ D_{\pm} &= \frac{1}{2}\sqrt{-\left(\frac{5}{4}y_1^2 + 4Q^2\right) \pm \frac{32/(27\beta^2) + 11y_1^3}{8Q}}. \end{aligned} \tag{4.2.13}$$

Among the four roots of y obtained by eqs. 4.2.11 & 4.2.12, only two real roots are allowed for real Q associated with the D_+ case, otherwise all the roots be complex. In fact, Q is real as can be determined by the limiting value of β and physical considerations embedded in α. The real roots condition associated with D_+ by eq. 4.2.13 is given by:

$$-\left(\frac{5}{4}y_1^2 + 4Q^2\right) + \frac{32/(27\beta^2) + 11y_1^3}{8Q} \geqslant 0. \tag{4.2.14}$$

The three real roots, if they exist, will locate the extrema of the potential. The local minimum value of the potential corresponds to stable circular orbit; while the maxima values correspond to unstable circular orbits. As can be observed from the plots of the potential, Fig. 4.4, if $D_+ \neq 0$, unlike the Schwarzschild solution(characterized by a single unstable circular orbit) the SdS solution is characterized by two unstable circular orbits. Since β is remarkably very small, Taylor expansion can be used to obtain simple but significantly precise expressions of Q and D_+ given as:

$$Q = \frac{1}{6}\left(\frac{2}{\beta}\right)^{2/3} + \frac{(16\alpha^2 + 15y_1)}{36} - \frac{64}{243}(2^{2/3}\alpha^6\beta^{4/3}), \tag{4.2.15}$$

$$D_+ = \frac{1}{2}\left(\frac{2}{\beta}\right)^{2/3} - 2Q. \tag{4.2.16}$$

Then, the real roots of y corresponding to D_+ by equations 4.2.11, 4.2.15 and 4.2.16 are given by

$$y_2 = -\left(y_1 + \frac{4\alpha^2}{3}\right) + \frac{64}{81}(2^{2/3}\alpha^6\beta^{4/3}), \tag{4.2.17}$$

$$y_3 = \frac{1}{3}(y_1 - y_2) - \frac{1}{3}\left(\frac{2}{\beta}\right)^{2/3}. \tag{4.2.18}$$

The smallest stable circular orbit corresponding to one of the inflection points is obtained when y_1 and y_2 coincide. Using eqs. 4.2.6 and 4.2.17, and then restoring the original parameters back through the transformation eqs. 4.1.14 & 4.2.4 we obtain:

$$r = \frac{J^2}{r_g} - \frac{16}{27}\left(\frac{2\Lambda}{3r_g}\right)^{2/3}\frac{J^6}{r_g^3}. \tag{4.2.19}$$

The first term, J^2/r_g, of eq. 4.2.19 is the familiar circular radius solution of the Schwarzschild orbit. So the radial orbit shift in stable circular orbits due to the cosmological constant is

$$\triangle r = -\frac{16}{27}\left(\frac{2\Lambda}{3r_g}\right)^{2/3}\frac{J^6}{r_g^3}. \tag{4.2.20}$$

Another possible circular bound orbit will be obtained by the condition $D_+ = 0$, where by equation 4.2.11 y_2 and y_3 coincide. For this particular case, the relation in equation 4.2.14 can be used to construct a standard cubic equation for Q whose solution is given by a single real root,

$$Q = \frac{1}{2}\sqrt{\frac{5}{3}}|y_1|\sinh\left[\frac{1}{3}\sinh^{-1}\left\{\sqrt{\frac{3}{5}}\frac{1}{|y_1|^3}\left(\frac{32}{27\beta^2} + 11y_1^3\right)\right\}\right]. \tag{4.2.21}$$

The case where β is very small (generally true excepting the critical black hole cases) considerably requires large value of α so that equation 4.2.17 can be given by

$$\alpha \approxeq \frac{\sqrt{3}}{4}\left(\frac{2}{\beta}\right)^{1/3}. \tag{4.2.22}$$

Now using eqs. 4.2.11 & 4.2.22, the double roots y_2 and y_3 of this circular orbit is given by

$$y_2 = y_3 = \frac{y_1}{4} - \frac{1}{2}\sqrt{\frac{5}{3}}|y_1| \sinh\left[\frac{1}{3}\sinh^{-1}\left\{\sqrt{\frac{3}{5}}\frac{1}{|y_1|^3}\left(\frac{32}{27\beta^2}\right)\right\}\right]. \tag{4.2.23}$$

In the general case, the physical roots of the extrema of the potential in terms of the parameter x, upon using the transformation equation 4.2.4 in eqs. 4.2.6, 4.2.17 & 4.2.18 are given by:

$$x_1 = \frac{3\beta}{2}\sum_{j,k\geqslant 0}(-1)^k \frac{(2j+5k)!}{j!k!(j+4k+1)!}\left(\frac{3}{4\alpha^2}\right)^{j+k}\left(\frac{3\sqrt{3}}{2}\beta\right)^{2k}, \tag{4.2.24}$$

$$x_2 = 2\alpha^2\beta - x_1 - \frac{32}{27}(2^{2/3}\alpha^6\beta^{7/3}), \tag{4.2.25}$$

$$x_3 = \left(\frac{\beta}{2}\right)^{1/3} + \frac{1}{3}(x_1 - x_2). \tag{4.2.26}$$

Using the transformation equations 4.2.4 and equations 4.2.24 - 4.2.26 the physical roots of the extrema of the potential in terms of the radial distance r are given as:

$$r_1 = \frac{3}{2}r_g\sum_{j,k\geqslant 0}\frac{(-1)^k \times 3^{2j} \times (2j+5k)!}{j!k!(j+4k+1)!}\left(\frac{3\sqrt{3}\,r_g}{2J}\right)^{2j+2k}\frac{\Lambda^k}{2^{2k}}, \tag{4.2.27}$$

$$r_2 = \frac{2J^2}{r_g} - r_1 - \frac{32J^6}{27r_g^3}\left(\frac{2\Lambda}{3r_g}\right)^{2/3}, \tag{4.2.28}$$

$$r_3 = \sqrt[3]{\frac{3\,r_g}{2\Lambda}} + \frac{1}{3}(r_1 - r_2). \tag{4.2.29}$$

4.3 Result and discussion

Using Einstein Field equations, the general conserved equations of motion in SdS geometry with brief boundary conditions have been derived. Furthermore, the SdS horizon boundary

conditions were used in detailing and addressing the region, where the resulting conserved equations are being applied.

Applying, the developed equations we examined the general characteristics of the SdS potential for both massive and massless particles in some general cases. In free falling particles, there is no difference among Newtonian, Schwarzschild and general relativistic effective potentials for massless particles; but, will differ significantly depending on the β parameter for massive particles as discussed in sec. On the other hand, for particles possessing angular momentum different from zero, the SdS effective potential in both massive and massless particles behaves differently from both Sch and Newtonian ones whose significance is determined by the underlining parameters as discussed earlier.

The general physical characteristics of the potential for exploited representative cases have been plotted. Then, the plots have been used in characterizing the orbits of particles moving in the region of the potential field; where the brief description for various representative cases have been provided using Fig. 4.4. In fact, the analytical orbit solutions were also used to complement the description.

For massive particles, generally the SdS potential differs from both the Newtonian and the Schwarzschild potentials. Primarily, the SdS potential is characterized by three turning points where the particles velocities vanish, as usual. Also, the points of apsis for bound orbits are different among the three potentials; so that the eccentricities of the orbits become different. Especially, as the region of SdS application becomes effective, the differences will become more significant.

The plot as in Fig. 4.5 will be used to summarize the general overview of the potentials. For example, a particle owning total energy between E_4 and E_5 (Fig. 4.4) performs a bound orbit under the three potentials. But, the apsidal positions of the three orbits and hence the

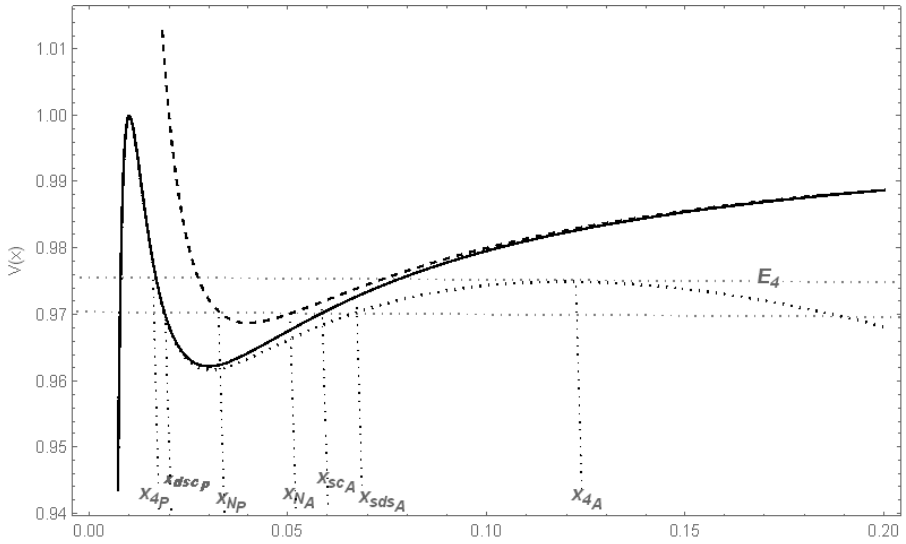

Figure 4.5: SdS effective potential: summary

eccentricities of the orbits are quite different. As, we see from the plot the perihelia positions $\mathrm{x}_{N_P}, \mathrm{x}_{Sc_P}, \mathrm{x}_{sds_p}$ for the Newtonian, Schwarzschild and SdS potentials and their corresponding aphelia positions $\mathrm{x}_{N_A}, \mathrm{x}_{Sc_A}, \mathrm{x}_{sds_A}$ are generally different. In fact, the perihelia of Schwarzschild and SdS slightly coincide; where we represented it as $\mathrm{x}_{dscp} \equiv \mathrm{x}_{Sc_P} \approx \mathrm{x}_{sds_P}$. However, this does not imply to possess the same eccentricity as the aphelion positions are reasonably differ.

Using appropriate boundary conditions, the effective potential was used to derive some special orbit equations and their solutions analytically.

For a quick overview of the effect of the cosmological constant, here, we examine the circular orbit special case, whose radius is given by eq. 4.2.19. For this particular case, a theoretical result for radial deviation of orbits (eq. 4.2.20) with respect to the classical Schwarzschild radius was generated, as given in Table 4.1. The choice of the systems considers small eccentricities, seeking circular orbit approximations, with some exceptions (due to lack of such observational data system). The latest observational data were used

in producing Table 4.1. The representative systems include: a) planetary system, b) binary stars (binary pulsars and SMBHs), c) orbits of stars and other binaries around galactic center, where the Milky-Way center is used as representative and d) orbit of binary galaxies, where the local group is used.

Table 4.1: Effect of Λ in circular orbits.

System	Orbiting object	$\Lambda\ (km^{-2})$ $\Lambda = 10^{-50}$ $\triangle r$ (μm)	$\Lambda = 10^{-46}$ $\triangle r$ (mm)	$\Lambda = 10^{-42}$ $\triangle r$ (m)	$\Lambda = 10^{-36}$ $\triangle r$ (km)	Data Sources
Solar system	Mercury	1.03	0.478	0.222	2.22	
	Earth	4.27	198	0.92	9.20	
	Jupiter	51.1	23.7	11	110	[129]
	Pluto	106	493	229	2290	
Binary stars						
Binary pulsars IGR J17062-6143 Intermediate mass $r_g \simeq 1.6\, r_{g\odot}$	low eccentricity orbiter chosen	$\sim 10^{-33}$	$\sim 10^{-33}$	$\sim 10^{-33}$	$\sim 10^{-32}$	[130]
Binary-SMBH $r_g \simeq 10^7\, r_{g\odot}$	low mass BH	493	229	106	1060	[131]
Milky-Way center *Disc-binary 1 Central-SMBH* $r_g \simeq 10^7\, r_{g\odot}$	Disc system $M \sim 50 M_\odot$	2.9×10^{-5}	4.3×10^{-5}	2.0×10^{-5}	2.0×10^{-5}	[132]
Binary-galaxies *MW-MC Central-SMBH* $r_g \simeq 10^{12}\, r_{g\odot}$	Clouds with M Model dependent	2.0×10^{15}	9.2×10^{14}	4.3×10^{14}	4.3×10^{15}	[133]

From the table, the following comments have been derived:

1) In the case of solar system, the effect of Λ on orbit radial perturbation is insignificant, just the order of μm to few $k$ms.

   - Also, the complicated interaction scenario of the solar system makes difficult to determine Λ effect precisely.

- Moreover, the orbits of the planets is not exactly circular.

2) In the case of low mass binary pulsars, the effect of Λ on circular orbit is negligible as can be observed from the table. The case of binary SMBHs is just identical to the solar system case.

3) The effect of Λ on circular orbits near AGNs is insignificant.

4) The effect of Λ on circular orbits will be significant in open and wide systems like binary-galaxies. As can be observed from the table, Λ effect is $\sim G$m to $\sim k$pc corresponding to low $\Lambda \sim 10^{-50} k\text{m}^{-2}$ to higher $\Lambda \sim 10^{-36} k\text{m}^{-2}$.

   - Actually, for the current standard value of $\Lambda \sim 10^{-46} k\text{m}^{-2}$, its effect is of the order of AU, quite observable!

Finally, we believe that the work of this chapter will benefit to study astrophysical dynamics in the SdS geometry. For example, in the more general elliptical orbit motions under the SdS geometry, the apsidal shifts of the orbits will be examined using the radial solutions given by eqs. 4.2.27- 4.2.29. On the other hand, we also note that the precession of bound elliptical orbits have been studied in chap. 6, where a two-body problem of this geometry have been developed to see the effect of Λ.

Chapter 5

The cosmological constant and the gravitational light bending

5.1 Introduction

In this chapter, we address the detailed derivations to our paper [134] by providing further supplementary comments and boundary conditions to enrich the thesis. The detailed review made therein the paper, has considered as a complementary review literature background of this chapter. Additionally, articles that have cited the paper are considered as review literature to this work.

Thus, this chapter provides the detail derivation of the equation of gravitational bending of light ray in the Schwarzschild-de Sitter background. The cosmological constant, the impact parameter and the angular distances to the source and the observer are considered as the important parameters of the equation.

The bending angle equation has considered in gravitational lensing to quantify the effect of cosmological constant. The detail work of this part has left to the reported article [134]. However, the detailing of orbit and bending angle equations developed here, shall be considered as supplementary and complementary future researches.

Finally, summary and conclusion will be given.

5.2 The photon orbit equation in SdS geometry

Using the GR orbit equations provided in ch. 4 (eqs 4.1.5, 4.1.10 and 4.1.11, where $\epsilon = 0$), we obtain a non-radial equation of motion as function of the azimuthal coordinate ϕ given as

$$\left(\frac{1}{r^2}\frac{dr}{d\phi}\right)^2 + \frac{1}{r^2} = \frac{1}{b^2} + \frac{1}{\ell^2} + \frac{r_g}{r^3}, \tag{5.2.1}$$

where b is the Schwarzschild impact parameter defined by

$$b = \frac{J}{\mathcal{E}}. \tag{5.2.2}$$

Using the closest radial approach r_o, where $dr/d\phi = 0$, eqs. 5.2.1 and 4.1.11 will be used to recast it as

$$b = \frac{r_o}{\sqrt{B(r_o)}}, \tag{5.2.3}$$

where, $B(r)$ is the time-time component of the metric given by eq. 4.1.11,

$$B(r) = 1 - \frac{r_g}{r} - \frac{r^2}{\ell^2}. \tag{5.2.4}$$

The modified impact parameter in the presence of Λ will be defined as

$$\frac{1}{b_\Lambda^2} = \frac{1}{b^2} + \frac{1}{\ell^2}. \tag{5.2.5}$$

Then, eq. 5.2.1 can be recast as

$$\left(\frac{1}{r^2}\frac{dr}{d\phi}\right)^2 + \frac{1}{r^2} = \frac{1}{b_\Lambda^2} + \frac{r_g}{r^3}. \tag{5.2.6}$$

The closest trajectory radial approach, r_0, to the gravitating object is determined by imposing the boundary condition, $dr/d\phi = 0$, whose solutions are given as

$$\begin{aligned}\left(\frac{r_0}{b_\Lambda}\right)\left[1-\left(\frac{r_0}{b_\Lambda}\right)^2\right] &= \frac{r_g}{b_\Lambda} \quad (\text{for } \Lambda \neq 0);\\ \left(\frac{r_0}{b}\right)\left[1-\left(\frac{r_0}{b}\right)^2\right] &= \frac{r_g}{b} \quad (\text{for } \Lambda = 0).\end{aligned} \tag{5.2.7}$$

The roots of r_0/b_Λ are

$$\begin{aligned}\left(\frac{r_0}{b_\Lambda}\right)_1 &= \frac{2}{\sqrt{3}}\sin\left[\frac{\pi}{6}+\frac{1}{3}\arccos\left(\frac{9}{2\sqrt{3}}\frac{r_g}{r_0}\right)\right];\\ \left(\frac{r_0}{b_\Lambda}\right)_2 &= -\frac{2}{\sqrt{3}}\sin\left[\frac{1}{3}\arccos\left(\frac{9}{2\sqrt{3}}\frac{r_g}{r_0}\right)\right];\\ \left(\frac{r_0}{b_\Lambda}\right)_3 &= \frac{2}{\sqrt{3}}\sin\left[\frac{\pi}{3}+\frac{1}{3}\arccos\left(\frac{9}{2\sqrt{3}}\frac{r_g}{r_0}\right)\right].\end{aligned} \tag{5.2.8}$$

Using Taylor expansion about the small quantity, r_g/b_Λ, eq 5.2.8 will yield

$$\begin{aligned}\left(\frac{r_0}{b_\Lambda}\right)_1 &= 1-\frac{1}{2}\left(\frac{r_g}{b_\Lambda}\right)-\frac{3}{8}(\frac{r_g}{b_\Lambda})^2+...,\\ \left(\frac{r_0}{b_\Lambda}\right)_2 &= -1-\frac{1}{2}\left(\frac{r_g}{b_\Lambda}\right)+\frac{3}{8}\left(\frac{r_g}{b_\Lambda}\right)^2+...,\\ \left(\frac{r_0}{b_\Lambda}\right)_3 &= \simeq \frac{r_g}{b_\Lambda} \;\Rightarrow r_0 \simeq r_g.\end{aligned} \tag{5.2.9}$$

In view of eq. 5.2.9, the only solution to the closest approach be $(r_0/b_\Lambda)_1$. Because, $(r_0/b_\Lambda)_2$ is negative which has no physical meaning; while $(r_0/b_\Lambda)_3$ lies outside of the region of interest for observation.

Considering $b \ll \ell$, and then using eq. 5.2.5 b_Λ is approximately given as

$$b_\Lambda \approx b - \frac{b^3}{2\ell^2}. \tag{5.2.10}$$

Now, using eqs. 5.2.9 and 5.2.10, the minimum distance to the gravitating object in SdS geometry is occurred at the radial coordinate, r_0, given by

$$r_0 = \underbrace{b\left(1-\frac{1}{2}\left(\frac{r_g}{b}\right)-\frac{3}{8}\left(\frac{r_g}{b}\right)^2+..\right)} - \frac{b^3}{2\ell^2}+... \tag{5.2.11}$$

The under-braced expression is the closest radial coordinate to that of the Schwarzschild geometry. Therefore, the cosmological constant reduces the impact parameter compared to the Schwarzschild geometry or, in other words, reduces the minimum radial distance to the origin.

The constant of motion, b (defined as the impact parameter in the case of Sch spacetime), defined by eq. 5.2.2, in terms of r_0 is exactly given by

$$b = \left(\frac{r_0^3}{r_0 - r_g}\right)^{\frac{1}{2}} \left[1 - \frac{r_0^3}{(r_0 - r_g)\ell^2}\right]^{-\frac{1}{2}}. \tag{5.2.12}$$

Whereas, its approximation to third order in r_g/r_0 and second order in Λ is given by

$$b \approx r_0 \left(1 + \frac{1}{2}\left(\frac{r_g}{r_0}\right) + \frac{3}{8}\left(\frac{r_g}{r_0}\right)^2 + \frac{r_0^2}{2\ell^2}\right). \tag{5.2.13}$$

5.2.1 Solution of the orbit equation

By now, we have sufficient information about the constants of the motion to solve the orbit equation given as in eq. 5.2.6.

In the absence of source mass ($r_g = 0$) we have a pure de Sitter space where its trivial solution is given by

$$\frac{1}{r} = \frac{\sin\phi}{b_\Lambda}. \tag{5.2.14}$$

In this case, the impact parameter is equal to the closest radial approach r_0.

In the general case, the integration of eq. 5.2.6 is not so simple. However, the radial coordinate transformation

$$r = \frac{1}{u}, \tag{5.2.15}$$

will be used to convert the orbit equation to the relatively simpler form given as

$$\left(\frac{du}{d\phi}\right)^2 + u^2 = \frac{1}{b_\Lambda^2} + r_g u^3. \tag{5.2.16}$$

The derivative of eq 5.2.16 with respect to ϕ, yield a non-linear second order ordinary differential (ODE) equation

$$\frac{d^2u}{d\phi^2} + u = \frac{3\,r_g}{2}\,u^2. \tag{5.2.17}$$

Introducing the dimensionless quantities $v(\phi)$ and α defined as

$$u(\phi) = \frac{v(\phi)}{r_0};\;\; \alpha = \frac{3\,r_g}{2r_0}, \tag{5.2.18}$$

eq. 5.2.17 is transformed to be recast as

$$\frac{d^2v}{d\phi^2} + v = \alpha v^2. \tag{5.2.19}$$

Note that, α is a small quantity. So, eq. 5.2.19 is the appropriate non-linear ODE equation to apply the standard perturbation method for its approximate solution. Thus, we can assume a series sum approximation of the form

$$v(\eta) = \sum_{n=0}^{\infty} \alpha^n v_n, \tag{5.2.20}$$

where η is the corresponding coordinate transformation to the perturbation given by

$$\eta = \phi\left(1 + \sum_{n=0}^{\infty} \alpha^n w_n\right). \tag{5.2.21}$$

The w_n's are the undetermined constants of multipliers corresponding to the degrees of α, that can be deduced from the initial boundary conditions. For significant physical observation, it is sufficient to carry the series sum to second order correction in α. Then, eqs. 5.2.20 and 5.2.21 will be respectively recast as

$$v(\eta) = v_0 + \alpha v_1 + \alpha^2 v_2, \tag{5.2.22}$$

$$\eta = \phi\left(1 + \alpha w_1 + \alpha^2 w_2\right). \tag{5.2.23}$$

Using eqs. 5.2.22 and 5.2.23 the differential eq. 5.2.20 will be given as

$$\alpha^2\left(\frac{d^2v_2}{d\eta^2}+v_2+2\omega_1\frac{d^2v_1}{d\eta^2}-2v_0v_1+2\omega_2\frac{d^2v_0}{d\eta^2}\right)$$
$$+\alpha\left(\frac{d^2v_1}{d\eta^2}+v_1+2\omega_1\frac{d^2v_0}{d\eta^2}-v_0^2\right)+\left(\frac{d^2v_0}{d\eta^2}+v_0\right)=0. \tag{5.2.24}$$

Equating the coefficients of α^n's to zero (where $n\in\{0,1,2\}$), we obtain three simultaneous second order linear differential equations in v_0, v_1 and v_2 respectively given by

$$\text{coff. } \alpha^0: \quad \frac{d^2v_0}{d\eta^2}+v_0=0; \tag{5.2.25}$$

$$\text{coff. } \alpha^1: \quad \frac{d^2v_1}{d\eta^2}+v_1+2\omega_1\frac{d^2v_0}{d\eta^2}-v_0^2=0; \tag{5.2.26}$$

$$\text{coff. } \alpha^2: \quad \frac{d^2v_2}{d\eta^2}+v_2+2\omega_1\frac{d^2v_1}{d\eta^2}-2v_0v_1+2\omega_2\frac{d^2v_0}{d\eta^2}=0. \tag{5.2.27}$$

The solution of v_0 is trivial. Then, replacing the solution of v_0, in eq. 5.2.26, we again trivially solve for v_1 and so on for v_2. The solutions are:

$$
\begin{aligned}
v_0(\eta) &= a_1 \sin\eta + a_1 \cos\eta; && (5.2.28)\\
v_1(\eta) &= \frac{(a_1^2+a_2^2)}{2} + (a_4 + w_1 a_2 - w_1 a_1 \eta)\cos\eta + (a_3 + w_1 a_2 \eta)\sin\eta \\
&\quad + \frac{(a_1^2-a_2^2)}{6}\cos 2\eta - \frac{a_1 a_2}{3}\sin 2\eta; && (5.2.29)\\
v_2(\eta) &= \frac{a_1 a_3 + a_2 a_4 + a_2^2\omega_1}{2} + \left(a_5 + \frac{a_1\,(3a_2^2 - a_1^2)}{48}\right)\sin\eta \\
&\quad + \left(\left(\omega_1 a_4 + \omega_2 a_2 + \frac{5a_2\,(a_1^2+a_2^2)}{12}\right)\eta - \frac{\omega_1^2 a_1}{2}\eta^2\right)\sin\eta \\
&\quad + \left(a_6 + \omega_1 a_4 + \omega_2 a_2 + \frac{a_2(11a_1^2+23a_2^2)}{48}\right)\cos\eta && (5.2.30)\\
&\quad + \left(\left(\omega_1^2 a_1 - \omega_1 a_3 - \omega_2 a_1 - \frac{5a_1\,(a_1^2+a_2^2)}{12}\right)\eta - \frac{\omega_1^2 a_2}{2}\eta^2\right)\cos\eta \\
&\quad + \left(-\frac{(a_1 a_4 + a_2 a_3 + \omega_1 a_1 a_2)}{3} + \frac{\omega_1(a_1^2-a_2^2)}{3}\eta\right)\sin 2\eta \\
&\quad + \left(\frac{(a_1 a_3 - a_2 a_4 - \omega_1 a_2^2)}{3} + \frac{2\omega_1 a_1 a_2}{3}\eta\right)\cos 2\eta \\
&\quad + \frac{a_1(3a_2^2-a_1^2)}{48}\sin 3\eta + \frac{a_1(a_2^2-3a_1^2)}{48}\cos 3\eta;
\end{aligned}
$$

where a_1, a_2, ..., a_6, ω_1 and ω_2 are constants of integration.

To give the $v_n's$ in terms of ϕ, the transformation eq. 5.2.21 will be used. So, to third order in α we have

$$
\begin{aligned}
\eta &= \phi(1+\alpha\omega_1+\alpha^2\omega_2)^{-1} \simeq \phi - \alpha\phi\left(\omega_1 + \alpha(\omega_2 - \omega_1^2)\right); \\
\sin n\eta &\simeq \sin n\phi - n\alpha\phi\left(\omega_1 + \alpha(\omega_2-\omega_1^2)\right)\phi\cos n\phi; && (5.2.31)\\
\cos n\eta &\simeq \cos n\phi + n\alpha\phi\left(\omega_1 + \alpha(\omega_2-\omega_1^2)\right)\phi\sin n\phi.
\end{aligned}
$$

Using eqs. 5.2.20 and 5.2.28 - 5.2.31, $v(\phi)$ is given by

$$\begin{aligned}
v(\phi) &= \frac{\alpha}{2}(a_1^2+a_2^2)+\frac{\alpha^2}{2}(a_1a_3+a_2a_4+\omega_1a_2^2)\\
&+\left(a_1+a_3\alpha+\frac{a_1\,(3a_2^2-a_1^2)+48a_5}{48}\alpha^2\right)\sin\phi\\
&+\left(2\omega_1a_2\alpha+\alpha^2\left(2\omega_1a_4+2\omega_2a_2-\omega_1^2a_2+\frac{5a_2\,(a_1^2+a_2^2)}{12}\right)-2\omega_1^2a_1\alpha^2\phi\right)\phi\sin\phi\\
&+\left(a_2+\alpha(a_4+\omega_1a_2)+\alpha^2\left(\omega_1a_4+\omega_2a_2+a_6+\frac{a_2(11a_1^2+23a_2^2)}{48}\right)\right)\cos\phi\\
&+\left(-2\omega_1a_1\alpha+\alpha^2\left(3\omega_1^2a_1-2\omega_2a_1-2\omega_1a_3-\frac{5a_1\,(a_1^2+a_2^2)}{12}\right)-2\omega_1^2a_2\alpha^2\phi)\right)\phi\cos\phi\\
&+\left(-\frac{a_1a_2}{3}\alpha-\frac{\alpha^2}{3}(\omega_1a_1a_2+a_1a_4+a_2a_3)+\frac{2\alpha^2\omega_1(a_1^2-a_2^2)}{3}\phi\right)\sin2\phi\\
&+\left(\frac{(a_1^2-a_2^2)}{6}\alpha+\alpha^2\frac{(a_1a_3-a_2a_4-\omega_1a_2^2)}{3}+\frac{4\omega_1a_1a_2}{3}\alpha^2\phi\right)\cos2\phi\\
&+\frac{\alpha^2a_1(3a_2^2-a_1^2)}{48}\sin3\phi+\frac{\alpha^2a_2(a_2^2-3a_1^2)}{48}\cos3\phi. \qquad (5.2.32)
\end{aligned}$$

There are eight constants and so need eight independent equations. The two boundary conditions at $\phi=\pi/2$ where $v(\phi)=1$ and $dv/d\phi=0$ are used to form six independent equations when the corresponding coefficients of α: α^0, α^1 and α^2 are being equated. The seventh and eighth equations can be constructed from the boundary condition at the position of the source $v(\phi)=v_{SO}$ and position of the observer $v(\phi)=v_{OB}$. Here, it has to be clear that the trajectory equation contains implicitly the deflection angles at the source and at the observer as constants of integration.

Thus, the six independent equations obtained by the two boundary conditions ($\phi=\pi/2$ where $v(\phi)=1$ and $dv/d\phi=0$) being evaluated at the closest approach are:

$$\begin{aligned}
a_1 &= 1;\quad a_2 = 0;\quad a_3 = -\frac{1}{3};\quad a_4 = \pi\omega_1;\\
a_5 &= \frac{2}{9}-\frac{\pi^2\omega_1^2}{2};\quad a_6 = \pi\omega_2-\frac{\pi\omega_1(15\omega_1+2)}{6}+\frac{5\pi}{24}. \qquad (5.2.33)
\end{aligned}$$

Using eq. 5.2.32 and 5.2.33, we obtain

$$\begin{aligned} v(\phi) &= \sin\phi + \frac{\alpha}{2}\left(1 + \frac{\cos 2\phi}{3} - \frac{2\sin\phi}{3} + \omega_1(\pi - 2\phi)\cos\phi\right) \\ &\quad -\frac{\alpha^2}{3}\left(1 + \frac{\sin 3\phi}{16} + \frac{\cos 2\phi}{3} - \frac{29}{48}\sin\phi - \frac{5}{8}(\pi - 2\phi)\cos\phi\right) \\ &\quad + \frac{\alpha^2(\pi - 2\phi)}{6}\Big(6\,\omega_2 - \omega_1\big[2\sin 2\phi + 3\pi\omega_1(\pi - 2\phi)\sin\phi\big]\Big). \end{aligned} \tag{5.2.34}$$

Eq. 5.2.34 is the proper solution of the orbit equation with two undetermined constants of integrations, ω_1 and ω_2; to be determined by the remaining two boundary conditions related to $v_{_{SO}}$ and $v_{_{OB}}$ as described earlier.

5.2.2 Perturbation along the radial coordinate: orbit special solution

In the special case where the perturbation is carried along the radial coordinate alone imposes an additional constrain, that the coordinate transformation given by eq. 5.2.23 leads to congruency of η and ϕ; since there is no perturbation effected along ϕ, i.e.,

$$\eta = \phi.$$

Then, follows

$$\omega_1 = \omega_2 = 0. \tag{5.2.35}$$

Then, the complete orbit solution of the photon in a centrally gravitating object in this special case is given by

$$\begin{aligned} v(\phi) &= \sin\phi + \frac{\alpha}{2}\left(1 + \frac{1}{3}\cos 2\phi - \frac{2}{3}\sin\phi\right) \\ &\quad -\frac{\alpha^2}{3}\left(1 + \frac{1}{16}\sin 3\phi + \frac{1}{3}\cos 2\phi - \frac{29}{48}\sin\phi - \frac{5}{8}(\pi - 2\phi)\cos\phi\right). \end{aligned} \tag{5.2.36}$$

Eq. 5.2.36 satisfies all the boundary conditions required at the closest radial approach to third order correction in the small quantity α; whereas in the case of article [134], the

correction was held to second order only.

Note that eq. 5.2.36 holds true for both Schwarzschild and SdS geometry. The difference comes only in the presence of Λ, intrinsic to r_0 in the case of SdS geometry whose relation is explicitly given by eq. 5.2.12, whereas it is absent in the case of Schwarzschild geometry.

5.3 The Deflection Angle

In asymptotically flat spacetime, like the Schwarzschild spacetime, the difference in angular coordinates of the source ϕ_s and the observer ϕ_{ob} is defined as the bending angle when the source and the observer are at infinitely large distances away from the lens. In such cases, the orbit solution, eq. 5.2.36, immediately yields the classical Schwarzschild bending angle up to the third order correction in α. But, in the general case when spacetime is not asymptotically flat, the bending angle will be different. Because, the source and observer distances matter on the horizon of observation as spacetime curves (for the detailed review see [134] and the references therein).

So, in the SdS case (where spacetime is not asymptotically flat), the derivation of the bending angle involves the source, the deflector and the observer.

Thus, following the trajectory of the photon the true bending angle at arbitrary observation point along the path is determined by the angle between the light ray at the source and at the observer. This angle is just the difference between the coordinate invariant angle ψ (the angle between the three vector $\mathbf{k}$ of the photon and the radial vector $\mathbf{r}$) and the angular coordinate ϕ at that position,

$$\delta = \psi - \phi. \tag{5.3.1}$$

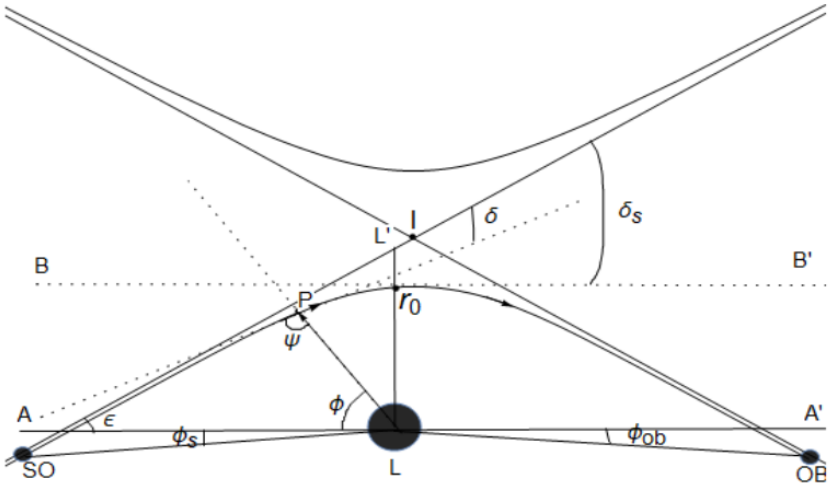

Figure 5.1: Lensing setup in gravitational light bending in SdS spacetime.

5.3.1 The lensing setup and bending angle derivation

The lensing setup is displayed as in Fig. 5.1, where eq. 5.2.36 is mainly used for the drawings. In the drawings:

- The photon trajectory is displayed with the lower half parabola emanating from the source "SO" then passing through an arbitrary point, "P", then passing through the closest radial position "r_0" and then being received at the observer point "OB". The upper branch parabola is a manifestation of the SdS geometry, that appears to exhibit a symmetric virtual lensing system.
- $\overline{LL'}$ represents the polar axis.
- $\overline{AA'}$ stands for the optic axis.
- The positions of the source, lens and the observer are respectively represented by SO, L and OB.

- The line $\overline{L'(SO)}$ is the undeflected photon trajectory when there is no lens.
- The line $\overline{I(OB)}$ is the observers line of sight perceiving the source's image at I.
- ψ is the coordinate invariant angle at the arbitrary point, P, on the trajectory of the photon; where the deflection angle at this point is represented by δ. At the source and the observer, it is represented respectively as ψ_s and ψ_{ob}.
- ϕ is the angular coordinate at the arbitrary point P. At the source and the observer, it is represented respectively as ϕ_s and ϕ_{ob}. In the special case when the source is being located on the optic axis ($\phi_s = 0$), the half bending angle δ_s from the source; on the way to the minimum radial position r_0 is just the angle between the undeflected line $\overline{L'(SO)}$ and the optic axis, ϵ. Similarly, the half bending angle δ_{ob} at the observer will be defined.

Now upon using eq. 5.3.1 and the lensing setup description, in the general case where the source and the observer being located respectively at small angular positions ϕ_s and ϕ_{ob}, the total deflection angle δ is given by

$$\delta = \psi_s + \psi_{ob} - (\phi_s + \phi_{ob}). \tag{5.3.2}$$

The orbit solution given by eq. 5.2.36 will be series expanded both at the source ($r = r_s$) around $\phi = 0$ and the observer ($r = r_{ob}$) around $\phi = \pi$ whose leading terms are given as

$$\phi = \phi_s + \phi_{ob} = -\frac{4M}{r_o} + (r_o + M)\left(\frac{1}{r_s} + \frac{1}{r_{ob}}\right) + \dots, \tag{5.3.3}$$

where we have recalled: $\alpha = 3r_g/(2r_o)$ and then used the relation $r_g = 2M$.

The invariant angle ψ case needs a further geometrical interpretation. However, in case of small deviations along the particle geodesy (the photon, in our case), ψ will be approximated by its tangent value at any point. [135], derives this tangent from the cosine of the

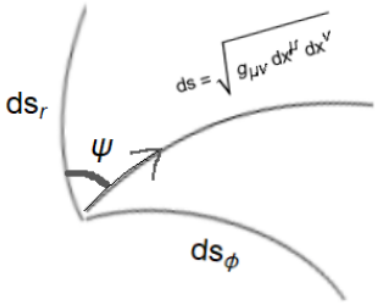

Figure 5.2: The invariant angle, ψ, between the 3-**k** vector of photon and the radial vector **r** at an arbitrary point P along the orbit.

angle in the projected 2-D Euclidean surface. Here, we use directly the orthogonality of the coordinate changes (r, ϕ) on the surface of the geodesy at the point of interest (see Fig. 5.2) so that

$$\tan\psi = \frac{ds_\phi}{ds_r}\,, \tag{5.3.4}$$

where ds_ϕ and ds_r are the projection of the line element, ds, along the ϕ and r coordinate changes respectively. Then, eq. 5.3.4 will be recast as

$$\tan\psi = \frac{\sqrt{g_{\phi\phi}}}{\sqrt{g_{rr}}}\frac{d\phi}{dr} = r\sqrt{B(r)}\,\frac{d\phi}{dr}, \tag{5.3.5}$$

where in the SdS spacetime the metric components $g_{\phi\phi}$ and g_{rr} are respectively given by (see ch. 3)

$$g_{\phi\phi} = r^2;\;\; g_{rr} = \left(1 - \frac{r_g}{r} - \frac{r^2}{\ell^2}\right)^{-1} = \frac{1}{B(r)}. \tag{5.3.6}$$

Using eqs. 5.2.1, 5.2.3 and 5.3.6, equation 5.3.5 will be recast as

$$\tan\psi = \frac{r_o}{r}\left[\frac{B(r_o)}{B(r)} - \frac{r_o^2}{r^2}\right]^{-1/2}. \tag{5.3.7}$$

Taylor expanding the right hand side expression of eq 5.3.7 around the small quantities: $r_o/r, r_g/r, r/\ell, r_g/r_o, r_o/\ell$ and then using $r_g = 2M$, we obtain

$$\begin{aligned} \tan\psi &= \frac{M+r_o}{r}\left(1-\frac{M}{r}\right)+... \\ &\quad -\frac{1}{4\ell^2}\left[2(M+r_o)(r+M)+\frac{r_o^3}{r}\left(1-\frac{M}{r}\right)\right]+... \end{aligned} \tag{5.3.8}$$

Using the small approximation for $\tan\psi \simeq \psi$, as discussed earlier and splitting it to the source (where $r = r_s$) and the observer (where $r = r_{ob}$), eq. 5.3.8 is recast as

$$\begin{aligned} \psi &= \psi_s + \psi_{ob} \\ &= (M+r_o)\left(\frac{1}{r_s}+\frac{1}{r_{ob}}-M\left(\frac{1}{r_s^2}+\frac{1}{r_{ob}^2}\right)\right)+... \\ &\quad -\frac{1}{4\ell^2}\left[2(M+r_o)(2M+r_s+r_{ob})+r_o^3\left(\frac{1}{r_s}+\frac{1}{r_{ob}}-M\left(\frac{1}{r_s^2}+\frac{1}{r_{ob}^2}\right)\right)\right]+... . \end{aligned} \tag{5.3.9}$$

Now using eqs. 5.3.1, 5.3.3 and 5.3.9, the total deflection angle with leading terms in terms of the closest radial approach is given as

$$\begin{aligned} \delta &= \frac{4M}{r_o}-M(M+r_o)\left(\frac{1}{r_s^2}+\frac{1}{r_{ob}^2}\right)+... \\ &\quad -\frac{1}{4\ell^2}\left[2(M+r_o)(2M+r_s+r_{ob})+r_o^3\left(\frac{1}{r_s}+\frac{1}{r_{ob}}-M\left(\frac{1}{r_s^2}+\frac{1}{r_{ob}^2}\right)\right)\right]+... . \end{aligned} \tag{5.3.10}$$

Assuming $M \ll r$ for all r's, all expressions with factor M+r will be split to terms of lower order where the r factor term is being considered in the lead terms; and the M factor term is being considered in the higher order ones. In this case, using the approximation for r_o given by eq. 5.2.11 in eq. 5.3.10, the total deflection angle in terms of the measurable quantity b with leading terms is given by

$$\begin{aligned} \delta &= \frac{4M}{b}-Mb\left(\frac{1}{r_s^2}+\frac{1}{r_b^2}\right)+\frac{2Mb\Lambda}{3} \\ &\quad -\frac{b\Lambda}{6}(r_s+r_{ob})-\frac{b^3\Lambda}{12}\left(\frac{1}{r_s}+\frac{1}{r_{ob}}\right)+\frac{Mb^3\Lambda}{12}\left(\frac{1}{{r_s}^2}+\frac{1}{{r_{ob}}^2}\right)+... \end{aligned} \tag{5.3.11}$$

Eq. 5.3.11 is exactly the same as the result obtained in the previous work reported as in [134].

5.3.2 Comment on earlier results: slight modification

The third term of eq. 5.3.11 arises only from the first term ($4M/r_o$) of eq. 5.3.10 in the approximation of r_o where the other higher order terms have been truncated. However, other considerable Λ coupled terms having equal footing with the third term of eq. 5.3.10 have been oddly consumed in the truncated higher order terms. In the case of [134], the blunder arises in the assumption just made to derive eq. 5.3.11 from eq. 5.3.10.

The blunder arises in the splitting of $M + r_o$ as lower and higher order factors in the assumption. In order to reveal this, it is important to see the expansion of this factor using the series approximation of r_o given by eq. 5.2.11, where

$$M + r_o \approx M + b\left(1 - \frac{M}{b} - \frac{3M^2}{2b^2} - ...\right) = b - \frac{3M^2}{2b} - ... \tag{5.3.12}$$

Plugging eq. 5.3.12 into eq. 5.3.10 reduces the third term of eq. 5.3.11 by half factor, where the change comes mainly from the Λ coupled term (third term of eq 5.3.10). Other additional terms will be consumed to the truncated higher order terms, while the other leading terms remain un affected.

Thus, the corrected total bending angle in the SdS spacetime is given by

$$\begin{aligned} \delta &= \frac{4M}{b} - Mb\left(\frac{1}{r_s^2} + \frac{1}{r_b^2}\right) + \frac{Mb\Lambda}{3} \\ &\quad -\frac{b\Lambda}{6}\left(r_s + r_{ob}\right) - \frac{b^3\Lambda}{12}\left(\frac{1}{r_s} + \frac{1}{r_{ob}}\right) + \frac{Mb^3\Lambda}{12}\left(\frac{1}{{r_s}^2} + \frac{1}{{r_{ob}}^2}\right) + ... \end{aligned} \tag{5.3.13}$$

5.4 Summary and conclusion

We derived the trajectory equation of light from its geodesy in the more general standard perturbation method that holds true for both, the Schwarzschild and the SdS spacetimes. In the derivations, the integration constants were all determined with appropriate boundary conditions of the geodesy. Conversely, it is possible to see that the final solution completely satisfies all the boundary conditions of the light geodesy.

The geodesic equation of light, eq. 5.2.1, demonstrates the appearance of Λ that the geodesic equation of light indeed includes Λ; which is considered to be an intrinsic geometrical consequence of the SdS spacetime. Actually, Λ disappears from the solution of the geodesic eq. 5.2.36. However, intrinsically it exists in the parameters of the solution. To reveal this obscured fact, it is sufficient to refer the radial closest approach r_o ($\alpha = 3M/r_o$) that has already included Λ by way of eqs. 5.2.3 and 5.2.5.

Another important issue to comment is, the criticism raised in some recent literatures (see for example [136]) where in the bending eq. 5.3.11 when $M \rightarrow 0, \delta \nrightarrow 0$, as problematic "claiming that lensing without source". However, this is a blunder, just equivalent to observe the ray coming from the source in a straight ruler on flat spacetime. Because, whatsoever M is, Λ itself curves spacetime in the opposite sense to the effect of M; a manifestation of the intrinsic geometrical property of Λ, whose background is a pure de Sitter geometry (see for example [135, 137]). Moreover, other extensive recent studies (see for example [138] and the references therein) show that the inclusion of Λ both in light bending and gravitational lensing is a prevailing geometrical intrinsic property of the embedding spacetime. Consequently, other fresh and recent investigations (see for example [139, 140]) show the influence of the cosmological constant on the shadow of black holes as a result

of gravitational lensing in strong gravity regime; where the observer point of view is taken into account by way of the appropriate comoving coordinates.

On the other hand, the application of the bending equation is used to quantify the effect of cosmological constant in gravitational lensing system. The detail work of this part is left to the reported article [134]. Actually, the paper sufficiently covers all the basic and necessary background literature reviews on whether Λ is a real geometrical effect or not, in gravitational bending of light. Furthermore, all the boundary conditions imposed on the selected model lensing system remains valid here. Thus, the slight modification made here has no essence on the physics used, except increasing the magnitude of Λ effect. However, emphasis is given here on detailing the orbit and bending equations of light for considering supplementary and complementary future researches.

Finally, we conclude that the cosmological constant influences light bending and gravitational lensing independent of coordinate transformations.

Chapter 6

Gravitational two body problem in SdS geometry

If the gravitational potential energy between two bodies deviates slightly from Newton's gravitational law, then the ellipse of the orbit gradually rotates leading to apsidal precessions (see for example [141]). This precession corresponds to the rotation of the Laplace-Runge-Lenz vector (LRL), which points along the line of apsides. The LRL vector is a constant of motion chiefly used to describe the shape and orientation of the orbit of bodies around one another, such as a planet revolving around a star. In the general view, the conservation of the vector corresponds to a particle moving freely on the surface of a four-dimensional hyper-sphere so that the whole problem is symmetric under certain rotations of the four-dimensional space (see for example [142], [143]). Various generalizations of the LRL vector have been defined (see for example [141], [143], [144], [145], [146], [147]) to incorporate the effects of relativity, and other fields. Customarily, perturbation is being used to derive the additional (but small) effects with the aid of the LRL vector.

The inclusion of Λ effect in the precession of planetary orbits have been carried out with different approaches (see for example [122, page 305], [148], [149], [150], [151], [152]) where some of the results are highly approximated while others are claimed as "exact."

However, due to the smallness of Λ, observations have not yet constrained the theoretical results. Probably, it will take some more periods of observational advances to come to conclusion.

Regardless of the efforts, some of the theoretical results seem paradoxical. Because, the secular first-order effect of Λ to the precession of the planetary orbits has the multiplicative factor $(1-e^2)^n$ where $n > 0$. So, smaller eccentricities result to larger Λ effects over larger eccentricities contrary to expected increasing Λ effect with distance. Therefore, constraining Λ effects in planetary orbits need further developments.

Thus, in this chapter we develop GR two-body problem equations different from the previous approaches. Essentially, the developed equations are expected to reproduce the Newtonian theory of gravitation if the later can successfully account observations. So an extension of the standard Post-Newtonian (PN) expansion is considered in linearization of the field equations in a region where we are going to implement the model with the SdS metric.

The organization of the work is: In section 1 we provide the boundary conditions where and how the SdS linearization and PN expansions will work. In section 2 we linearize the field equations in the Post-Newtonian expansion with the Schwarzschild-de Sitter (SdS) metric. In section 3 we derive the energy momentum tensor for higher order corrections in the PN expansion in SdS metric. In section 4, the energy momentum tensor developed is used to derive the Lagrangian and Hamiltonian of n system of gravitationally interacting particles to the fourth order correction in the velocity(v^4) of the particles. In section 5, we apply the results of section 4 to two-body system then derive the precession of orbits of the system. Finally, in section 6 we discuss the results of the new development to remark.

6.1 Conditions for the application of Post-Newtonian expansion and linearization of EFE in SdS

The general assumption, that EFE can be tested observationally in the context of Newtonian formalism under weak-field approximation, is being valid if the later accounts for a successful observation. So, in a region where the Post Newtonian expansion and linearization of the fields going to be implemented with the SdS metric be subjected to this general assumption. This is possible in a region where the effect of Λ is very small but considerably competent with higher PN corrections (if required). This region is precisely determined by the conditions we have described in 4.1.2. On the other hand, the operational conditions for the weak-field approximation in the specified region (of the SdS geometry), will be addressed with oversimplified description as undergoing.

In Newtonian gravitation, as a particle falls from the outer region of a gravitating system with varying potential Φ to the inner region, then gravity accelerates it to a kinetic energy

$$\frac{1}{2}mv^2 \sim \mid m\Phi \mid_{max};\ \ v \ll c\,. \tag{6.1.1}$$

Where m is mass of the particle, v is the speed of the particle and c is the speed of light in vacuum. Whereas, Φ is the Newtonian potential normalized to zero at sufficiently far distance from the gravitating system.

The condition given by eq. 6.1.1 implies

$$\mid \Phi \mid \ll c^2. \tag{6.1.2}$$

Using the conditions imposed by eqs. 6.1.1 & 6.1.2 to the perfect fluid given by eq. 3.1.31, the speed of sound in the fluid environment is approximately given by

$$v_s = (dP/d\rho)^{1/2} \sim (P/\rho)^{1/2} \sim \mid T^{ij}/T^{00} \mid^{1/2} \ll 1, \tag{6.1.3}$$

where P is the pressure of the fluid, ρ is the density of the fluid and T^{00} and T^{ij} are the total energy momentum and stress energy momentum tensor of the fluid, respectively.

By eq. 6.1.3 the stress component of the energy momentum tensor is very much smaller than the total energy momentum density of the system.

By now we have sufficient and necessary conditions for the weak-field approximation of GR equations to test in terms of the Newtonian formalism. To implement these conditions for the development of the detailed work as outlined in sec. 6.1, the parametric expansions will be practically carried out in either of the following procedures.

i) The higher correction potentials are obtained by series expansion of the metrics with the Newtonian potentials, hence the Post Newtonian(PN) formalism. The zero components of the metrics are considered to be Euclidean metrics.

ii) The perturbing potential $h_{\mu\nu}$ to the flat Minkowski metrics $\eta_{\mu\nu}$ are considered to be linear with the Newtonian potentials, whenever being considered as their first order corrections. In this case, the Minkowski metrics play role in raising and lowering indices everywhere in the differential equations.

In the presence of positive cosmological constant, the Post Newtonian expansion will be carried out by considering the Newtonian potential and the potential that arises from the cosmological constant as a single potential in the Euclidean background spacetime. On the other hand, the linearization case will be achieved in two possible ways: 1) Keep both potentials together as a single potential analogous to the Post Newtonian expansion, but the Minkowski spacetime is being used as the background. 2) Consider the potential that arises from the cosmological constant as a higher correction to the Schwarzschild spacetime background in the specified region.

In this work we follow the linearization method where the first approach is being implemented, i.e., linearization of the fields with SdS metric in the Minkowski background. Furthermore, in view of the small value of the cosmological constant we keep the cosmological constant term to first degree order, and avoid all cross terms with the cosmological constant terms (except in a prevailing condition to permit) during the linearization.

6.2 Linearization of EFEs in SdS spacetime

The SdS metric $g_{\mu\nu}$ in spherical coordinate system, eq. 3.2.19, in terms of the generalized Newtonian potential Φ_N can be recast as

$$ds^2 = -\left(1 + \frac{2\Phi_N}{c^2} - \frac{\Lambda}{3}r^2\right)dt^2 + \frac{dr^2}{\left(1 + \frac{2\Phi_N}{c^2} - \frac{\Lambda}{3}r^2\right)} + r^2 d\Omega^2. \tag{6.2.1}$$

The metric perturbation in the Minkowski background is given by

$$g_{\mu\nu} \approx \eta_{\mu\nu} + h_{\mu\nu}; \quad g^{\mu\nu} \approx \eta^{\mu\nu} - h^{\mu\nu}, \tag{6.2.2}$$

where $\eta_{\mu\nu}$ is the Minkowski metric with signature (-, +, +, +).

Considering the presumed boundary conditions (as discussed earlier), the perturbing potentials $h_{\mu\nu}$ and their derivatives with respect to the space-coordinates are of the order of v^2/c^2, v^4/c^4, and so on for h_{00} and h_{ij}; while for h_{0i} the potentials are of the order of v^3/c^3, v^5/c^5, etc. On the other hand, every derivative of the potentials with respect to the time-coordinate increases each order by v/c additional factor. Subsequently, upon using eqs. 3.1.17, 3.1.23 & 6.2.2 we observe that the relevant Ricci tensor components being used in EFEs, for the weak field approximation possess the same order of perturbations.

Thus, the relevant Ricci tensors to the fourth order correction in the perturbing potentials, as we will see soon, are given as:

$$\begin{aligned} R_{00} &= R_{00}^{(2)} + R_{00}^{(4)}, \\ R_{ij} &= R_{ij}^{(2)}, \\ R_{0i} &= R_{0i}^{(3)}. \end{aligned} \tag{6.2.3}$$

The time-time component, R_{00}, of the Ricci tensor to the fourth order perturbation in the Newtonian potentials is given by

$$\begin{aligned} R_{00} &= \frac{1}{c}\frac{\partial}{\partial t}\left(\frac{\partial h_{i0}}{\partial x^i} - \frac{1}{2c}\frac{\partial h_i^i}{\partial t}\right) - \frac{1}{2}\nabla^2 h_{00} + \frac{1}{2}h^{ij}\frac{\partial^2 h_{00}}{\partial x^i \partial x^j} \\ &\quad -\frac{1}{4}\left(\frac{\partial h_{00}}{\partial x^i}\right)^2 + \frac{1}{4}\frac{\partial h_{00}}{\partial x^j}\left(2\frac{\partial h_j^i}{\partial x^i} - \frac{\partial h_i^i}{\partial x^j}\right). \end{aligned} \tag{6.2.4}$$

Using the harmonic coordinate condition,

$$g^{\mu\nu}\Gamma^{\alpha}_{\mu\nu} = 0, \tag{6.2.5}$$

we get the relation

$$\frac{\partial h_{i0}}{\partial x^i} - \frac{1}{2c}\frac{\partial h_i^i}{\partial t} = 0. \tag{6.2.6}$$

Now using the relation given by eq. 6.2.6, eq. 6.2.4 will be recast as

$$\begin{aligned} R_{00} &= -\frac{1}{2}\nabla^2 h_{00} + \frac{1}{2}h^{ij}\frac{\partial^2 h_{00}}{\partial x^i \partial x^j} - \frac{1}{4}\left(\frac{\partial h_{00}}{\partial x^i}\right)^2 \\ &\quad +\frac{1}{4}\frac{\partial h_{00}}{\partial x^j}\left(2\frac{\partial h_j^i}{\partial x^i} - \frac{\partial h_i^i}{\partial x^j}\right). \end{aligned} \tag{6.2.7}$$

The first term in equation 6.2.7 is second order in the perturbing potential h, while all the remaining terms are of fourth order in h.

So,

$$R_{00}^{(2)} = -\frac{1}{2}\nabla^2 h_{00}^{(2)}, \tag{6.2.8}$$

$$R_{00}^{(4)} = -\frac{1}{2}\nabla^2 h_{00}^{(4)} + \frac{1}{2}h_{ij}^{(2)}\frac{\partial^2 h_{00}^{(2)}}{\partial x^i \partial x^j} - \frac{1}{4}\left(\frac{\partial h_{00}^{(2)}}{\partial x^i}\right)^2 + \frac{1}{4}\frac{\partial h_{00}^{(2)}}{\partial x^j}\left(2\frac{\partial h_{ij}^{(2)}}{\partial x^i} - \frac{\partial h_{ii}^{(2)}}{\partial x^j}\right). \tag{6.2.9}$$

Where $h_{00}^{(2)}$, $h_{ij}^{(2)}$, and $h_{00}^{(4)}$ are all considered to be the sum of the corresponding Newtonian and that of the Λ potentials given as

$$h_{00}^{(2)} = h_{00}^{N(2)} + h_{00}^{\Lambda(2)}, \tag{6.2.10}$$

$$h_{00}^{(4)} = h_{00}^{N(4)} + h_{00}^{\Lambda(4)}, \tag{6.2.11}$$

$$h_{ij}^{(2)} = h_{ij}^{N(2)} + h_{ij}^{\Lambda(2)}. \tag{6.2.12}$$

The superscripts ^{N} and $^\Lambda$ stand for the Newtonian and cosmological potentials, respectively.

In view of equation 6.1.1, the fourth order correction in h obtained from R_{ij} is insignificant. Hence, only the second order correction in h to the Newtonian potentials is relevant. So, using equation 6.2.2 in the expansion of the space-space component of the Ricci tensor, we obtain

$$R_{ij}^{(2)} = \frac{1}{2}\frac{\partial^2 h_{00}^{(2)}}{\partial x^i \partial x^j} - \frac{1}{2}\frac{\partial^2 h_{kk}^{(2)}}{\partial x^i \partial x^j} + \frac{1}{2}\frac{\partial^2 h_{jk}^{(2)}}{\partial x^i \partial x^k} + \frac{1}{2}\frac{\partial^2 h_{ik}^{(2)}}{\partial x^j \partial x^j} - \frac{1}{2}\nabla^2 h_{ij}^{(2)}. \tag{6.2.13}$$

Using the harmonic coordinate condition (eq. 6.2.5), eq. 6.2.13 is reduced to yield

$$R_{ij}^{(2)} = -\frac{1}{2}\nabla^2 h_{ij}^{(2)}. \tag{6.2.14}$$

The space-time component of the Ricci tensor corrections contributes odd orders only, which begin from the third order. Thus, in our case, the significant space-time component

of the Ricci tensor is of third order. So, using eq. 6.2.2 in the expansion of the space-time component of the Ricci tensor, we obtain

$$R^{(3)}_{i0} = \frac{1}{2c}\frac{\partial^2 h^{(2)}_{ij}}{\partial t \partial x^j} + \frac{1}{2}\frac{\partial^2 h^{(2)}_{0j}}{\partial x^i \partial x^j} - \frac{1}{2c}\frac{\partial^2 h^{(2)}_{jj}}{\partial t \partial x^i} - \frac{1}{2}\nabla^2 h^{(3)}_{i0}. \tag{6.2.15}$$

Using eqs. 6.2.6 & 6.2.15, $R^{(3)}_{i0}$ is recast as

$$R^{(3)}_{i0} = \frac{1}{2c}\frac{\partial^2 h^{(2)}_{ij}}{\partial t \partial x^j} - \frac{1}{4c}\frac{\partial^2 h^{(2)}_{jj}}{\partial t \partial x^i} - \frac{1}{2}\nabla^2 h^{(3)}_{i0}. \tag{6.2.16}$$

In summary, the important Ricci tensors are given by eqs. 6.2.8, 6.2.9, 6.2.14 & 6.2.16 that we recast them as

$$R^{(2)}_{00} = -\frac{1}{2}\nabla^2 h^{(2)}_{00}, \tag{6.2.17}$$

$$\begin{aligned} R^{(4)}_{00} &= -\frac{1}{2}\nabla^2 h^{(4)}_{00} + \frac{1}{2}h^{(2)}_{ij}\frac{\partial^2 h^{(2)}_{00}}{\partial x^i \partial x^j} \\ &\quad -\frac{1}{4}\left(\frac{\partial h^{(2)}_{00}}{\partial x^i}\right)^2 + \frac{1}{4}\frac{\partial h^{(2)}_{00}}{\partial x^j}\left(2\frac{\partial h^{(2)}_{ij}}{\partial x^i} - \frac{\partial h^{(2)}_{ii}}{\partial x^j}\right), \end{aligned} \tag{6.2.18}$$

$$R^{(2)}_{ij} = -\frac{1}{2}\nabla^2 h^{(2)}_{ij}, \tag{6.2.19}$$

$$R^{(3)}_{i0} = \frac{1}{2c}\frac{\partial^2 h^{(2)}_{ij}}{\partial t \partial x^j} - \frac{1}{4c}\frac{\partial^2 h^{(2)}_{jj}}{\partial t \partial x^i} - \frac{1}{2}\nabla^2 h^{(3)}_{i0}. \tag{6.2.20}$$

Note that, the Lagrangian of the system being used is determined by the underlying metric of the system; whereas, the gravitational content of the metric is imbedded in the background geometry and the perturbing potentials. To obtain the solutions of the perturbing potentials, in particular, it is important to express the exact Einstein field equations with the positive cosmological constant; where the relevant Ricci tensors (derived earlier) are being used.

So, the exact Einstein field equations in this case is given as

$$R_{\mu\nu} = \frac{8\pi G}{c^4} S_{\mu\nu}\ , \tag{6.2.21}$$

where

$$S_{\mu\nu} = T_{\mu\nu} - \frac{1}{2} g_{\mu\nu} T^{\lambda}_{\lambda} + \frac{\Lambda c^4}{8\pi G} g_{\mu\nu}. \tag{6.2.22}$$

In view of eqs. 3.1.31, 6.2.2, 6.2.17 - 6.2.22 and the developments (more on the energy momentum tensor) of the upcoming section (sec. 6.3), the significant $S_{\mu\nu}$-components relevant to the exact field equations to use are: $S^{(0)}_{00}$, $S^{(2)}_{00}$, $S^{(0)}_{ij}$ and $S^{(1)}_{i0}$, respectively given as

$$\begin{aligned}
S^{(0)}_{00} &= \frac{1}{2}\left(T^{(0)}_{00} - \frac{\Lambda c^4}{4\pi G}\right), && (6.2.23)\\
S^{(2)}_{00} &= \frac{1}{2}\left(T^{(2)}_{00} + T^{(2)}_{ii} + \frac{\Lambda c^4}{4\pi G} h^{(2)}_{00}\right), && (6.2.24)\\
S^{(0)}_{ij} &= \frac{1}{2}\delta_{ij}\left(T^{(0)}_{00} + \frac{\Lambda c^4}{4\pi G}\right), && (6.2.25)\\
S^{(1)}_{i0} &= T^{(1)}_{i0}. && (6.2.26)
\end{aligned}$$

6.3 The Energy Momentum Tensor

The contravariant form of the energy momentum tensor of n discrete particles is given as (see for example [120])

$$T^{\mu\nu} = \sum_n \frac{m_n c}{\sqrt{-g}} \frac{dx^{\mu}_n}{d\tau} \frac{dx^{\nu}_n}{dt} \delta(\mathbf{r} - \mathbf{r_n}). \tag{6.3.1}$$

Its equivalent covariant form is

$$T_{\alpha\beta} = \sum_n \frac{m_n c}{\sqrt{-g}} g_{\alpha\mu} g_{\beta\nu} \frac{dx^{\mu}_n}{d\tau} \frac{dx^{\nu}_n}{dt} \delta(\mathbf{r} - \mathbf{r_n}). \tag{6.3.2}$$

By eq. 6.3.2 the time-time component of the energy-momentum tensor is given by

$$T_{00} = \sum_n \frac{m_n c}{\sqrt{-g}} \left((g_{00})^2 \frac{dx^0_n}{d\tau} \frac{dx^0_n}{dt} + g_{0i} g_{0j} \frac{dx^i_n}{d\tau} \frac{dx^j_n}{dt} \right) \delta(\mathbf{r} - \mathbf{r_n}). \tag{6.3.3}$$

The second term of eq. 6.3.3 is of order $o(v^8)$, and hence negligible. So the significant T_{00} is given as

$$T_{00} = \sum_n \frac{m_n c^3}{\sqrt{-g}} (g_{00})^2 \frac{dt}{d\tau} \delta(\mathbf{r} - \mathbf{r_n}). \tag{6.3.4}$$

Using equations 3.1.1 & 6.3.4 we obtain

$$T_{00} = \sum_n m_n c^2 (-g)^{-1/2} (-g_{00})^{3/2} \left(1 + 2\frac{g_{0i}}{g_{00}}\frac{v_n^i}{c}\frac{g_{ij}}{g_{00}} + \frac{v_n^i v_n^j}{c^2}\right)^{-1/2} \delta(\mathbf{r} - \mathbf{r_n}), \tag{6.3.5}$$

where g, the determinant of $g_{\mu\nu}$ is given as

$$g = Det\, g_{\mu\nu} = \begin{vmatrix} g_{00} & g_{01} & g_{02} & g_{03} \\ g_{10} & g_{11} & g_{12} & g_{23} \\ g_{10} & g_{11} & g_{12} & g_{23} \\ g_{10} & g_{11} & g_{12} & g_{23} \end{vmatrix}. \tag{6.3.6}$$

In expanding equation 6.3.6, for example along the first row or the first column, the significantly relevant term is given as

$$\begin{aligned} g &\approx g_{00} \begin{vmatrix} g_{11} & g_{12} & g_{23} \\ g_{11} & g_{12} & g_{23} \\ g_{11} & g_{12} & g_{23} \end{vmatrix} \\ &= g_{00} |g_{ij}|, \end{aligned} \tag{6.3.7}$$

where $|g_{ij}|$ is the determinant of the space-space components.

Plugging eq. 6.3.7 in eq. 6.3.5, we obtain

$$T_{00} = \sum_n m_n c^2 (|g_{ij}|)^{-1/2} (-g_{00}) \left(1 + 2\frac{g_{0i}}{g_{00}}\frac{v_n^i}{c} + \frac{g_{ij}}{g_{00}}\frac{v_n^i v_n^j}{c^2}\right)^{-1/2} \delta(\mathbf{r} - \mathbf{r_n}). \tag{6.3.8}$$

Observing the diagonal property of g_{ij}, and so using equations 6.2.2 and 6.3.8, T_{00} is given as

$$T_{00} = \sum_n m_n c^2 (1 + h_{ii})^{-1/2} (1 - h_{00}) \left(1 - 2h_{0i}\frac{v_n^i}{c} - (1 + h_{00})\frac{v_n^2}{c^2} + ...\right)^{-1/2} \delta(\mathbf{r} - \mathbf{r_n}). \tag{6.3.9}$$

Finally, upon using the relation $h_{ij} = \delta_{ij} h_{00}$, the time-time component of the energy-momentum tensor to the fourth order correction in v is given by

$$T_{00} = \sum_n m_n c^2 \left(1 - \frac{5}{2}h_{00}^{(2)} + \frac{1}{2}\frac{v_n^2}{c^2} + \frac{3}{8}\frac{v_n^2}{c^2} + h_{0i}^{(3)}\frac{v_n^i}{c} - \frac{5}{2}h_{00}^{(4)} + \frac{3}{2}(h_{00}^{(2)})^2 - \frac{5}{4}h_{00}^{(2)}\frac{v_n^2}{c^2}\right)\delta(\mathbf{r} - \mathbf{r_n}). \tag{6.3.10}$$

Using eqs. 6.3.2 & 6.3.10, the zero and the second order corrections of T_{00} are respectively given by:

$$T_{00}^{(0)} = \sum_n m_n c^2 \delta(\mathbf{r} - \mathbf{r_n}), \tag{6.3.11}$$

$$T_{00}^{(2)} = \sum_n m_n c^2 \left(-\frac{5}{2}h_{00}^{(2)} + \frac{1}{2}\frac{v_n^2}{c^2}\right)\delta(\mathbf{r} - \mathbf{r_n}). \tag{6.3.12}$$

Using eqs. 6.2.2 & 6.3.2, the spatial-spatial component of the energy-momentum tensor up to the fourth order correction in v is given by

$$T_{ij} = \sum_n m_n v_n^i v_n^j \left(1 + h_{00} + \frac{v_n^2}{2c} + 2h_{i0}v_n^j c\right)\delta(\mathbf{r} - \mathbf{r_n}). \tag{6.3.13}$$

Now using eq. 6.3.13, the spatial-spatial component of the energy-momentum tensor to the second order correction in v is given by

$$T_{ij} = \sum_n m_n v_n^i v_n^j \delta(\mathbf{r} - \mathbf{r_n}). \tag{6.3.14}$$

The space-time (mixture) component of the energy-momentum tensor, by equation 6.3.2, is given by

$$T_{i0} = -T^{i0} = -\sum_n \frac{m_n c^2}{\sqrt{-g}} v_n^i \frac{dt}{d\tau}\delta(\mathbf{r} - \mathbf{r_n}). \tag{6.3.15}$$

Expanding $d\tau$ and g with similar procedures as contemplated in earlier discussions, the space-time energy-momentum tensor component, T_{i0}, to the third order correction in v is given by

$$T_{i0} = -\sum_n m_n v_n^i c \left(1 + \frac{v^2}{2c^2} - h_{00}^{(2)}\right)\delta(\mathbf{r} - \mathbf{r_n}). \tag{6.3.16}$$

To the second order in v, T_{i0} is given by

$$T_{i0} = -\sum_n m_n v_n^i c\delta(\mathbf{r} - \mathbf{r_n}). \tag{6.3.17}$$

6.4 Solutions of the perturbing potentials

As we have discussed in previous sections, the perturbing potentials are part of the contents of gravitation that were used to define the exact Einstein field equations. Thus, the solutions of the perturbing potentials are expected to be derived from the exact EFEs. Moreover, the intended boundary conditions so far discussed should be used appropriately.

Accordingly, using eqs. 6.2.17-6.2.26, the corresponding correlations among the Ricci and effective energy-momentum tensors being used to derive the perturbing potentials are given by

$$R_{00}^{(2)} = \frac{4\pi G}{c^4}\left(T_{00}^{(0)} - \frac{\Lambda c^4}{4\pi G}\right), \tag{6.4.1}$$

$$R_{00}^{(4)} = \frac{4\pi G}{c^4}\left(T_{00}^{(2)} + T_{ii}^{(2)} + \frac{\Lambda c^4}{4\pi G}h_{00}^{(2)}\right), \tag{6.4.2}$$

$$R_{ij}^{(2)} = \frac{4\delta_{ij}\pi G}{c^4}\left(T_{00}^{(0)} + \frac{\Lambda c^4}{4\pi G}\right), \tag{6.4.3}$$

$$R_{i0}^{(3)} = \frac{8\pi G}{c^4}T_{i0}^{(1)}. \tag{6.4.4}$$

1) The second order time-time component perturbing potential: $h_{00}^{(2)}$

Using equations 6.2.17, 6.3.11 and 6.4.1 we obtain

$$\nabla^2 h_{00}^{(2)} = -\frac{8\pi G}{c^4}\left(\sum_n m_n c^2\delta(\mathbf{r} - \mathbf{r_n}) - \frac{\Lambda c^4}{4\pi G}\right). \tag{6.4.5}$$

The relation

$$\nabla^2\left(\frac{1}{\mid \mathbf{r} - \mathbf{r}_n \mid}\right) = -4\pi\delta(\mathbf{r} - \mathbf{r}_n), \tag{6.4.6}$$

is used to re-express equation 6.4.5 as

$$\nabla^2 h_{00}^{(2)} = \frac{2}{c^2}\left(\nabla^2\left\{G\sum_n \frac{m_n}{\mid \mathbf{r}-\mathbf{r}_n \mid}\right\} + \Lambda c^2\right). \tag{6.4.7}$$

The embraced expression in equation 6.4.7 is noticeably the negative of the first kind of Newtonian potential. So, we will attempt to write a modified potential of the form

$$\Phi = \Phi_{_N} + \Phi_{_\Lambda}, \tag{6.4.8}$$

where $\Phi_{_N}$ is the classical Newtonian potential given by

$$\Phi_{_N} = -G\sum_n \frac{m_n}{\mid \mathbf{r}-\mathbf{r}_n \mid}. \tag{6.4.9}$$

$\Phi_{_\Lambda}$ is the potential that arises as the first kind from cosmological constant.

Using the relation

$$\nabla^2 r^2 = 6, \tag{6.4.10}$$

the potential that arises as the first kind from cosmological constant is given by

$$\Phi_{_\Lambda} = -\frac{\Lambda\, c^2}{6} r^2. \tag{6.4.11}$$

Now, using eqs. 6.4.8, 6.4.9 & 6.4.11 eq. 6.4.7 can be recast as

$$\nabla^2 h_{00}^{(2)} = -\frac{2}{c^2}\nabla^2\Phi. \tag{6.4.12}$$

Then, eq. 6.4.12 immediately yields the solution of $h_{00}^{(2)}$ given by

$$h_{00}^{(2)} = -\frac{2}{c^2}\Phi \tag{6.4.13}$$

The corresponding first class Newtonian and Λ-content potentials are respectively given by

$$h_{00}^{N(2)} = -\frac{2}{c^2}\Phi_{_N}, \tag{6.4.14}$$

$$h_{00}^{\Lambda(2)} = -\frac{2}{c^2}\Phi_{_\Lambda}. \tag{6.4.15}$$

2) The second order space-space component perturbing potential: $h_{ij}^{(2)}$

Evaluating eq. 6.2.17 to 6.4.1, 6.2.19 to 6.4.3, and then combining the results yield

$$\nabla^2 h_{ij}^{(2)} = \delta_{ij}\,(\nabla^2 h_{00}^{(2)} - 4\,\Lambda). \tag{6.4.16}$$

Now, using eqs. 6.4.7 - 6.4.9, 6.4.12, 6.4.16 we obtain

$$\nabla^2 h_{ij}^{(2)} = -\delta_{ij}\,\frac{2}{c^2}\,\nabla^2\Phi', \tag{6.4.17}$$

where Φ' is given by

$$\Phi' = \Phi_{_N} - \Phi_{_\Lambda} \tag{6.4.18}$$

Therefore, the solution of $h_{ij}^{(2)}$ is given by

$$h_{ij}^{(2)} = -\delta_{ij}\,\frac{2}{c^2}\,\Phi' \tag{6.4.19}$$

3) The fourth order time-time component perturbing potential: $h_{00}^{(4)}$

Evaluating eq. 6.2.18 to eq. 6.4.2 and then developing it further using equations 6.3.12, 6.3.14, 6.4.13 and 6.4.19, we obtain

$$\begin{aligned}\nabla^2 h_{00}^{(4)} - \frac{4}{c^4}\,\Phi'\nabla^2\Phi + \frac{2}{c^4}\left(\frac{\partial\Phi}{\partial x^i}\right)^2 + \frac{2}{c^4}\left(\frac{\partial\Phi}{\partial x^i}\right)\left(\frac{\partial\Phi'}{\partial x^i}\right)\\ = -\frac{8\pi G}{c^4}\left(\sum_n m_n\left\{5\frac{\Phi}{c^2} + \frac{3}{2}v_n^2\right\}\delta(\mathbf{r}-\mathbf{r_n}) + \frac{\Phi\nabla^2\Phi_{_\Lambda}}{2\pi G}\right).\end{aligned} \tag{6.4.20}$$

Using the relation given by equation 6.4.6 and the relations

$$\frac{\partial^2}{\partial x^2}\left(\Phi^2\right) = \nabla^2\left(\Phi^2\right) = 2\left(\frac{\partial\Phi}{\partial x}\right)^2 + 2\Phi\nabla^2\Phi, \tag{6.4.21}$$

$$\Phi' = \Phi_{_N} - \Phi_{_\Lambda} = \Phi - 2\Phi_{_\Lambda}, \tag{6.4.22}$$

$$\nabla^2(\Phi\Phi_{_\Lambda}) = 2\left(\frac{\partial\Phi_{_\Lambda}}{\partial x^i}\right)\left(\frac{\partial\Phi}{\partial x^i}\right) + \Phi\nabla^2\Phi_{_\Lambda} + \Phi_{_\Lambda}\nabla^2\Phi, \tag{6.4.23}$$

in equation 6.4.20 we get

$$\nabla^2\left(h_{00}^{(4)}+\frac{2\,\Phi^2}{c^4}-\frac{2\,\Phi_{_\Lambda}\Phi}{c^4}\right)=-\frac{8\pi G}{c^4}\sum_n m_n\left(\frac{\Phi^s}{c^2}+\frac{3}{2}v_n^2\right)\delta(\mathbf{r}-\mathbf{r_n})+\nabla^2\Phi^c. \tag{6.4.24}$$

Φ^c is the additional coupling between the Newtonian and that of cosmological constant potentials of order $\Phi_{_\Lambda}\Phi$. Φ^s is the second potential due to the other particle, which upon using equations 6.4.8, 6.4.9 and 6.4.11 is given by

$$\Phi^s=-G\sum_{n\prime}\frac{m_{n\prime}}{\mid\mathbf{r}_n-\mathbf{r}_{n'}\mid}-\frac{\Lambda c^2}{6}\mathbf{r}_n^2. \tag{6.4.25}$$

Using the relation given by eq. 6.4.6, eq. 6.4.24 can be recast as

$$\nabla^2\left(h_{00}^{(4)}+\frac{2\Phi^2}{c^4}-\frac{2\Phi_{_\Lambda}\Phi}{c^4}\right)=\nabla^2\left(\frac{2G}{c^4}\sum_n\frac{m_n\Phi_n^s}{\mid\mathbf{r}-\mathbf{r}_n\mid}+\frac{3\,G}{c^4}\sum_n\frac{m_nv_n^2}{\mid\mathbf{r}-\mathbf{r}_n\mid}+\Phi^c\right). \tag{6.4.26}$$

Finally, by equation 6.4.26, the solution of $h_{00}^{(4)}$ is given by

$$h_{00}^{(4)}=-\frac{2\,\Phi^2}{c^4}+\frac{2\Phi_{_\Lambda}\Phi}{c^4}+\frac{2\,G}{c^4}\sum_n\frac{m_n\Phi_n^s}{\mid\mathbf{r}-\mathbf{r}_n\mid}+\frac{3\,G}{c^4}\sum_n\frac{m_nv_n^2}{\mid\mathbf{r}-\mathbf{r}_n\mid}+\Phi^c. \tag{6.4.27}$$

4) The third order time-space component perturbing potential: $h_{i0}^{(3)}$

Relating eq. 6.2.20 to eq. 6.4.4, we get

$$\frac{1}{2\,c}\frac{\partial^2h_{ij}^{(2)}}{\partial t\partial x^j}-\frac{1}{4\,c}\frac{\partial^2h_{jj}^{(2)}}{\partial t\partial x^i}-\frac{1}{2}\nabla^2h_{i0}^{(3)}=\frac{8\pi G}{c^4}T_{i0}^{(1)}. \tag{6.4.28}$$

Now, plugging the solution of $h_{ij}^{(2)}$ (eq. 6.4.19) and the relevant energy momentum tensor $T_{i0}^{(3)}$ given by eq. 6.3.17 into eq. 6.4.28, we obtain

$$\nabla^2h_{i0}^{(3)}=\frac{16\pi G}{c^4}\sum_n m_nv_n^ic\,\delta(\mathbf{r}-\mathbf{r}_n)+\frac{1}{c^3}\frac{\partial^2\Phi'}{\partial t\partial x^i}. \tag{6.4.29}$$

Using the relation given by eq. 6.4.6 in eq. 6.4.29 and then regrouping, we obtain

$$\nabla^2\left(h_{i0}^{(3)}+\frac{4\,G}{c^3}\sum_n\frac{m_nv_n^i}{\mid\mathbf{r}-\mathbf{r}_n\mid}\right)=\frac{1}{c^3}\frac{\partial^2\Phi'}{\partial t\partial x^i}. \tag{6.4.30}$$

Since we are looking for linear solutions, therefore, we reconstruct equation 6.4.30 as

$$\nabla^2 \left(h_{i0}^{(3)} + \frac{4\,G}{c^3} \sum_n \frac{m_n v_n^i}{\mid \mathbf{r} - \mathbf{r}_n \mid} \right) = \nabla^2 \left(\frac{1}{c^3} \frac{\partial^2 f}{\partial t \partial x^i} \right). \tag{6.4.31}$$

Then, the linear solution to $h_{i0}^{(3)}$ is given by

$$h_{i0}^{(3)} = -\frac{4\,G}{c^3} \sum_n \frac{m_n v_n^i}{\mid \mathbf{r} - \mathbf{r}_n \mid} + \frac{1}{c^3} \frac{\partial^2 f}{\partial t \partial x^i}, \tag{6.4.32}$$

where the auxiliary solution to f is obviously given by

$$\nabla^2 f = \Phi' = \Phi_{_N} + \Phi_{_\Lambda} = -G \sum_n \frac{m_n}{\mid \mathbf{r} - \mathbf{r}_n \mid} + \frac{\Lambda\, c^2}{6}\, \mathbf{r}^2. \tag{6.4.33}$$

Using the relations (in static spherical coordinates)

$$\nabla^2 r = \frac{2}{r}, \tag{6.4.34}$$

$$\nabla^2 r^4 = 20\, r^2, \tag{6.4.35}$$

f is given by

$$f = -\frac{G}{2} \sum_n m_n \mid \mathbf{r} - \mathbf{r}_n \mid + \frac{\Lambda\, c^2}{120}\, r^4. \tag{6.4.36}$$

Plugging eq. 6.4.36 into eq. 6.4.32, we obtain

$$h_{i0}^{(3)} = -\frac{G}{2\,c^3} \sum_n m_n \left(\frac{8\, v_n^i}{|\mathbf{r} - \mathbf{r}_n|} + \frac{\partial^2}{\partial t \partial x^i} |\mathbf{r} - \mathbf{r}_n| \right) + \frac{\Lambda}{120\, c} \left(\frac{\partial^2}{\partial t\, \partial x^i}\, \mathbf{r}^4 \right). \tag{6.4.37}$$

A further simplification of $h_{i0}^{(3)}$ will be obtained upon simplifying the expressions $(\frac{\partial^2}{\partial t\, \partial x^i}\, R)$ and $(\frac{\partial^2}{\partial t\, \partial x^i}\, \mathbf{r}^4)$ of eq. 6.4.37; where $\mathbf{r} - \mathbf{r}_n$ is represented by $\mathbf{R}$, while its corresponding magnitude $|\mathbf{r} - \mathbf{r}_n|$ is represented by R.

By vector algebra we will immediately derive the relation

$$\frac{\partial R}{\partial t} = \mathbf{v}_{_R} \cdot \hat{\mathbf{u}}_{_R}\,, \tag{6.4.38}$$

where $\mathbf{v}_{_R}$ is the difference in velocity between the particles located at $\mathbf{r}_n$ and $\mathbf{r}$ whose direction is parallel to $\mathbf{R}$, and $\hat{\mathbf{u}}_{_R}$ is the unit vector along $\mathbf{R}$.

Then, using eq. 6.4.38, the expression ($\frac{\partial^2}{\partial t\,\partial x^i}R$) will be given by

$$\frac{\partial^2 R}{\partial t\,\partial x^i} = \frac{\partial}{\partial x^i}\mathbf{v}_{_R}\cdot\hat{\mathbf{u}}_{_R} + \mathbf{v}_{_R}\cdot\frac{\partial}{x^i}\hat{\mathbf{u}}_{_R}. \tag{6.4.39}$$

With little algebra, $\frac{\partial}{x^i}\mathbf{v}_{_R}$ and $\frac{\partial}{x^i}\hat{\mathbf{u}}_{_R}$ are respectively given by

$$\frac{\partial}{\partial x^i}\mathbf{v}_{_R} = \left(\frac{v^i_{_R} - u^i_{_R}(\mathbf{v}_{_R}\cdot\hat{\mathbf{u}}_{_R})}{R}\right)\hat{\mathbf{u}}_i, \tag{6.4.40}$$

$$\frac{\partial}{\partial x^i}\hat{\mathbf{u}}_{_R} = \frac{u^i_{_R}}{R}\left(\hat{\mathbf{u}}_i - \hat{\mathbf{u}}\right). \tag{6.4.41}$$

Now using eqs. 6.4.40 - 6.4.41 and expressing $\mathbf{v}_{_R}$ in terms of $\mathbf{v}_{_n}$, eq. 6.4.39 is recast as

$$\frac{\partial^2 R}{\partial t\,\partial x^i} = \frac{-v^i_{_n} + u^i_{_n}(\mathbf{v}_{_n}\cdot\hat{\mathbf{u}}_{_n})}{|\mathbf{r}-\mathbf{r}_n|}. \tag{6.4.42}$$

With similar procedure, but less effort, the expression ($\frac{\partial^2}{\partial t\,\partial x^i}\,\mathbf{r}^4$) is given by

$$\frac{\partial^2}{\partial t\,\partial x^i}\,\mathbf{r}^4 = 4\,r^2\left(v^i_n + 2\,(\mathbf{v}_{_n}\cdot\hat{\mathbf{u}}_{_n})u^i_{_n}\right). \tag{6.4.43}$$

Finally, using eqs. 6.4.37, 6.4.42 and 6.4.43, $h^{(3)}_{i0}$ given by

$$\begin{aligned} h^{(3)}_{i0} &= -\frac{G}{2\,c^3}\sum_n \frac{m_n}{|\mathbf{r}-\mathbf{r}_n|}\left(7\,v^i_n + u^i_{_n}(\mathbf{v}_{_n}\cdot\hat{\mathbf{u}}_{_n})\right) \\ &\quad + \frac{\Lambda}{30\,c}\,r^2\left(v^i_n + 2\,(\mathbf{v}_{_n}\cdot\hat{\mathbf{u}}_{_n})u^i_{_n}\right). \end{aligned} \tag{6.4.44}$$

6.5 Lagrangian of the System

The Lagrangian of a particle in the gravitational field of another particle is given by

$$L_n = -m_n c\,\frac{d\tau}{dt}. \tag{6.5.1}$$

Using eqs. 3.1.1, 6.2.2 and 6.5.1 the Lagrangian of the system to the fourth order correction in v is given by

$$L_n = -m_n c^2 \left(1 - h_{00} - 2\,h_{0i}\frac{v_n^i}{c} - (\delta_{ij} + h_{ij})\frac{v_n^i v_n^j}{c^2}\right)^{1/2}. \tag{6.5.2}$$

Using Taylor expansion, and then neglecting the rest mass energy, eq. 6.5.2 yields

$$\begin{aligned} L_n &= m_n c^2 \left(\frac{h_{00}^{(2)} + h_{00}^{(4)}}{2} + h_{0i}^{(3)}\frac{v_n^i}{c} + \frac{1}{2}h_{ij}^{(2)}\frac{v_n^i v_n^j}{c^2} + \frac{(h_{00}^{(2)})^2}{8} + \frac{h_{00}^{(2)}}{4}\frac{v_n^2}{c^2}\right) \\ &\quad + \frac{m_n v_n^2}{2} + \frac{m_n v_n^4}{8\,c^2}. \end{aligned} \tag{6.5.3}$$

The net force acting on one of the particles (say the n' particle) due to the others is given by

$$\mathbf{f}_{\mathbf{n}'} = \left(\frac{\partial L_{n'}}{\partial \mathbf{r}}\right)_{\mathbf{r}=\mathbf{r}_{n'}}. \tag{6.5.4}$$

Then, the total Lagrangian of n system of interacting particles is given by

$$L = \sum_n \int \left(\frac{\partial L_{n'}}{\partial \mathbf{r}}\right)_{\mathbf{r}=\mathbf{r}_{n'}} dr. \tag{6.5.5}$$

Equation 6.5.5 will be used to normalize sufficiently far away distances (in the vicinity the intended boundaries as outlined in the previous discussions) to interacting distances. Then, the proper Lagrangian of the system is given by

$$L = \sum_n (L_{n'})_{\mathbf{r}=\mathbf{r}'_n}, \tag{6.5.6}$$

where $L_{n'}$ is given by eq 6.5.3.

Plugging the simplified forms of the perturbing potentials, $h_{00}^{(2)}$, $h_{ij}^{(2)}$, $h_{00}^{(4)}$ and $h_{i0}^{(3)}$ respectively given by equations 6.4.13, 6.4.19 , 6.4.27 and 6.4.44 in equation 6.5.3 will provide the appropriate Lagrangian of one of the n system of particles. Then, using the result

in equation 6.5.6, a little vector algebra will provide the simplified final form of the total Lagrangian of the n body system given by

$$\begin{aligned} L &= \sum_n \frac{m_n v_n^2}{2}\left(1+3\sum_{n'}\frac{G m_{n'}}{c^2\, r_{nn'}}\right)+\sum_n \frac{m_n v_n^4}{8\,c^2}+\sum_n\sum_{n'}\frac{G m_n m_{n'}}{2\, r_{nn'}} \\ &\quad -\sum_n\sum_{n'}\frac{G m_n m_{n'}}{4\,c^2 r_{nn'}}\left(7\,\mathbf{v}_n\cdot\mathbf{v}_{n'}+(\mathbf{v}_n\cdot\hat{\mathbf{u}}_{nn'})(\mathbf{v}_n\cdot\hat{\mathbf{u}}_{nn'})\right)+\sum_n\frac{\Lambda c^2\, m_n r_n^2}{6} \\ &\quad -\sum_n\sum_{n'}\sum_{n''}\frac{G^2 m_n m_{n'} m_{n''}}{2\,c^2\, r_{nn'}\, r_{nn''}}+\sum_n\frac{\Lambda\, m_n}{30}\, r_n^2\,(v_n^2+2\,(\mathbf{v}_n\cdot\hat{\mathbf{u}}_n)^2) \\ &\quad -\sum_n\sum_{n'}\frac{G\Lambda m_n m_{n'}}{12\,c^2 r_{nn'}}\, r_n^2+\sum_n\frac{\Lambda^2 c^2 m_n r_n^4}{72}-\sum_n\frac{\Lambda m_n v_n^2 r_n^2}{12}, \end{aligned} \tag{6.5.7}$$

where n stands for the first particle and n' stands for the second particle in the interaction while $n''=n$ or $n''=n'$.

The center of mass $\mathbf{R}_{cm}$ of the system in the second order correction in v in the presence of Λ is given by

$$\mathbf{R}_{cm}=\frac{1}{E}\sum_n \mathbf{r}_n\left(m_n c^2+\frac{m_n v_n^2}{2}-{\sum_{n'}}'\frac{G\, m_n m_{n'}}{2\, r_{nn'}}-\frac{\Lambda c^2\, m_n r_n^2}{6}\right). \tag{6.5.8}$$

E is the total energy of the system to second order correction in v in the modified Newtonian potential due to cosmological constant. Perhaps, the order correction in Λ will be even much less than the second order correction in v. However, the inclusion of Λ benefits to see whether there is any significant effect due to its appearance in any of the contributing terms in the final result. Thus, with this remark E is given by

$$E=\sum_n\left(m_n c^2+\frac{m_n v_n^2}{2}-{\sum_{n'}}'\frac{G\, m_n m_{n'}}{2\, r_{nn'}}-\frac{\Lambda c^2\, m_n r_n^2}{6}\right). \tag{6.5.9}$$

6.6 The two body problem

In this section we derive the Lagrangian of gravitationally interacting two massive spineless uncharged particles. Then, using the resulting Lagrangian we derive the Hamiltonian of the system. Finally, applying Hamilton-Jacobi equations we derive the precession of the orbits of two body system.

6.6.1 Lagrangian, Hamiltonian and radial momentum of the system

The Lagrangian of the two body system in the SdS metric will be derived from eq. 6.5.7, by putting $n = 1$, $n' = 2$ and $n'' = 1$ or $n'' = 2$. Then we have,

$$\begin{aligned} L &= \frac{m_1 v_1^2}{2} + \frac{m_2 v_2^2}{2} + \frac{1}{8\,c^2}\,(m_1 v_1^4 + m_2 v_2^4) \\ &\quad + \frac{G\,m_1 m_2}{r} - \frac{G^2\,m_1 m_2 (m_1 + m_2)}{2\,c^2\,r^2} \\ &\quad + \frac{G\,m_1 m_2}{2\,c^2\,r}\left(3\,(v_1^2 + v_2^2) - 7\,\mathbf{v}_1\cdot\mathbf{v}_2 - (\mathbf{v}_1\cdot\hat{\mathbf{u}})(\mathbf{v}_2\cdot\hat{\mathbf{u}})\right) \\ &\quad + \frac{\Lambda c^2}{6}(m_1 r_1^2 + m_2 r_2^2) + \frac{\Lambda}{60}\,(m_1 v_1^2 r_1^2 + m_2 v_2^2 r_2^2) \\ &\quad - \frac{G\,\Lambda\,m_1 m_2}{12\,c^2\,r}(r_1^2 + r_2^2) + \frac{\Lambda^2\,c^2}{72}\,(m_1 r_1^4 + m_2 r_2^4), \end{aligned} \tag{6.6.1}$$

where r is the distance between the particles.

The Lagrangian is used to develop the simplified forms of the Hamiltonian and the radial momentum of the system. In the simplifying processes, certainly there exist various approaches; where a vanishing net linear momentum about the center of mass of the system is the most common technique adopted. In the case of two-body system, the equivalent of vanishing net linear momentum about the center of mass of the system is the same as:

$$\mathbf{p}_1 + \mathbf{p}_2 = 0, \tag{6.6.2}$$

where, $\mathbf{p}_1$ and $\mathbf{p}_2$ are the linear momenta of particle 1 and 2 respectively.

The Hamiltonian of the system will be derived from the Legendre transform of the Lagrangian,

$$H = \sum_i \dot{q}_i p_i - L, \tag{6.6.3}$$

where $\dot{q}_i$ is the velocity of the i's particle in the generalized coordinate q.

Now representing $\mathbf{p}_1$ by $\mathbf{p}$ and then using equations 6.6.1 - 6.6.3, the Hamiltonian of the system about the center of mass up on considering the perturbing potentials to the fourth order correction in v is given by

$$\begin{aligned}
\mathcal{H} \;=\; & \frac{p^2}{2\mu} - \frac{G\mu M}{r} - \frac{p^4}{8\,c^2\mu^3}\left(1 - \frac{3\mu}{M}\right) \\
& -\frac{G}{2\,c^2 r}\left(p^2\,(1+\frac{3M}{\mu}) + (\mathbf{p}\cdot\hat{\mathbf{u}})^2\right) + \frac{G^2\mu M^2}{2\,c^2 r^2} \\
& -\frac{\Lambda c^2}{6}(m_1 r_1^2 + m_2 r_2^2) - \frac{\Lambda\, p^2}{60\,\mu\, M}\left(m_2 r_1^2 + m_1 r_2^2\right) \\
& +\frac{G\Lambda\mu M}{12\,c^2 r}(r_1^2 + r_2^2) - \frac{\Lambda^2 c^2}{72}(m_1 r_1^4 + m_2 r_2^4),
\end{aligned} \tag{6.6.4}$$

where M and μ are the total and reduced masses, respectively given by

$$M = m_1 + m_2;\;\; \mu = \frac{m_1 m_2}{m_1 + m_2}. \tag{6.6.5}$$

The Post-Newtonian radial momentum $\mathbf{p}_r$ in terms of the constants of motion, the total energy E, the total angular momentum $\mathbf{J}$ and the cosmological constant Λ will be derived as follows:

1. Since the system is conservative, $\mathcal{H} = E$.

2. The total momentum $\mathbf{p}$ is given by:

$$\mathbf{p}^2 = \mathbf{p}_\phi^2 + \mathbf{p}_{rad}^2 \tag{6.6.6}$$

where $\mathbf{p}_\phi$ is the azimuthal component of the momentum given by:

$$\mathbf{p}_\phi^2 = \frac{\mathbf{J}^2}{r^2}, \tag{6.6.7}$$

whereas $\mathbf{p}_{rad}$ is the radial component composed of the Newtonian momentum $\mathbf{p}_r$ and that resulted from the corresponding cosmological constant. In view of equation 4.1.10 it is given by:

$$\mathbf{p}_{rad}^2 = \mathbf{p}_r^2 - \frac{\Lambda c^2}{3}(\mathbf{r}_1^2 + \mathbf{r}_2^2). \tag{6.6.8}$$

3. Following the method by [153] the higher Post-Newtonian potential terms will be reasonably approximated by the second order energy corrections as seen by equation 6.5.9.

4. Finally, using the center of mass motion equation where the velocity $V_{cm} = dR_{cm}/dt$ vanishes, after a vigorous algebraic calculations 6.6.4 be recast as:

$$\begin{aligned} E &= \frac{1}{2\mu}\left(\mathbf{p}_r^2 + \frac{\mathbf{J}^2}{r^2}\right) - \frac{G\mu M}{r} - \frac{1}{2c^2\mu}\left(1 - \frac{3\mu}{M}\right)\left(E + \frac{G\mu M}{r}\right)^2 - \frac{G}{2c^2 r}\mathbf{p}_r^2 \\ &\quad - \frac{G\mu}{c^2 r}\left(1 + \frac{3M}{\mu}\right)\left(E + \frac{G\mu M}{r}\right) + \frac{G^2\mu M^2}{2c^2 r^2} - \frac{\Lambda c^2 \mu\, r^2}{2} + F(\Lambda, m_1, m_2), \end{aligned} \tag{6.6.9}$$

where higher order terms free of Λ are kept to fourth order in v, while the other higher order correction terms both linear and conjugated to Λ are being represented by $F(\Lambda, m_1, m_2)$.

Then, neglecting higher order terms and involving some little algebra we obtain the required p_r compactly given as

$$p_r = \int \sqrt{\alpha(r) + \frac{\delta_E}{r^2} + \delta_\Lambda\, r^2}, \tag{6.6.10}$$

where the function $\alpha(r)$ and the small constants δ_E and δ_Λ are given by

$$\alpha(r) = A + \frac{B}{r} - \frac{J^2}{r^2}; \quad \delta_E = \frac{6G^2\mu^2 M^2}{c^2}; \quad \delta_\Lambda = \Lambda c^2 \mu^2. \tag{6.6.11}$$

A and B are constants given by

$$\begin{aligned} A &= 2\mu E + \frac{E^2}{c^2}\left(1 - \frac{3\mu}{M}\right); \\ B &= 2G\mu^2\left(M - \frac{E}{c^2}\right) + \frac{G\mu E}{c^2}\left(8M + \frac{E}{c^2}(1 - \frac{3\mu}{M})\right). \end{aligned} \tag{6.6.12}$$

6.6.2 Precession of orbits of two-body system

In this section we derive the precession of orbits of two-body system using Hamilton-Jacobi Equation. The Hamiltonian of the system is as given by equation 6.6.4 from which we have already developed the conjugate radial momentum. So, here, we need only the form of the trajectory equation.

The Hamilton-Jacobi equation for a massive particle in a centrally symmetric gravitational field is given by:

$$g^{\mu\nu}\frac{\partial S}{\partial x^\mu}\frac{\partial S}{\partial x^\nu} + mc^2 = 0, \tag{6.6.13}$$

where S is the action that generates the Hamiltonian.

Following the standard method, generally the action assumes of the form:

$$S = -E_0 t + J\phi + S_r, \tag{6.6.14}$$

where E_0 is the total zero order energy of the system, J is the angular momentum of the system, ϕ is the angular position and S_r is component of the action that depends only on radial position.

The trajectory of a particle in such centrally symmetric system is given by

$$\frac{\partial S}{\partial J} = \text{constant}. \tag{6.6.15}$$

Using equations 6.6.14 and 6.6.15, the trajectory is given by

$$\phi = \text{constant} - \frac{\partial S_r}{\partial J}. \tag{6.6.16}$$

By Hamilton-Jacobi canonical momentum equations p_r is given as:

$$p_r = \frac{\partial S}{\partial r} = \frac{\partial S_r}{\partial r}. \tag{6.6.17}$$

Then,

$$S_r = \int p_r dr, \tag{6.6.18}$$

where p_r is given by equation 6.6.10.

Taylor expansion of p_r with respect to the small quantities δ_E and δ_Λ and then using the first order approximation, S_r is given by

$$\begin{aligned} S_r &= \int \sqrt{\alpha(r)}\, dr + \frac{\delta_E}{2} \int \frac{dr}{r^2\sqrt{\alpha(r)}} + \frac{\delta_\Lambda}{2} \int \frac{r^2 dr}{\sqrt{\alpha(r)}} \\ &= S_r^{(0)} - \frac{\delta_E}{2\,J} \frac{\partial S_r^{(0)}}{\partial J} + \frac{\delta_\Lambda}{2} \int \frac{r^2 dr}{\sqrt{\alpha(r)}}, \end{aligned} \tag{6.6.19}$$

where

$$S_r^{(0)} = \int \sqrt{\alpha(r)}\, dr \tag{6.6.20}$$

corresponds to the Newtonian ellipse.

The last term of eq. 6.6.19 will be transformed to an easily integrable form upon using the elliptical orbit equation

$$r = \frac{a(1-e^2)}{1 + e\cos\phi}, \tag{6.6.21}$$

where a is the semi-major axis, e the eccentricity and ϕ is the true anomalous angle of the ellipse. Thus, using eqs. 6.6.11 and 6.6.21, $S_r^{(\Lambda)}$ is given as

$$S_r^{(\Lambda)} = \frac{\delta_\Lambda}{2} \int \frac{r^2 dr}{\sqrt{\alpha(r)}} \to \frac{\delta_\Lambda}{2} \int_0^\pi \frac{\varepsilon(e)\,\kappa(J)\,\sin\phi\, d\phi}{\Big(\chi(J) + \varepsilon(e)\cos\phi\Big)^4 \sqrt{1 - \varepsilon^2(e)\cos^2\phi}} = \frac{\delta_\Lambda}{2} F(J). \tag{6.6.22}$$

where the parameters $\kappa(J)$, $\chi(J)$ and $\varepsilon(e)$ are given by

$$\kappa(J) = \frac{16\,J^7}{B^4}\chi(\mathrm{J}); \quad \chi(J) = \frac{B}{\sqrt{B^2 + 4AJ^2}}; \quad \varepsilon(e) = \frac{e}{\sqrt{2-e^2}}. \tag{6.6.23}$$

$F(J)$ is the integration result compactly given by

$$F(J) = \kappa(J) f\left(\chi(J)\right) \tag{6.6.24}$$

where the function $f\left(\chi(J)\right)$ is given as

$$f\left(\chi(J)\right) = \left\{ \begin{array}{l} \dfrac{\varepsilon\sqrt{1-\varepsilon^2}\,(3\chi^2(2-6\chi^2+9\chi^4)+2\varepsilon^2(1-\chi^2-15\chi^4)+\varepsilon^4(4+11\chi^2))}{(1-\chi^2)^3(\chi^2-\varepsilon^2)^3} \\ + \dfrac{\chi\,(3+2\,\chi^2)}{2(1-\chi^2)^{7/2}} \ln\left[\dfrac{\chi^2\,(1-2\varepsilon^2)+2\,\chi\,\varepsilon\sqrt{(1-\chi^2)\,(1-\varepsilon^2)}+\varepsilon^2}{(\chi^2-\varepsilon^2)}\right] \end{array} \right\}. \tag{6.6.25}$$

Now using eqs. 6.6.19 - 6.6.22 $\triangle S_r$ is given by

$$\begin{aligned} \triangle S_r &= \triangle S_r^{(0)} - \frac{\delta_E}{2}\triangle\Big(\frac{1}{J}\frac{\partial S_r^{(0)}}{\partial J}\Big) + \frac{\delta_\Lambda}{2}\triangle F(J) \\ &= \triangle S_r^{(0)} - \frac{\delta_E}{2J^2}\frac{\partial S_r^{(0)}}{\partial J}\triangle J - \frac{\delta_E}{2J}\frac{\partial \triangle S_r^{(0)}}{\partial J} + \frac{\delta_\Lambda}{2}\frac{\partial F(J)}{\partial J}\triangle J. \end{aligned} \tag{6.6.26}$$

The precession of the orbit of the binary about its center of mass in terms of the angular change $\Delta\phi$ per revolution by equation 6.6.16 is given by

$$\begin{aligned} \triangle\phi &= -\triangle\left(\frac{\partial S_r}{\partial J}\right) = -\frac{\partial}{\partial J}(\triangle S_r), \\ &= -\frac{\partial \triangle S_r^{(0)}}{\partial J} + \frac{\partial}{\partial J}\left(\frac{\delta_E}{2J^2}\frac{\partial S_r^{(0)}}{\partial J}\triangle J\right) - \frac{\delta_E}{2J^2}\frac{\partial \triangle S_r^{(0)}}{\partial J} \\ &\quad -\frac{\delta_\Lambda}{2}\frac{\partial^2 F(J)}{\partial J^2}\triangle J - \frac{\delta_\Lambda}{2}\frac{\partial F(J)}{\partial J}\frac{\partial \triangle J}{\partial J}. \end{aligned} \tag{6.6.27}$$

Neglecting higher order corrections in both, with and without Λ, eq. 6.6.27 will be recast as

$$\triangle\phi = -\frac{\partial \triangle S_r^{(0)}}{\partial J} - \frac{\delta_E}{2J^2}\frac{\partial \triangle S_r^{(0)}}{\partial J} - \frac{\delta_\Lambda}{2}\frac{\partial F(J)}{\partial J}\frac{\partial \triangle J}{\partial J}. \tag{6.6.28}$$

Since, $\triangle S_r^{(0)}$ is the zero order change corresponding to the fixed Newtonian ellipse (see for example [153]) so that

$$\triangle\phi^{(0)} = -\frac{\partial \Delta S_r^{(0)}}{\partial J} = \frac{\partial \triangle J}{\partial J} = 2\pi. \tag{6.6.29}$$

Using eqs. 6.6.11, 6.6.28 - 6.6.29, the total angular change becomes

$$\triangle\phi = 2\pi + \frac{6\pi G^2\mu^2 M^2}{J^2c^2} - \pi\Lambda c^2\mu^2\,\frac{\partial F(J)}{\partial J}. \tag{6.6.30}$$

Obviously, the second term is the well known orbit change due to mass gravitation given by

$$\triangle\phi_E = \frac{6\pi G^2\mu^2 M^2}{J^2c^2}, \tag{6.6.31}$$

while the third term is the angular change contribution from the dark energy sector (in the form of cosmological constant) given by

$$\triangle\phi_\Lambda = -\pi\Lambda c^2\mu^2\,\frac{\partial F(J)}{\partial J}. \tag{6.6.32}$$

Expressing J and F as a function of χ, $\frac{\partial F(J)}{\partial J}$ will be given as

$$\frac{\partial F(J)}{\partial J} = -\frac{B^2}{4A^3}\frac{(1-\chi^2)^3}{\chi^2}\left((4\chi^2+3)f(\chi) - \chi(1-\chi^2)\frac{\partial f(\chi)}{\partial\chi}\right) \tag{6.6.33}$$

Finally, using eqs. 6.6.25 and 6.6.32 - 6.6.33 the angular change contribution of the cosmological constant will be precisely determined provided the parameters of the motion $A,\ B,\ a,\ e\ \&\ J$ are known from observation.

Some special cases

1) A and B are being approximated by their leading terms (classical equivalent)

Then, by eq. 6.6.12

$$A \simeq 2\mu E = \frac{G\mu^2 M}{a} = \frac{J^2}{a^2(1-e^2)};\quad B \simeq 2G\mu^2 M = 2aA, \tag{6.6.34}$$

where E and J are the classical total energy and momentum given by

$$E = \frac{G\mu M}{2\,a};\quad J = \sqrt{G\mu^2 M a(1-e^2)}. \tag{6.6.35}$$

Using eqs. 6.6.34 - 6.6.35, eq. 6.6.22 is easily transformed to

$$S^{(\Lambda)} = \frac{\delta_\Lambda a(1-e^2)^{7/2}}{2J}\int_{1-e^2}^{1}\frac{du}{u^4\sqrt{\epsilon_1+\epsilon_2 u-\epsilon_3 u^2}} \tag{6.6.36}$$

where

$$\begin{aligned}\epsilon_1 &= 2-e^2-e(1-e^2)(1+2e);\\ \epsilon_2 &= 2e(1-e^2)(1-e);\quad \epsilon_3 = e(1-e^2).\end{aligned} \tag{6.6.37}$$

Then,

$$\triangle\phi_\Lambda = -\frac{\partial\triangle S^{(\Lambda)}}{\partial J} = \frac{\pi\delta_\Lambda a^4(1-e^2)^{7/2}}{J^2}\int_{1-e^2}^{1}\frac{du}{u^4\sqrt{\epsilon_1+\epsilon_2 u-\epsilon_3 u^2}}. \tag{6.6.38}$$

Using eqs. 6.6.11 and 6.6.35 eq 6.6.38 be recast as

$$\triangle\phi_\Lambda = -\frac{\partial\triangle S^{(\Lambda)}}{\partial J} = \frac{\pi\Lambda c^2 a^3(1-e^2)^{5/2}}{GM}\int_{1-e^2}^{1}\frac{du}{u^4\sqrt{\epsilon_1+\epsilon_2 u-\epsilon_3 u^2}}. \tag{6.6.39}$$

In terms of the Keplerian period, eq. 6.6.39 is recast as

$$\triangle\phi_\Lambda = \frac{\Lambda c^2 P_p^2\,(1-e^2)^{5/2}}{4\pi}\int_{1-e^2}^{1}\frac{du}{u^4\sqrt{\epsilon_1+\epsilon_2 u-\epsilon_3 u^2}}. \tag{6.6.40}$$

where the Keplerian period is given by

$$P_p = 2\pi\left(\frac{a^3}{GM}\right)^{1/2}. \tag{6.6.41}$$

2) Integrating by series expansion

Integrating by series expansion of ${S_r}^{(\Lambda)}$ about the small quantity $1/r$ will lead to

$${S_r}^{(\Lambda)} = \frac{\delta_\Lambda}{2}\int\frac{r^2dr}{\sqrt{\alpha(r)}} \simeq -\frac{\delta_\Lambda J^2}{4A^{3/2}}\,r + ... \tag{6.6.42}$$

Then, the non-averaged instantaneous angular change contribution due to Λ with the series leading term is approximated as

$$\triangle\phi_{\Lambda_{ins}} = -\frac{\partial\triangle S^{(\Lambda)}}{\partial J} \simeq -\frac{\delta_\Lambda J}{2A^{3/2}}\frac{\partial\triangle J}{\partial J}\,r + ... \simeq -\pi\frac{\delta_\Lambda J}{A^{3/2}}\,r \tag{6.6.43}$$

In averaging over the Keplerian period, eq. 6.6.43 will be recast as

$$\triangle\phi_\Lambda =\simeq -\frac{\pi}{P_p}\frac{\delta_\Lambda J}{A^{3/2}}\int_0^{P_p} r dt. \tag{6.6.44}$$

The time integral will be converted to the useful angular integral upon using the conservation of angular momentum

$$J = \mu\, r^2\dot{\phi}, \tag{6.6.45}$$

so that eq. 6.6.44 will be recast as

$$\begin{aligned}\triangle\phi_\Lambda &\simeq -\frac{\pi}{P_p}\frac{\delta_\Lambda J}{A^{3/2}}\int_0^{2\pi}\frac{\mu\, r^3}{J}\, d\phi. \\ &= -\frac{\pi}{P_p}\frac{\delta_\Lambda J}{A^{3/2}}\int_0^{2\pi}\frac{\mu\, r^3}{J}\, d\phi. \end{aligned}\tag{6.6.46}$$

Finally, using the approximate classical value of A and plugging eq. 6.6.21, into eq. 6.6.46 the angular change due to the cosmological constant is given by

$$\triangle\phi_\Lambda = -\frac{\Lambda c^2 {P_p}^2(1-e^2)^{1/2}(1+\frac{e^2}{2})}{4\pi}. \tag{6.6.47}$$

For nearly circular orbits, eq. 6.6.47 will be approximated as

$$\triangle\phi_\Lambda = -\frac{\Lambda c^2 {P_p}^2(1-e^2)^{1/2}}{4\pi}. \tag{6.6.48}$$

In general, the mean angular change corresponding to the cosmological constant has the form

$$\triangle\phi_\Lambda = -\frac{\Lambda c^2 {P_p}^2}{4\pi} f(e), \tag{6.6.49}$$

where $f(e)$ is only as a function of the ellipticity e of the orbit.

The mean change of the angular frequency of the orbits when the averaging is being taken over the Keplerian period is

$$< \dot{\omega}_\Lambda >= \frac{1}{P_p}\int_0^{P_p} \omega_\Lambda dt = \frac{\triangle\phi_\Lambda}{P_p} = -\frac{\Lambda c^2 P_p}{4\pi} f(e), \tag{6.6.50}$$

so that basically the earlier derivations corresponding to the mean angular change remains the same except the two differ in factor of P_p.

As an alternative derivation of the mean frequency change, following [141, chapter 12], the secular precession of angular velocity due to Λ over the unperturbed Keplerian period P is given by:

$$< \dot{\omega}_\Lambda > = \frac{1}{P_p}\int_0^{P_p} \frac{\partial \triangle \mathcal{H}_\Lambda}{\partial J} dt = \frac{1}{P_p}\frac{\partial}{\partial J}\left(\int_0^{P_p} \triangle\mathcal{H}_\Lambda dt\right), \tag{6.6.51}$$

where $\triangle\mathcal{H}_\Lambda$ is the leading perturbing potential contributed from Λ. With the aid of eq. 6.6.9, it is given by

$$\triangle\mathcal{H}_\Lambda = -\frac{\Lambda c^2}{2}\mu\, r^2. \tag{6.6.52}$$

Using eqs. 6.6.45 and 6.6.52 in eq. 6.6.51, we obtain

$$< \dot{\omega}_\Lambda > = \frac{1}{P_p}\frac{\partial}{\partial J}\left(J\int_0^{2\pi}\left(\frac{\mu r^2}{J}\right)^2 d\phi\right), \tag{6.6.53}$$

where the integrand of eq. 6.6.53 is observed to be the square of the instantaneous classical angular velocity of the system. Using the general field equations derived in ch. 4, particularity eq. 4.1.7 (see also), it can be expressed as

$$\left(\frac{\mu r^2}{J}\right)^2 = \frac{r^3}{GM}. \tag{6.6.54}$$

Then, using eqs. 6.6.21 and 6.6.54 in eq. 6.6.53, the final precession in orbit frequency is

given by

$$\begin{aligned} < \dot{\omega}_\Lambda > &= -\frac{\Lambda c^2}{2P_p}\int_0^{2\pi}\frac{r^3}{GM}d\phi, \\ &= -\frac{\Lambda c^2 P_p\sqrt{1-e^2}\,(1+\frac{e^2}{2})}{4\pi}. \end{aligned} \tag{6.6.55}$$

Eq. 6.6.55 is in agreement with eq. 6.6.47.

The form of $\mathbf{J}^2$ in the presence of Λ

Since, both the Newtonian attractive force between the particles and the repulsive force of the cosmological constant are radial so that the angular momentum $\mathbf{J}$ is a conserved quantity. Thus, the Laplace-Runge-Lenz vector $\mathbf{A}$ is the easiest way to construct $\mathbf{J}^2$. Following [141, section 3.9], in the presence of cosmological constant, we find the modified Laplace-Runge-Lenz vector given by

$$\mathbf{A} = \mathbf{p}\times\mathbf{J} - G\mu^2 M\hat{\mathbf{r}} + \mathbf{A}_\Lambda, \tag{6.6.56}$$

where $\mathbf{A}_\Lambda$ is the new vector due to Λ in modification to the old Laplace-Runge-Lenz vector $\mathbf{p}\times\mathbf{J} - G\mu^2 M\hat{\mathbf{r}}$, given by

$$\mathbf{A}_\Lambda = G\mu M m_\Lambda\hat{\mathbf{r}} + \frac{\Lambda\, m_\Lambda(\mu - M)}{3}\int \mathbf{r}\times(\mathbf{r}\times\dot{\mathbf{r}})dt. \tag{6.6.57}$$

m_Λ is considered to represent an equivalent mass parameter contribution of Λ. From geometrical perspective, m_Λ may be computed by assuming an ellipsoidal vacuum filled with uniform density $-(\Lambda c^2)/(4\pi G)$ whose principal axis be parallel to the plane of motion of the binary.

The second term in eq. 6.6.57 is of $O(\Lambda^2)$ and is insignificant. Then, considering the first term (besides the implicit Λ content within $\mathbf{p}$ and $\mathbf{J}$), the classical ellipse equation is

modified to be given by (the intermediate procedures are the same as [141, section 3.9])

$$\frac{1}{r} = \frac{G\mu^2 M(1-\sigma_\Lambda)}{J^2}(1 + e\cos\phi), \tag{6.6.58}$$

where the eccentricity e, and the small quantity σ are respectively defined by

$$e = \frac{A}{G\mu^2 M(1-\sigma_\Lambda)};\ \ \sigma_\Lambda = \frac{m_\Lambda}{M}. \tag{6.6.59}$$

The maximum magnitude of σ be obtained if the geometry is being assumed to be spherical, so that

$$|\sigma_\Lambda|_{max} \leq |\frac{\rho_{vac}V_{vac}}{M}| = \frac{\frac{\Lambda c^2}{4\pi G} \times \frac{4\pi}{3}a^3}{M} = \frac{1}{3}\left(\frac{\Lambda c^2 {P_p}^2}{4\pi}\right). \tag{6.6.60}$$

At the apsis where $r = r_{min};\ \phi = 0$ and $r = r_{max};\ \phi = \pi + \delta\phi$. Using this boundary conditions, eq. 6.6.58 yields

$$r_{min} + r_{max} = \frac{J^2}{G\mu^2 M(1-\sigma_\Lambda)}\left(\frac{1}{1+e} + \frac{1}{1-e\cos(\delta\phi)}\right), \tag{6.6.61}$$

where $\delta\phi$ is the half period precession angle due to the relativistic effect.

Taylor expand of $\cos\delta\phi$ in eq. 6.6.61 is of $(\delta\phi^2)$, and hence does not contribute to first order correction in $\delta\phi$. Thus, to the significant first order correction in $\delta\phi$, eq. 6.6.61 yields

$$J^2 = G\mu^2 M a(1-\sigma_\Lambda)(1-e^2), \tag{6.6.62}$$

where $2a = r_{min} + r_{max}$ is twice the semi-major axis of the ellipse swept by the binary motion.

So the additional Λ contribution to the precession of orbit parameters can be included through J by way of eq. 6.6.62. However, this additional value is relatively very small compared to the result obtained using the classical J already used. For example, the coupled Λ

effect contained in the angular precession due to gravitation given by eq. 6.6.31 upon using the improved J is

$$\begin{aligned} |\triangle\phi_{E_\Lambda}| &\simeq \frac{6\pi GM}{c^2a(1-e^2)}\,|\sigma_\Lambda| \\ &\leq \frac{6\pi GM}{c^2a(1-e^2)}\left|\frac{1}{3}\left(\frac{\Lambda c^2 {P_p}^2}{4\pi}\right)\right| \\ &\leq \frac{1}{3}\left|\frac{\Lambda c^2 {P_p}^2}{4\pi}\right|, \end{aligned} \tag{6.6.63}$$

to first order series expansion in the small quantity σ_Λ.

Thus, fairly, the decoupled Λ term (eq. 6.6.49) just derived using the classical J will precisely determine the effect of Λ in the precision of the orbit provided that $f(e) \neq 0$. However, in case $f(e) = 0$, the non-vanishing additional term obtained from the coupling as seen by eq. 6.6.63 would be used to see the Λ effect.

6.7 Result and Discussion

With the general assumption, that EFE being observationally tested in the context of Newtonian formalism, the weak-field approximation in a region where the effect of Λ is very small but considerably competent with higher Post-Newtonian corrections has been derived with appropriate boundary conditions. Methodologically, we have used the Post-Newtonian expansion of the perturbing potentials, and thus developed an extension of the standard Post-Newtonian expansion to derive GR two-body problem equations in SdS geometry. Also, the details of the boundary conditions where and how the SdS linearization and PN expansions will work have been provided.

Actually, we did develop the Lagrangian and Hamiltonian of many body problems that will be used to derive relevant equations of the system. However, we focused on the two-body

problem where we have further imposed boundary conditions to derive observable conserved physical quantities including energy and momentum.

As application of the new development, the precession of orbits in SdS geometry were derived using Hamilton-Jacobi equation; where the Hamiltonian already developed from the PN expansion formalism is being used. In the detailed derivation of the precession of the orbits, the formal approach of using small deviations resulting to the precession corresponding to rotation of the Laplace-Runge-Lenz vector (LRL) pointing along the line of apsides was used for the incorporation of Λ effect. Moreover, an additional term of the LRL vector has been derived that helps to see the effect of Λ.

The analytical result of the work shows the effect of Λ on precession of orbits that depend on the parameters of the orbits. Especially, the dependence of Λ effect with respect to eccentricity of the orbit is indebted to other parameters of the orbit. However, in the limiting cases the results of the new approach will agree with the previous results as shown in the simplifying cases as discussed in sec. **??**.

Moreover, in the new development there is no vanishing effect of Λ obtained as in the case of earlier works (see for example [149, 150]) corresponding to $\sqrt{1-e^2} = 0$, at $e = 1$. In the new development, even though the value obtained by the classical approximation of J vanishes, still the improved LRL vector coupled to it will yield a non-vanishing value observed by eq. 6.6.63.

In table 6.1, we present some representative orbit precessions calculated using our new development with the inclusion of Λ, where the latest observational data is being used. The representative binary systems include: a) planetary system (solar and alpha century), b) binary stars (binary pulsars and SMBHs), c) orbits of stars and other binaries around galactic center where the Milky-Way center is used as representative and d) orbit of binary galaxies

where the local group is used.

Finally, the following conclusions have been derived;

1) In the case of planetary system, the precessional effect of Λ compared to that of the classical Einstein effect is $\lesssim 10^{-9}$, which is insignificant.

2) In the case of binary stars and systems orbiting around galactic centers, the relative precession of Λ compared to that of the classical Einstein precession is $\lesssim 10^{-20}$, which is too small to consider.

3) The effect of Λ on the precession of orbits of two-body system will be significant in open wide systems like binary-galaxies. As can be observed from the table, Λ is much dominant over the Einstein classical precession.

4) The results obtained in the new development well agrees with the earlier results obtained by others for low eccentricities (as can be inferred from the table). However, for large eccentricities the results deviate up to 10^2 order.

5) The results obtained in the new development will be improved, if the parameters of the orbits are being used with increased observational precisions (instead of the simple assumptions used here as in table 6.1).

Table 6.1: Orbit precession of binaries covering from solar system to binary galaxies.

System	e	a	P_p	$\Delta\phi_E\ (\prime\prime)$	$\Delta\phi_{E\Lambda_{max}}\ (\prime\prime)$	$\Delta\phi_{\Lambda_n}\ (\prime\prime)$	$\Delta\phi_{\Lambda_s}\ (\prime\prime)$	$\Delta\phi_{nr}; \dot{\omega}_{nr}$	$\Delta\phi_{sr}; \dot{\omega}_{sr}$	Reference
Planetary system										
Solar system										
Mercury	0.2056	0.387 au	87.95 d	43.0	2.2×10^{-19}	2.8×10^{-12}	1.3×10^{-12}	6.4×10^{-14}	2.9×10^{-14}	[129]
Earth	0.0167	1.0 au	1.0 yr	3.84	3.3×10^{-19}	8.9×10^{-13}	5.4×10^{-12}	2.3×10^{-13}	1.4×10^{-12}	[129]
Comet-Halley	0.967	17.94 au	76.1 yr	0.043	2.2×10^{-17}	3.3×10^{-8}	1.0×10^{-10}	7.6×10^{-7}	2.4×10^{-9}	[129]
Exo-Solar system										
Aldebaran-b	0.1	1.46 pc	$1.725\ yr$	1.61	4.2×10^{-19}	9.3×10^{-12}	9.2×10^{-12}	5.8×10^{-12}	5.7×10^{-12}	[154]
Binary stars										
Binary pulsars										
IGR J17062-6143	0.03	1169.2 km	$37.97'$	6.2×10^2	2.8×10^{-25}	1.2×10^{-16}	3.9×10^{-16}	1.8×10^{-19}	6.2×10^{-19}	[130]
B1913+16	0.617	701514 km	$0.323\ d$	2.0×10^5	1.3×10^{-20}	4.8×10^{-14}	3.7×10^{-15}	2.4×10^{-19}	1.9×10^{-20}	[155]
Binary-SMBH	0.3	121.7 au	150 d	5.8×10^{20}	1.1×10^{-9}	8.4×10^{-17}	2.4×10^{-17}	1.4×10^{-37}	4.2×10^{-38}	[131]
Milky-Way center										
Closest star S_2	0.881	8.313pc	15.6 yr	1.3×10^{10}	2.8×10^{-7}	2.8×10^{-9}	4.0×10^{-11}	2.1×10^{-19}	3.0×10^{-21}	[156]
Gas cloud-G2	0.9384	1.92 pc	$137\ yr$	1.9×10^6	3.2×10^{-9}	4.0×10^{-8}	2.5×10^{-10}	2.0×10^{-14}	1.3×10^{-16}	[157]
Disc-binary 1	0.01	1.0 au	0.365 d	3.8×10^9	3.3×10^{-16}	5.3×10^{-16}	5.4×10^{-15}	1.4×10^{-25}	1.4×10^{-24}	[132]
Disc-binary 2	0.9	20 au	1.033 d	3.6×10^{11}	2.5×10^{-13}	5.8×10^{-13}	6.6×10^{-15}	1.6×10^{-24}	1.9×10^{-26}	[132]
Binary-galaxies										
MW-MC	0.5	0.1Mpc	2 Gyr	2.7×10^{-7}	9.4×10^{-8}	0.073	0.0093	2.7×10^5	3.4×10^4	[133]
M31-M33	0.76	127kpc	2.4 Gyr	4.5×10^{-7}	2.3×10^{-7}	0.23	0.0084	5.1×10^5	1.9×10^4	[158]

Parameters: a is the semi-major axis given in au, pc or km; e is the eccentricity; P_p is the Keplerian period given in minutes ($'$); all the precession angles are given in arc seconds ($''$) per century. $\Delta\phi_E\ (\prime\prime)$ is the classical Einstein precession, $\Delta\phi_{E\Lambda_{max}}\ (\prime\prime)$ is the coupling precession component, $\Delta\phi_{\Lambda_n}\ (\prime\prime)$ represents the new precession and $\Delta\phi_{\Lambda_s}\ (\prime\prime)$ represents the precession derived in earlier works by others (taken as standard here). $\Delta\phi_{nr}$ and $\Delta\phi_{sr}$ represent the relative(ratio) angular precessions of the new and the "standard," respectively with respect to $\Delta\phi_E$; while $\dot{\omega}_{nr}$ and $\dot{\omega}_{sr}$ are representing the corresponding relative precession frequencies.

Chapter 7

Radiation from radially in falling particles to black holes in SdS geometry

Radiation from radially in falling particles into Schwarzschild Black Holes has been studied since 1960's (see for example [159], [160]). In this regard, today, there is a great deal of seminal works in various frameworks that includes: Einstein's linearized and non-linearized field equations(in the classical field theory framework), quantum field theory, Quantum optics, etc., (see for example [161], [162], [163]). However, there are limited studies under the more general SdS spacetime geometry, where the Schwarzschild is a special case. So, in this chapter we derive radiation of small particles in falling to BHs in the SdS geometry. Then, examine the effect of Λ on the spectrum of the radiation.

Here, the radiation considers only the electromagnetic component from a small charged particle interacting with a neutral BH in the specified geometry. The gravitational radiation case is probably not significant, where the particle's mass is too small to perturb the metric.

The organization of the work is as follows: in sec. 7.1 we derive the redshift due to the geometrical effect and discus on the results. In sec. 7.2 we derive the energy spectrum of the radiation and discuss on the results. In the final sec. 7.3, we provide our conclusions.

7.1 The redshift in the SdS Spacetime

The gravitational redshift z is defined by the ratio between emitted frequency ν_e and observed frequency ν_0 as in eq. 3.3.29

$$\frac{\nu_e}{\nu_o} = 1 + z. \tag{7.1.1}$$

The relative frequency, ν_e/ν_o, in SdS will be derived from the line element

$$\begin{aligned} ds^2 &= -f(r)dt^2c^2 + \frac{dr^2}{f(r)} + r^2 d\Omega^2, \\ \text{where} \qquad & f(r) = 1 - \frac{r_g}{r} - \frac{r^2}{\ell^2}. \end{aligned} \tag{7.1.2}$$

The proper time $d\tau$ of the line element, eq. 7.1.2, is given by

$$d\tau^2 = -f(r)dt^2c^2. \tag{7.1.3}$$

The frequency of a particle at r travelling in the SdS spacetime is related to the proper time as

$$\nu_(r) = \frac{1}{d\tau(r)}. \tag{7.1.4}$$

Then, the frequency ratio at the source to observer by eqs. 7.1.1 and 7.1.4 is given by

$$\frac{\nu_e}{\nu_o} = \left(\frac{f(r_o)}{f(r_e)}\right)^{1/2}. \tag{7.1.5}$$

In the Schwarzschild spacetime, the frequency ν_e of a photon emitted at a distance r_e from a black hole is related to the frequency ν_∞ observed at infinity by

$$\frac{\nu_e}{\nu_\infty} = f(r_e)^{-1/2} = \left(1 - \frac{r_g}{r_e}\right)^{-1/2}. \tag{7.1.6}$$

But, in the SdS spacetime this is not the case. Since, as r becomes large the term containing cosmological constant curves spacetime too. Both of the radial distances necessarily enter

into the redshift equation given by

$$\frac{\nu_e}{\nu_o} = \left(\frac{1 - (\frac{r_g}{r_o} + \frac{r_o^2}{\ell^2})}{1 - (\frac{r_g}{r_e} + \frac{r_e^2}{\ell^2})} \right)^{1/2}. \tag{7.1.7}$$

The effect of the cosmological constant can be easily recognized by recasting eq. 7.1.7 as

$$\frac{\nu_e}{\nu_o} = \left(\frac{1 - \frac{r_g}{r_o}}{1 - \frac{r_g}{r_e}} \right)^{1/2} \left(\frac{1 - \frac{r_o^2/\ell^2}{(1 - r_g/r_o)}}{1 - \frac{r_e^2/\ell^2}{(1 - r_g/r_e)}} \right)^{1/2}. \tag{7.1.8}$$

For the zero cosmological constant ($\Lambda = 0$), at a very large observation point eq. 7.1.7 just reduces to the Schwarzschild geometry redshift relation given by that of eq. 7.1.6. However, for non zero cosmological constant ($\Lambda \neq 0$) it is given by

$$\frac{\nu_e}{\nu_o} \approxeq \left(\frac{1 - \frac{r_o^2}{\ell^2}}{1 - \frac{r_g}{r_e}} \right)^{1/2}, \text{ for } r_o \gg r_g. \tag{7.1.9}$$

7.1.1 Significance of Λ in the redshift

In order to determine the effect of Λ in the redshift, we define the unit-less quantities $\frac{r_e}{r_g}$, $\frac{r_o}{\ell}$ & the β parameter (eq. 4.1.14) respectively as

$$\frac{r_e}{r_g} = 1 + 10^{-\zeta}, \quad \frac{r_o}{\ell} = 10^{-\eta}, \quad \beta = 10^{-\xi}. \tag{7.1.10}$$

The parameters, ς and η are designed to accommodate respectively the precisions related to position of emission with respect to r_g and the position of observation with respect to the cosmological length ℓ. While, ξ represents the possible β parameter ranging from $\frac{2}{3\sqrt{3}}$ (for critical black holes) to 10^{-22} (when $\Lambda = 10^{-52} m^{-2}$) for smaller black holes of mass $\sim 10 M_\odot$. Then, the general equation for the relative redshift, eq. 7.1.7 is given by

$$\frac{\nu_e}{\nu_o} = \sqrt{\frac{10^{-(2\eta+\xi)} \left(1 + 10^{\zeta}\right) \left[10^{(2\eta+\xi)} - (10^{\xi} + 10^{3\eta})\right]}{1 - 10^{-2(\zeta+\xi)} \left(1 + 10^{\zeta}\right)}}. \tag{7.1.11}$$

At very large observation point, eq. 7.1.9 yields

$$\frac{\nu_e}{\nu_o} = \sqrt{(1+10^{\zeta})\,(1-10^{-2\eta})},\ \text{as } r_o \to \text{large}. \tag{7.1.12}$$

The limiting case, given by eq. 7.1.9 will provide a simple and quick overview of the cosmological constant effect in the radiation redshift. For example, if an emission takes place at r_e as closer as 10^{-8} from r_g and an observer be located at $r_o \sim 1Gpc$ from a black hole of mass $10^8 M_{\odot}$, so that $\zeta = 8$, $\eta \simeq 1.0$ and $\xi \simeq 15$, the relative redshift be 9950. However, in the vanishing cosmological constant it becomes 10000. A considerable difference!

A theoretical numerical data generated from the general eq. 7.1.11 is shown as in Table 7.1. The table is theoretically designed to represent a range of feasible sample representative systems of in the universe; that believed to give a general overview of the redshift relation with respect to the emission and observation points with representative black holes as small, massive and supermassive ones indicated through the parameters defined as in eq. 7.1.10.

As can be observed from the table, for small black holes (eg. $\xi = 15$) when the observation points are taken closer to the holes (eg. $\eta = 8$), there is no significant redshift difference between the Schwarzschild spacetime and that of the SdS spacetime; irrespective of the accuracy level taken into account for how far the emission point being closer to the Schwarzschild radius. On the other hand, in this case, the level of accuracy for how close the emission point goes to the Schwarzschild radius, shows an increasing redshift that reaches infinity at the Schwarzschild radius. However, for points of observations being closer to the cosmological length, the redshift differences become very large between the two spacetime geometries. In this case, for a given point of emission, the redshift remains the same under Schwarzschild geometry, irrespective of the observation point while under the SdS geometry the redshift varies with the location of point of observation. It decreases with increasing observation distance from the source to vanish or even blueshifted.

Table 7.1: The redshift in SdS for in falling particles to black holes.

		$\xi = 15$		$\xi = 4$	
ζ	η	SdS $\frac{\nu_e}{\nu_o}$ $(\Lambda \neq 0)$	Schwarzschild $\frac{\nu_e}{\nu_o}(\Lambda = 0)$	SdS $\frac{\nu_e}{\nu_o}$ $(\Lambda \neq 0)$	Schwarzschild $\frac{\nu_e}{\nu_o}(\Lambda = 0)$
	8	1.00499	1.00499	–	–
-2	0.3	0.869655	1.00499	0.869583	1.00489
	10^{-3}	0.0681214	1.00499	0.0673777	1.00494
	8	1.04881	1.04881	–	–
-1	0.3	0.907575	1.04881	0.907455	1.0487
	10^{-3}	0.0710918	1.04881	0.0703121	1.04876
	8	31.6386	31.6386	–	–
3	0.3	27.3781	31.6386	27.3744	31.6354
	10^{-3}	2.14457	31.6386	2.12105	31.637
	8	10^6	10^6	–	–
12	0.3	865339	10^6	865224	999900
	10^{-3}	67783.4	10^6	67039.9	999950
	8	10^8	10^8	–	–
16	0.3	8.65339×10^7	10^8	8.65224×10^7	9.999×10^7
	10^{-3}	6.77834×10^6	10^8	6.70399×10^6	9.9995×10^7

However, for sizable black holes including the critical black holes (eg. $\xi = 4$), totally the redshift relation behaves different in the two geometries.

7.2 Energy received at observation point from radially in falling particles towards a black hole in SdS geometry

The energy received (dE_{rec}) at r_o far away from the source is related to the energy emitted(dE_{em}) at r_e near the source by

$$dE_{rec} = \frac{\nu_o}{\nu_e} \times dE_{em}. \tag{7.2.1}$$

Using eqs. 7.1.9 and 7.2.1, the energy received per unit time at the position r_o (far from a particle) emitted at the position r_e (near from the source) is given by

$$\frac{dE_{rec}}{dt} = \left(\frac{1-\frac{r_g}{r_e}}{1-\frac{r_o^2}{\ell^2}}\right)^{1/2} \times \frac{dE_{em}}{dt}. \tag{7.2.2}$$

Following the method adopted by D.K.Ross [160], the energy emitted per unit time by an accelerating charge ze, where retardation effects have been taken into account is given by

$$\frac{dE_{em}}{dt} = -\left(\frac{\dot{v}^2}{c^3}\frac{z^2e^2}{6\pi\epsilon_0}\right) \times \frac{1}{(1-v^2)^3}. \tag{7.2.3}$$

Then, the energy received at the observer when the redshift effect is taken into account through terms of order v^3 (related to significance) by using eqs. 7.2.2 - 7.2.3 is approximately given by

$$\frac{dE_{rec}}{dt} = -\left(\frac{\dot{v}^2}{c^3}\frac{z^2e^2}{6\pi\epsilon_0}\right) \times (1+3v^2) \times \left(\frac{1-\frac{r_g}{r_e}}{1-\frac{r_o^2}{\ell^2}}\right)^{1/2}. \tag{7.2.4}$$

The redshift correction is not only important near the Schwarzschild radius as in the absence of the cosmological constant but all observation points, where r_o goes closer to the cosmological length i.e., $\ell = \sqrt{\frac{3}{\Lambda}}$, is important. That means the location of the observer enters in the radiation received to increase the magnitude. Of course, the position of the observer is important in addition to the near emission position.

7.2.1 Integral boundary conditions and solutions: Euler-Lagrange equations

To integrate eq. 7.2.4 we need the form of v and $\dot{v}$ for a small particle of mass m falling in SdS spacetime in the vicinity of the gravitating object. Thus, these quantities of motion can be derived from the Lagrangian L of the particle in the gravitational field of the black

hole given by

$$L = -m\frac{ds}{dt}, \tag{7.2.5}$$

where ds is the line element given by eq. 3.1.1

$$ds^2 = g_{\mu\nu}dx^\mu dx^\nu. \tag{7.2.6}$$

The Euler-Lagrange equation for the coordinate x^λ is given by

$$\frac{\partial L}{\partial x^\lambda} - \frac{d}{dt}\left(\frac{\partial L}{\partial \dot{x}^\lambda}\right) = 0, \tag{7.2.7}$$

where the dot over x shows the ordinary derivative with respect to time.

Using eqs. 7.2.5 - 7.2.7, the Euler-Lagrange equations for the coordinate x^λ is given by

$$\dot{x}^\mu \dot{x}^\nu \frac{\partial g_{\mu\nu}}{\partial x^\lambda} - 2\frac{d}{dt}\left(\frac{g_{\mu\lambda}\dot{x}^\mu}{\sqrt{g_{\mu\nu}\dot{x}^\mu\dot{x}^\nu}}\right) = 0. \tag{7.2.8}$$

Since, the metric $g_{\mu\nu}$ in SdS geometry does not explicitly depend on time, so eq. 7.2.8 for $x^\lambda = t$ is integrated to give a constant, say C, given by

$$g_{tt}\frac{dt}{ds} = C, \tag{7.2.9}$$

where g_{tt} is the time-time component of the SdS metric given as in eq. 7.1.2.

Considering the case where the particle is to fall from far distance at r_o with velocity v_o towards the hole, then the constant C is given by

$$C = \left(\frac{f_0}{1 - v_o^2 f_o^{-2}}\right)^{1/2}, \tag{7.2.10}$$

where we adopted $f(r_o) \equiv f_o$, etc.

For non relativistic particles, eq. 7.2.10 will be approximately given as

$$C \approx f_o^{1/2}\left(1 + \frac{1}{2}v_o^2 {f_o}^{-2}\right)^{1/2}. \tag{7.2.11}$$

For a particle falling from rest at this point,

$$C = f_o^{1/2}. \tag{7.2.12}$$

C takes values ranging from zero to its maximum value, $C_{max}^2 = 1 - 3\left(\frac{r_g}{2\ell}\right)^{2/3}$ for a particle released from rest at $r_{_{0mx}} = \left(\frac{\ell^2 r_g}{2}\right)^{1/3}$. With the exception of this maximum value, any C between zero and this maximum value will be a constant for two release positions from rest on either side of $r_{_{0mx}}$, towards ℓ or towards r_g decreasing monotonically to reach its zero value at these extremal positions. The two possible release positions for a single value of C by the use of eqs. 7.1.2 and 7.2.12 are given by

$$r_{_{o1}} = \frac{2\ell}{\sqrt{3}}\sqrt{1-C^2}\,\cos\left(\frac{1}{3}\arccos\left(-\frac{3\sqrt{3}r_g}{2\ell}\left(1-C^2\right)^{-3/2}\right)\right), \tag{7.2.13}$$

$$r_{_{02}} = \frac{2\ell}{\sqrt{3}}\sqrt{1-C^2}\sin\left(\frac{1}{3}\arcsin\left(\frac{3\sqrt{3}r_g}{2\ell}\left(1-C^2\right)^{-3/2}\right)\right). \tag{7.2.14}$$

For non-critical black holes, these release positions are approximately given by

$$r_{_{o1}} \approx \sqrt{1-C^2}\,\ell, \tag{7.2.15}$$

$$r_{_{02}} \approx \frac{r_g}{1-C^2}. \tag{7.2.16}$$

Using eq. 7.2.9, the velocity v and the acceleration $\dot{v}$ of the particle at any r in the region of SdS application are respectively given by

$$v = f\left(1-\frac{f}{C^2}\right)^{1/2}, \tag{7.2.17}$$

$$\dot{v} = f\left(1-\frac{3f}{2C^2}\right)\left(\frac{r_g}{r^2}-\frac{2r}{\ell^2}\right). \tag{7.2.18}$$

The particle attains extremal velocities at two postions near the cosmological length and the Schwarzschild radius respectively given by

$$r_{_{vm1}} = \frac{2\ell}{\sqrt{3}}\left(1-\frac{2}{3}C^2\right)^{1/2}\cos\left(\frac{1}{3}\arccos\left(-\frac{3\sqrt{3}\,r_g}{2\ell}\left(1-\frac{2C^2}{3}\right)^{-3/2}\right)\right), \quad (7.2.19)$$

$$r_{_{vm2}} = \frac{2\ell}{\sqrt{3}}\left(1-\frac{2}{3}C^2\right)^{1/2}\arcsin\left(\frac{3\sqrt{3}\,r_g}{2\ell}\left(1-\frac{2C^2}{3}\right)^{-3/2}\right). \quad (7.2.20)$$

For non-critical black holes, these extremal velocity positions are approximately given by

$$r_{_{vm1}} \approx \sqrt{1-\frac{2}{3}C^2}\,\ell, \quad (7.2.21)$$

$$r_{_{vm2}} \approx r_g\left(1-\frac{2}{3}C^2\right)^{-1}. \quad (7.2.22)$$

Comparing the release position and the position where the extremum velocity occurs, upon using eqs. 7.2.15 and 7.2.21, that the particle is moving away. This analysis may lead to an assertion for the manifestation of expansion of the universe in the context of cosmological constant or else that needs further investigation. Since, this is not our main investigation issue; here we focus on the case of the falling towards the hole. So, the extremum velocity for the fall is given by eq. 7.2.20 whose approximation is given by that of eq. 7.2.22. As can be determined from the equation, for a particle being released from rest near r_{0mx}, where $C \approx 1$, the maximum velocity attained in the SdS spacetime occurs at $r_{_{vmx}} \approx 3r_g$. However, a particle being released from rest at the extremal positions r_g and ℓ will achieve this extremal velocity at $r_{_{vmx}} \approx r_g$, which is a rather vanishing velocity (as we can see soon in the forthcoming paragraph). In general, wherever the particle falls from, the extremal velocity occurs at some position in the range $r_g \leq r_{_{vmx}} \leq 3r_g$. On the other hand, in the case of Schwarzschild spacetime, $3r_g$ seems the favoured natural occurrence position of maximum velocity for all far fall positions. However, falls from nearby r_g assume to attain their extremal velocities nearly at the same positions both in SdS and Schwarzschild

geometries.

Up on using eqs. 7.1.2 and 7.2.20 in eq. 7.2.17 the exact maximum velocity of the particle will be obtained. However, instead of eq. 7.2.20 if its equivalent approximation given by eq. 7.2.22 will be used to yield easily

$$v_{_{max}} = \frac{2\sqrt{3}}{9}C^2. \tag{7.2.23}$$

In the vicinity of eq. 7.2.23, the largest velocity that a falling particle into a black hole can attain is $\frac{2\sqrt{3}}{9}$; being attained at about $3r_g$ under the special case where the particle is to fall from rest near $r_{_{0mx}}$ ($C \approx 1$). In the general case where the particle is falling from any position away from $r = \frac{2\sqrt{3}}{9}$, the value of the extremal velocity decreases monotonically as the release point goes towards the extremal positions r_g or ℓ. Of course, the value vanishes at the extremal positions.

On the other hand, in the Schwarzschild spacetime for all far distant falls, where $r_g/r_o \ll 1$, $C \approx 1$ and so the particle always possess $v_{_{max}} = \frac{2\sqrt{3}}{9}$ around $3r_g$. However, as the distance of fall gets closer to the hole, the extremal velocity becomes very small.

Table 7.2, provides a general overview of the evolution of the extremal velocities in both geometries with respect to release positions.

Table 7.2: Effect of cosmological constant on extremal velocity of particles radially falling into black holes.

The special case when the point of release be closer to the cosmological length ($r_o \to \ell$).				
	$\Lambda \neq 0$			$\Lambda = 0$
$\frac{r_o}{\ell}$	C^2	$\frac{r_{vmx}}{r_g}$	v_{max}	
0.995	0.01	1.01	0.00385	$C^2 \simeq 1$;
0.949	0.1	1.07	0.0385	$\frac{r_{vmx}}{r_g} \simeq 3$;
0.707	0.5	1.5	0.192	$v_{max} \simeq 0.385$;
0.1	0.99	2.94	0.381	for all $\frac{r_o}{\ell}$ cases.
0.01	0.9999	3	0.385	
The special case when the point of release be closer to the Schwarzschild radius ($r_o \to r_g$).				
$\frac{r_o}{r_g}$	C^2	$\frac{r_{vmx}}{r_g}$	v_{max}	
100	0.99	2.941	0.381	
10	0.9	2.5	0.346	No significance differences
2	0.5	1.5	0.192	between the
1.11	0.1	1.07	0.0385	$\Lambda = 0$ and $\Lambda \neq 0$ cases.
1.01	0.01	1.01	0.00385	

7.2.2 Integration of energy received

Eq. 7.2.4 is used to derive the energy received at the observation point. Integration of this equation in terms of r is a complicated task. However, transforming the integrand from dr to df* will simplify the integration. Thus, using eqs. 7.2.4, 7.2.17 and 7.2.18, the rate of

*

$$
\begin{aligned}
f &= 1 - \frac{r_g}{r} - \frac{r^2}{\ell^2} \\
\Rightarrow \frac{df}{dr} &= \frac{r_g}{r^2} - \frac{2r}{\ell^2} \\
& \quad r\text{in terms of f is given by} \\
r &= \frac{2\,\ell}{\sqrt{3}}\sqrt{1-f}\,\sin\left(\frac{1}{3}\arcsin\left(\frac{3\sqrt{3}r_g}{2\ell(1-f)^{3/2}}\right)\right) \\
&\approx \frac{r_g}{1-f}
\end{aligned}
$$

energy received per unit f is given by

$$-\frac{dE_{rec}}{df} = \frac{e^2 z^2}{6\pi\epsilon_0 c^3}\frac{f^{3/2}}{f_o\sqrt{1-\frac{f}{f_o}}}\left(\frac{(1-f)^2}{r_g}-\frac{2r_g}{l^2(1-f)}\right) \times\left(1-\frac{3f}{2f_o}\right)^2\left(1+3f^2\left(1-\frac{f}{f_o}\right)\right). \tag{7.2.24}$$

Integrating eq. 7.2.24, we obtain

$$E_{rec}(f) = \frac{e^2 z^2}{6\pi\epsilon_0\, c^3}\Bigg\{\frac{f_o^{11/2}\arcsin\left(\sqrt{f_o^{-1}f}\right)}{131072\, r_g}\left(A(f)-\frac{128\, r_g^2}{\ell^2 f_o^{10}}B(f)\right) + \frac{(3-4f_o)(3-2f_o)^2 r_g}{2\,\ell^2 f_o^4\sqrt{1-f_o^{-1}}}C(f)+\frac{\sqrt{f-\frac{f^2}{f_o}}}{13762560 f_o^3 r_g}\left(D(f)-\frac{2688\, r_g^2}{\ell^2}E(f)\right)\Bigg\}, \tag{7.2.25}$$

where $A(f)$, $B(f)$, $C(f)$, $D(f)$ and $E(f)$ are respectively given by

$$
\begin{aligned}
A(f) &= -1089 + 2556 f_o^{-1} - 12832 f_o^{-2} + 24064 f_o^{-3} - 13824 f_o^{-4}; \\
B(f) &= 39 + 84 f_o^{-1} + 632 f_o^{-2} + 4672 f_o^{-3} - 34944 f_o^{-4} + 59904 f_o^{-5} - 27648 f_o^{-6}; \\
C(f) &= \ln\left[\frac{\left(1-\sqrt{f}\right)\left(1+f_o^{-1}\sqrt{f}+\sqrt{1-f_o^{-1}}\sqrt{1-f_o^{-1}f}\right)}{\left(1+\sqrt{f}\right)\left(1-f_o^{-1}\sqrt{f}+\sqrt{1-f_o^{-1}}\sqrt{1-f_o^{-1}f}\right)}\right]; \\
D(f) &= -10321920 f^8 + 645120(36+25f_o) f^7 \qquad (7.2.26) \\
&\quad -46080(288+804f_o+137f_o^2) f^6 \\
&\quad +3840 f_o \left(7008+3884f_o+11f_o^2\right) f^5 \\
&\quad -384 f_o \left(32256+30432f_o+284f_o^2-121f_o^3\right) f^4 \\
&\quad +48 f_o \left(161280+139776f_o+12832f_o^2-2556f_o^3+1089f_o^4\right) f^3 \\
&\quad -56 f_o^2 \left(84480+24064f_o-12832f_o^2+2556f_o^3-1089f_o^4\right) f^2 \\
&\quad +70 f_o^3 \left(13824-24064f_o+12832f_o^2-2556f_o^3+1089f_o^4\right) f \\
&\quad +105 f_o^4 \left(13824-24064f_o+12832f_o^2-2556f_o^3+1089f_o^4\right); \\
E(f) &= 1152\left(12-17f_o\right) f^4 + 48\left(360-516f_o+181f_o^2\right) f^3 \\
&\quad +8\left(2880-5160f_o+1508f_o^2-13f_o^3\right) f^2 \\
&\quad +10\left(3456-6336f_o+2520f_o^2-28f_o^3-13f_o^4\right) f \\
&\quad +5\left(13824+2304f^5-26496f_o+11712f_o^2-632f_o^3-84f_o^4-39f_o^5\right).
\end{aligned}
$$

In the classical Schwarzschild spacetime where the particle is considered to fall from infinity ($f_o = 1$) to f_{min} (the metric specified at the point where the radiation is received)

eq. 7.2.25 is given by

$$\begin{aligned} E_{rec} &= \frac{375e^2z^2}{262144\pi r_g\epsilon_0}\Bigg\{\left(\frac{\pi}{2}-\arcsin[f_{min}^{1/2}]\right)+\sqrt{f_{min}-f_{min}^2}\Bigg(1+\frac{2f_{min}}{3} \\ &-\frac{259144f_{min}^2}{5625}+\frac{4998736f_{min}^3}{39375}-\frac{8044928f_{min}^4}{39375} \\ &+\frac{2791168f_{min}^5}{7875}-\frac{1258496f_{min}^6}{2625}+\frac{124928f_{min}^7}{375}-\frac{32768f_{min}^8}{375}\Bigg)\Bigg\}. \end{aligned} \tag{7.2.27}$$

Introducing the substitution $x = r_g/r_{min}$ and using $f_{min} = 1-r_g/r_{min}$ in the Schwarzschild spacetime, then eq. 7.2.27 is given by

$$\begin{aligned} E_{rec} &= \frac{375e^2z^2}{524288\pi r_g\epsilon_0}\Bigg\{\left(\pi-2\arcsin\left[\sqrt{1-x}\right]\right) \\ &-2\sqrt{(x-x^2)}\Bigg(1+\frac{2}{3}x-\frac{62536}{5625}x^2+\frac{1263184}{39375}x^3 \\ &+\frac{3161728}{39375}x^4-\frac{660736}{1575}x^5+\frac{1559552}{2625}x^6-\frac{137216}{375}x^7+\frac{32768}{375}x^8\Bigg)\Bigg\}. \end{aligned} \tag{7.2.28}$$

This is exactly the same as that of equation (13) derived as in [160] given by

$$E_{rec} = 2m_e\left(\frac{r_e}{r_g}\right)\left(\frac{I}{12}\right)z^2, \tag{7.2.29}$$

where m_e is the electron rest mass, r_e is the classical electron radius($r_e = \frac{e^2}{4\pi\epsilon_0 m_e}$) and I in our case is given by

$$\begin{aligned} I &= 0.0171661\Bigg\{\left(\pi-2\arcsin\left[\sqrt{1-x}\right]\right) \\ &-2\sqrt{(x-x^2)}\Bigg(1+\frac{2}{3}x-\frac{62536}{5625}x^2+\frac{1263184}{39375}x^3+\frac{3161728}{39375}x^4 \\ &-\frac{660736}{1575}x^5+\frac{1559552}{2625}x^6-\frac{137216}{375}x^7+\frac{32768}{375}x^8\Bigg)\Bigg\}. \end{aligned} \tag{7.2.30}$$

The I in our expression appears to differ from that of equation (14) as in [160]. But a straightforward expansion and algebraic arrangements of either of the two shows that both

expressions are identical (see the footnote*).

Indeed, the adopted method mimics the previous results obtained by others on the special case where the investigation was carried out under the Schwarzschild geometry. To get an insight of the non-zero cosmological constant effect, we consider the special case where the particle falls from sufficiently large distance, comparable with cosmological length. For example, for a particle to fall from $r_o = \frac{1}{2}\,\ell$, $f_o \approx 1$ so that the Schwarzschild radiation given by eq. 7.2.28 remains valid. On the other hand, in the SdS radiation $f_o \approx 1 - r_o^2/\ell^2 = 3/4$, quite different from the Schwarzschild case. So for the SdS radiation case, eq. 7.2.25

*For example the expression $\pi - 2\arcsin\left[\sqrt{1-x}\right]$ in our work is the same as that of $\frac{\pi}{2} - \arcsin[1-2x]$ as in [160] as follows.

$$
\begin{aligned}
\text{Let } y &= \arcsin\left[\sqrt{1-x}\right] \\
\Rightarrow \quad & \sin^2[y] = \frac{1-\cos[2y]}{2} = 1-x \\
\Rightarrow \quad & -\cos[2y] = \sin[2y - \frac{\pi}{2}] = 1-2x \\
\Rightarrow \quad & y = \frac{1}{2}\arcsin[1-2x] + \frac{\pi}{4} \\
\text{Then follows,} \quad & \pi - 2\arcsin\left[\sqrt{1-x}\right] = \frac{\pi}{2} - \arcsin[1-2x].
\end{aligned}
$$

recast as

$$
\begin{aligned}
E_{rec} \;=\; & \frac{578625\sqrt{3}}{1073741824\pi}\frac{e^2z^2}{r_g\epsilon_0}\Bigg\{\left(\pi-2\arcsin\left[\frac{2}{\sqrt{3}}f_{\min}^{1/2}\right]\right)\\
& +\frac{4}{3}\sqrt{3f_{\min}-4f_{\min}^2}\Bigg(1+\frac{8}{9}f_{\min}-\frac{116561536}{2893125}f_{\min}^2\\
& +\frac{7939941376}{60755625}f_{\min}^3-\frac{12859899904}{60755625}f_{\min}^4+\frac{2775842816}{7290675}f_{\min}^5\\
& -\frac{7218397184}{12151125}f_{\min}^6+\frac{2449473536}{5207625}f_{\min}^7-\frac{2147483648}{15622875}f_{\min}^8\Bigg)\Bigg\} \qquad (7.2.31)\\
& -\frac{3003\sqrt{3}}{131072\pi}\frac{e^2z^2r_g}{\epsilon_0\ell^2}\Bigg\{\left(\pi-2\arcsin\left[\frac{2f_{\min}^{1/2}}{\sqrt{3}}\right]\right)+\frac{4}{3}\sqrt{3f_{\min}-4f_{\min}^2}\times\\
& \left(1+\frac{8}{9}f_{\min}-\frac{44672}{45045}f_{\min}^2+\frac{19456}{6435}f_{\min}^3-\frac{32768}{45045}f_{\min}^4+\frac{262144}{27027}f_{\min}^5\right)\Bigg\}.
\end{aligned}
$$

Imposing further assumptions, such as neglecting the relatively very small terms of order $\frac{r_g}{l^2}$ where the region of fall is being considered near Schwarzschild domination, eq. 7.2.31 with reasonable accuracy be given by

$$
\begin{aligned}
E_{rec} \;=\; & \frac{578625\sqrt{3}}{1073741824\pi}\frac{e^2z^2}{r_g\epsilon_0}\Bigg\{\left(\frac{\pi}{2}-\arcsin\left[\frac{5-8x}{3}\right]\right)\\
& +\frac{4}{1640401875}\sqrt{(1-x)(4x-1)}\Bigg(116220089+1110751160\,x \qquad (7.2.32)\\
& +3932876672\,x^2+13424983040\,x^3-206735835136\,x^4\\
& +548757831680\,x^5-628998799360\,x^6+344100700160\,x^7-75161927680\,x^8\Bigg)\Bigg\}.
\end{aligned}
$$

Equation 7.2.32 can compactly be given as

$$
E_{rec}=\frac{e^2}{4\pi\epsilon_0 M}\left(\frac{I'}{12}\right)z^2, \qquad (7.2.33)
$$

where I' is given by

$$\begin{aligned} I' &= 0.0224011\Bigg\{\left(\frac{\pi}{2}-\arcsin\left[\frac{5-8x}{3}\right]\right) \\ &+\frac{4}{1640401875}\sqrt{(1-x)(4x-1)}\Bigg(116220089+1110751160x \\ &+3932876672x^2+13424983040x^3-206735835136x^4+548757831680x^5 \\ &-628998799360x^6+344100700160x^7-75161927680x^8\Bigg)\Bigg\}. \end{aligned} \tag{7.2.34}$$

For a particle falling into the Schwarzschild radius where $x = 1$, eqs. 7.2.30 and 7.2.34 will reduce respectively to $I = 0.0171661\pi$ and $I' = 0.0224011\pi$. Then, radiations in the Schwarzschild and SdS backgrounds are respectively given by

$$E_{rec,Sch} = 0.00898817m_e\left(\frac{r_e}{r_g}\right)z^2; \tag{7.2.35}$$

$$E_{rec,SdS} = 0.0117292m_e\left(\frac{r_e}{r_g}\right)z^2. \tag{7.2.36}$$

Thus, radiations from particles in falling into black holes significantly differ when calculated in the Schwarzschild and SdS backgrounds. So, the cosmological constant has significant effect in radiations resulted from in falling particles to massive objects if an appreciable distance from the hole is being considered.

7.3 Conclusions

Radiations from particles in falling into black holes significantly differ when calculated in the Schwarzschild and SdS backgrounds. So, the cosmological constant has significant effect in radiations resulted from an in falling particles to massive objects if an appreciable distance from the hole is being considered. Moreover, in the Schwarzschild background, a charged particle of magnitude ze when falling from a large distance of cosmological length

order into a black hole radiates an electromagnetic energy given by eq. 7.2.35. This energy is considered to escape to infinity. But in the case of SdS background the same particle falling from the same position of fall to the black hole radiates a greater amount of energy given by eq. 7.2.36. However, the destiny of where this amount of energy will reside needs further investigation.

Part III

Future perspective and summary

Chapter 8

Future perspectives

In this chapter, we provide our views regarding the criticisms of Einstein modified field equations, attributed to the cosmological constant. Then, we provide some supplementary works to enrich the relevance of the cosmological constant as an intrinsic constant. As the background literature review, ch. 2, especially sec. 2.3 has considered to cover issues we raise here. Thus, whenever further investigation is required the chapter will serve as the background material.

8.1 Einstein field equations: the case of modification

Einstein modified equation has received criticisms that the introduction of Λ is a simple hand set constant without proper logical explanation. Yet, there is no concrete reasoning that challenges to invalidate the modification. Though the criticism is relevant in many ways pertaining to the literatures, we argue that the introduction is a logical approach by Einstein himself. As we know from Einstein's philosophy towards formalisms that simplicity is more important than extended mathematics, where in his belief that others can

do. Thus, we do expect that why the introduction is logically ostensible. Moreover, we claim that Einstein with an intention of "the others (like mathematicians) will do," (his) principle kept the explanation open. Furthermore, as experienced as he was, he had well knew the necessity of further mathematical and physical explanations, as such, doubtless to tackle in time he would had preferred to open as an issue. Moreover, the sustained progress and science products in relation to this issue will strengthen our idea in either ways as suggested.

Construction of Einstein tensor

In deriving his field equations, Einstein originally had constructed his tensor with the intention that the tensor would determine the geometry of the source of gravitation or curvature. Moreover, the theory is a metric theory from which his tensor was supposed to be constructed. Therefore, the metric tensor would have entered as a contribution to gravitation or curvature property in some form that imposes logically the introduction of a form of cosmological constant (may or may not be a constant). In actual logic, there is no reason to think it as a form that depends on some scalar or vector variable and or even time dependent. Since, $g_{\mu\nu}$ represents the geometry of spacetime itself, the properties of mass, stress, energy and momentum should not be seen as intrinsic properties of matter, but as relational properties that material systems have only in virtue of their relation to spacetime structure.

Thus, with this comment, we argue that the geometric part shall be relocated in the $g_{\mu\nu}$ or attached to it, the Λ case; while the energy issue (that raised concern from conservation perspective) need to be considered under dark energy content of the universe being added to the stress-tensor.

In effect, our suggestion will help to rediscover the construction of Einstein field equations; and will resolve the disagreement among the expertise view, in the inclusion of Λ where some of them follow from the energy conservation law while others consider it as geometrical issue.

8.2 The value of cosmological constant: a new approach

The cosmological constant, one of the key components of Einstein field equations, has received great attention since its introduction including its empirical value. Especially, during the early developments there were different theoretical models to obtain zero or none zero values that would have hung on till the development of sophisticated observational means. However, as current astronomical observations indicate that the universe is expanding at an accelerated phase that suggests a non-zero positive cosmological value in Einstein field equations. So far, the theoretical estimates for the value have involved quantum field theory that requires an energy cutoff at the Plank length. Here, we derive the theoretical value from different approach where the luminosity of the universe is being considered with key physical assumptions.

8.2.1 Cosmological constant value derived from universe's luminosity

Assuming the whole universe as a luminous body, the Eddington luminosity limit can be applied to define the maximum luminosity of the universe for outward universes (if exists any), where the minimum time be at least equivalent to the age of the universe. With this assumption, an observer located within the interior of our universe can define the luminosity in the reverse way where the minimum time now becomes the same as that of an outside

observer just located at the age of the universe.

Key assumptions and propositions

a) The maximum luminosity of the universe is determined at the Planck length given by

$$\frac{E_{max}}{t_{min}} = \gamma \frac{c^5}{2G} \tag{8.2.1}$$

where γ is the luminous matter component of the universe.

b) The source of the maximum energy used for the luminosity must come from the nuclear mass-energy conversion of the luminous part of the universe, given by

$$E_{max} = M_{_{LU}} c^2 \tag{8.2.2}$$

where $M_{_{LU}}$ is the maximum mass of the luminous part of the universe

c) The minimum time is the age of the universe as described earlier for an in inside observer. In view of eqs. 8.2.1 & 8.2.2, given by

$$t_{min} = t_{AU} = \frac{r_{g_{LU}}}{\gamma c} \tag{8.2.3}$$

Where, t_{min}, t_{AU} & $r_{g_{LU}}$ are representing the minimum time, the age of the universe and the Schwarzschild radius contributed from the luminous part of the universe respectively.

d) The weak-field approximation is used to constrain on the upper bound value of the cosmological constant.

Recall that the exact SdS metric time-time component is given by

$$g_{tt} = -1 + \frac{2GM}{c^2 r} + \frac{\Lambda}{3} r^2 \tag{8.2.4}$$

In the weak-field approximation this reduces to

$$g_{tt_{NL}}(r) \approx -1 + \frac{2GM}{c^2 r} \tag{8.2.5}$$

as discussed in chapter 3.

As we can see in the metric perturbation the neglected term is of second order in Newtonian potential i.e., $(r_g/r)^2$. This limiting case imposes on the upper value of the cosmological constant where the term with the cosmological constant expression in 8.2.4 be at most first order in the Newtonian potential.

So outside a concentrated mass where $r \geq r_g$,

$$\frac{\Lambda}{3} r^2 \leq \frac{r_g}{r} \tag{8.2.6}$$

In the extreme, special case where the equality in eq. 8.2.6 holds true

$$\Lambda_{max} = \frac{3 r_g}{r_{max}^3} \tag{8.2.7}$$

where the subscript $_{max}$ stands for the upper boundary value (the possible maximum value) for Λ and related quantities.

Since, outside the Schwarzschild radius $r \geq r_g$ the second order Newtonian potential is less than or equal to the first order, then

$$\frac{3 r_g^2}{r^4} \leq \Lambda_{max} \leq \frac{3 r_g}{r^3} \tag{8.2.8}$$

Additionally, in view of 8.2.4 and the limiting case of the metrics we have an additional condition

$$\frac{r_g}{r} + \frac{\Lambda_{max}}{3} r^2 \leq 1 \tag{8.2.9}$$

Using eqs. 8.2.8 & 8.2.9, we get two exact results:

$$\Lambda_1 = \frac{3}{8 r_g^2} \;\; \& \;\; \Lambda_2 = \frac{3\left(7 - 3\sqrt{5}\right)}{2 r_g^2} \tag{8.2.10}$$

where $\Lambda_2 > \Lambda_1$, so that the maximum value of the cosmological constant is given by

$$\Lambda = \frac{3\left(7-3\sqrt{5}\right)}{2r_{gmaxU}^2} \tag{8.2.11}$$

where r_{gmaxU} is the maximum Schwarzschild radius of the universe contributed from all gravitational masses, both baryonic and dark matter. Also, we can classify these into luminous and non-luminous masses respectively denoted as M_{LU} & M_{NLU}. Then r_{gmaxU} is given by

$$\begin{aligned} r_{g_{maxU}} &= \frac{2G}{c^2}(M_{LU}+M_{NLU}) \\ &= r_{g_{LU}}(1+\frac{M_{NLU}}{M_{LU}}) \end{aligned} \tag{8.2.12}$$

Using eqs. 8.2.3, 8.2.11 & 8.2.12 the maximum value of the cosmological constant value is expressed by

$$\begin{aligned} \Lambda &= \frac{3(7-3\sqrt{5})}{2\left[\gamma c t_{_{AU}}(1+\frac{M_{NLU}}{M_{LU}})\right]^2} \\ &= \frac{3(7-3\sqrt{5})}{2\left[\gamma c t_{_{AU}}(1+\frac{\alpha}{\gamma})\right]^2} \end{aligned} \tag{8.2.13}$$

where α is the ratio of non-luminous matter content of the universes, the dark matter plus the non-luminous baryonic content of the universe.

Finally, using the 2018 Planck satellite data [40]:

$\alpha \simeq 0.31$, $\gamma \simeq 0.005$, $t_{_{AU}} \simeq 13.82$ G year & $c = 3 \times 10^8 m/s$

$$\Lambda = 2.66 \times 10^{-52} m^{-2} \tag{8.2.14}$$

8.3 Conclusion

The vast number of exact solutions so far derived for EFE exhibits the richness and mathematical beauty of the field, where those physically interpreted ones have successfully passed all observations they have being tested. On the other hand, the remaining majorities and others that will possibly be derived in the future leave open research for its completeness where the cosmological constant therein inherits issues both explicitly and implicitly. Also, most viable modified gravity theories claim the cosmological constant in some other forms. Thus, the recent attention towards the cosmological constant in modern cosmology seems a compelling paradigm shift, considered to be stipulated as supplementary and complementary fundamental physics problem to be discovered.

Chapter 9

Summary and conclusion

Using Einstein field equations, the general conserved equations of motion in SdS geometry with brief boundary conditions have been derived. The SdS horizon boundary conditions were used in detailing and addressing the region, where the resulting conserved equations are being applied. The conserved equations were in turn, implemented to derive other important specific equations, including the SdS effective potential equation. Especially, the effective potential has used to derive orbit equations and their general characteristic features, for both massive and massless particles.

In examining the general characteristics of the SdS potential, we notice that in free falling particles, there is no difference among Newtonian, Schwarzschild and general relativistic effective potentials for massless particles; but, will differ significantly depending on the mass and region of interaction parameters for massive particles. On the other hand, for particles possessing angular momentum different from zero, the SdS effective potential in both massive and massless particles behaves differently from both Sch and Newtonian ones whose significance is determined by the underlining parameters that includes: the region of

interaction, mass of the gravitating system, the particles angular momentum, and others. In characterizing the potential, plots of some sample exploited representative cases have been used, while analytical orbit solutions were also used to complement the description.

For massive particles, generally the SdS potential differs from both the Newtonian and the Schwarzschild potentials. Primarily, the SdS potential is characterized by three turning points where the particles velocities vanish, as usual. Also, the points of apsis for bound orbits are different among the three potentials; so that the eccentricities of the orbits become different. Especially, as the region of SdS application becomes effective, the differences will become more significant.

Three special cases have examined to quantify the effect of Λ on orbits, where the results have summarized as follows:

1) Massive particles in circular orbits: In this special case, the deviation of circular orbits from that of the classical Schwarzschild counterpart has calculated using the radial solution of the effective potential. In seeking for circular orbit approximations, systems with small eccentricities have selected (with some exceptions, due to the lack of such observational data). Then, the latest observational data have used in producing numerical data table for the representative systems that includes: a) planetary system, b) binary stars (binary pulsars and SMBHs), c) orbits of stars, and other binaries around galactic center (where the Milky-Way center has used as representative) and d) orbit of binary galaxies (where the local group has used). The numerical results indicate that the effect of Λ at small scales, systems a) - c), is insignificant. However, it is quite significant in open and wide systems like binary-galaxies where the radius of the circular orbit shift will go probably beyond the order of $k$pc.

2) Light trajectory: In this case, the effective potential was used to derive photon orbit equation to derive the bending angle. In turn, the bending angle has used in gravitational lensing to quantify the effect of Λ. For the selected systems, the observed effect is of order of 2% compared to the classical Schwarzschild effect.

3) Massive particles in elliptical orbits: In this case, we developed a two-body problem in the SdS geometry to describe elliptical motions. Then, we were able to quantify the effect of Λ on orbit precession for selected astrophysical binaries, where a similar observational data with that of the circular orbit case have used. In fact, data selection has become easier in this case than the circular orbit, since almost all binaries poses non-zero ellipticities. The effect of Λ on precession of orbits of two-body system will be significant in open and wide systems like binary-galaxies. However, at small scales, systems within the Milky-Way galaxy, the effect of Λ is negligible.

Moreover, it is also possible to quantify the geometrical effect of Λ in terms of the apsidal shifts, where the radial solutions corresponding to the turning points of the effective potential will be used.

The cosmological constant has also significant effect in radiations resulted from an in falling particles to massive objects if an appreciable distance from the hole is considered. We have shown that, a charged particle of magnitude ze when falling from a large distance of the order of cosmological length to a black hole radiates a greater amount of electromagnetic energy compared to that of the Schwarzschild case. However, the destiny to where this amount of energy will reside needs further investigation. Of course, in the case of Schwarzschild spacetime, the same particle falling from the same position of fall has considered to escape to infinity as previous studies describe.

On the other hand, as we have addressed in the detailed review works, the GR based gravity theory is prominently passing all observational tests irrespective of the criticisms it has regularly faced. Yet, as discussed under the future perspectives, a lot of work remains to discover. For example, the cosmological constant nature itself remains as a fundamental physics problem to discover.

Finally, we believe that our work will benefit to fill some academic issues. In addition, it will also help as a reference for further researches.

References

[48] A. S. Eddington. *The mathematical theory of relativity*. Cambridge University Press, Cambridge, UK, 1 edition, 1923.

[1] V. M. Slipher. Spectrographic Observations of Nebulae. *Popular Astronomy*, 23:21–24, January 1915.

[2] V. M. Slipher. Nebulae. *Proceedings of the American Philosophical Society*, 56:403–409, 1917.

[3] A. Einstein. Zur allgemeinen Relativitätstheorie. *Sitzungsberichte der Königlich Preußischen Akademie der Wissenschaften (Berlin), Seite 778-786.*, 1915.

[4] A. Einstein. Zur allgemeinen Relativitätstheorie (Nachtrag). *Sitzungsberichte der Königlich Preußischen Akademie der Wissenschaften (Berlin), Seite 799-801.*, 1915.

[5] A. Einstein. Erklärung der Perihelbewegung des Merkur aus der allgemeinen Relativitätstheorie. *Sitzungsberichte der Königlich Preußischen Akademie der Wissenschaften (Berlin), Seite 831-839.*, 1915.

[6] A. Einstein. Die Feldgleichungen der Gravitation. *Sitzungsberichte der Königlich Preußischen Akademie der Wissenschaften (Berlin), Seite 844-847.*, 1915.

[7] A. Einstein. Die Grundlage der allgemeinen Relativitätstheorie. *Annalen der Physik*, 354:769–822, 1916.

[8] A. Einstein. Kosmologische betrachtungen zur allgemeinen relativitätstheorie.

Sitzungsberichte der Königlich Preußischen Akademie der Wissenschaften (Berlin), Seite 142-152., 1917.

[9] E. Hubble. A Relation between Distance and Radial Velocity among Extra-Galactic Nebulae. *Proceedings of the National Academy of Science*, 15:168–173, March 1929.

[10] G. Lemaître. Un Univers homogène de masse constante et de rayon croissant rendant compte de la vitesse radiale des nébuleuses extra-galactiques. *Annales de la Société Scientifique de Bruxelles*, 47:49–59, 1927.

[11] G. Lemaître. Expansion of the universe, A homogeneous universe of constant mass and increasing radius accounting for the radial velocity of extra-galactic nebulae. *MNRAS*, 91:483–490, March 1931.

[12] W. de Sitter. Einstein's theory of gravitation and its astronomical consequences. Third paper. *MNRAS*, 78:3–28, November 1917.

[13] A. Friedmann. Über die Krümmung des Raumes. *Zeitschrift fur Physik*, 10:377–386, 1922.

[14] A. Friedmann. Über die Möglichkeit einer Welt mit konstanter negativer Krümmung des Raumes. *Zeitschrift fur Physik*, 21:326–332, December 1924.

[15] A. M. Boesgaard and G. Steigman. Big bang nucleosynthesis - Theories and observations. *ARAA*, 23:319–378, 1985.

[16] P. J. E. Peebles, D. N. Schramm, E. L. Turner, and R. G. Kron. The case for the relativistic hot big bang cosmology. *Nature*, 352:769–776, August 1991.

[17] M. S. Turner. Cosmology Update 1998. *arXiv Astrophysics e-prints*, January 1999.

[18] A. G. Riess et al. *Observational Evidence from Supernovae for an Accelerating Universe and a Cosmological Constant*. *AJ*, 116:1009–1038, September 1998.

[19] S. Perlmutter et al. *Measurements of Omega and Lambda from 42 High-Redshift Supernovae*. *ApJ*, 517:565–586, June 1999.

[20] B. Ratra and P. J. E. Peebles. Cosmological consequences of a rolling homogeneous scalar field. *PhRvD*, 37:3406–3427, June 1988.

[21] S. M. Carroll. The Cosmological Constant. *Living Reviews in Relativity*, 4:1, February 2001.

[22] R. R. Caldwell. A phantom menace? Cosmological consequences of a dark energy component with super-negative equation of state. *Physics Letters B*, 545:23–29, October 2002.

[23] P. J. Peebles and B. Ratra. The cosmological constant and dark energy. *Reviews of Modern Physics*, 75:559–606, April 2003.

[24] P. G. Ferreira. Cosmological Tests of Gravity. *arXiv e-prints*, February 2019.

[25] T. Clifton, P. G. Ferreira, A. Padilla, and C. Skordis. Modified gravity and cosmology. *Physrep*, 513:1–189, March 2012.

[26] A. Joyce, B. Jain, J. Khoury, and M. Trodden. Beyond the cosmological standard model. *Physrep*, 568:1–98, March 2015.

[27] L. Lombriser and N. A. Lima. Challenges to self-acceleration in modified gravity from gravitational waves and large-scale structure. *Physics Letters B*, 765:382–385, February 2017.

[28] J. M. Ezquiaga and M. Zumalacárregui. Dark Energy After GW170817: Dead Ends and the Road Ahead. *Physical Review Letters*, 119(25):251304, December 2017.

[29] B. P. Abbott and et al . Observation of Gravitational Waves from a Binary Black Hole Merger. *PhRvL*, 116(6):061102, 2016.

[30] B. P. Abbott, R. Abbott, T. D. Abbott, F. Acernese, K. Ackley, C. Adams, T. Adams,

P. Addesso, R. X. Adhikari, V. B. Adya, and et al. GW170817: Observation of Gravitational Waves from a Binary Neutron Star Inspiral. *Physical Review Letters*, 119(16):161101, October 2017.

[31] T. Baker, E. Bellini, P. G. Ferreira, M. Lagos, J. Noller, and I. Sawicki. Strong Constraints on Cosmological Gravity from GW170817 and GRB 170817A. *Physical Review Letters*, 119(25):251301, December 2017.

[32] J. Edmund, Copeland, et al. Dark energy after GW170817, revisited. *Physical Review Letters*, 122(6):61301, 2019.

[33] Planck Collaboration, N. Aghanim, and et al. Planck 2018 results. VI. Cosmological parameters. *A&A*, 641:A6, 2020.

[34] T. M. C. Abbott et al. Dark Energy Survey year 1 results: Cosmological constraints from galaxy clustering and weak lensing. *PhRvD*, 98(4):043526, August 2018.

[35] D. M. Scolnic et al. The Complete Light-curve Sample of Spectroscopically Confirmed SNe Ia from Pan-STARRS1 and Cosmological Constraints from the Combined Pantheon Sample. *ApJ*, 859:101, June 2018.

[36] E. Komatsu, K. M. Smith, J. Dunkley, C. L. Bennett, B. Gold, G. Hinshaw, N. Jarosik, D. Larson, M. R. Nolta, L. Page, D. N. Spergel, M. Halpern, R. S. Hill, A. Kogut, M. Limon, S. S. Meyer, N. Odegard, G. S. Tucker, J. L. Weiland, E. Wollack, and E. L. Wright. Seven-year Wilkinson Microwave Anisotropy Probe (WMAP) Observations: Cosmological Interpretation. *ApJS*, 192:18, February 2011.

[37] Planck Collaboration, P. A. R. Ade, N. Aghanim, C. Armitage-Caplan, M. Arnaud, M. Ashdown, F. Atrio-Barandela, J. Aumont, C. Baccigalupi, A. J. Banday, and et al. Planck 2013 results. XVI. Cosmological parameters. *A&A*, 571:A16, November 2014.

[38] Planck Collaboration, R. Adam, P. A. R. Ade, N. Aghanim, Y. Akrami, M. I. R. Alves, F. Argüeso, M. Arnaud, F. Arroja, M. Ashdown, and et al. Planck 2015 results. i. overview of products and scientific results. *A&A*, 594:A1, September 2016.

[39] Planck Collaboration, P. A. R. Ade, N. Aghanim, M. Arnaud, M. Ashdown, J. Aumont, C. Baccigalupi, A. J. Banday, R. B. Barreiro, J. G. Bartlett, and et al. Planck 2015 results. xiii. cosmological parameters. *A&A*, 594:A13, September 2016.

[40] Planck Collaboration, Y. Akrami, et al. Planck 2018 results. X. Constraints on inflation. *arXiv e-prints*, July 2018.

[41] G. Hinshaw et al. Nine-year Wilkinson Microwave Anisotropy Probe (WMAP) Observations: Cosmological Parameter Results. *ApJS*, 208:19, October 2013.

[42] L. Heisenberg. A systematic approach to generalisations of General Relativity and their cosmological implications. *arXiv e-prints*, July 2018.

[43] D. J. Eisenstein et al. Detection of the Baryon Acoustic Peak in the Large-Scale Correlation Function of SDSS Luminous Red Galaxies. *ApJ*, 633:560–574, November 2005.

[44] S. Peirani and J. A. de Freitas Pacheco. Mass determination of groups of galaxies: Effects of the cosmological constant. *NewA*, 11(4):325–330, Jan 2006.

[45] Friedrich Kottler. Über die physikalischen Grundlagen der Einsteinschen Gravitationstheorie. *Annalen der Physik*, 361(14):401–462, Jan 1918.

[46] Willem de Sitter. On the relativity of inertia. Remarks concerning Einstein's latest hypothesis. *KNAB*, 19:1217–1225, Mar 1917.

[47] K. Schwarzschild. On the Gravitational Field of a Mass Point According to Einstein's Theory. *Abh. Konigl. Preuss. Akad. Wissenschaften Jahre 1906,92,*

Berlin,1907, 1916:189–196, Jan 1916.

[49] K. Lundmark. The determination of the curvature of space-time in de Sitter's world. *MNRAS*, 84:747–770, June 1924.

[50] J. S. Tenn. What else did v. m. slipher do? In M. J. Way and D. Hunter, editors, *Origins of the Expanding Universe: 1912-1932*, volume 471 of *Astronomical Society of the Pacific Conference Series*, page 235, April 2013.

[51] C. O'Raifeartaigh. The contribution of v. m. slipher to the discovery of the expanding universe. In M. J. Way and D. Hunter, editors, *Origins of the Expanding Universe: 1912-1932*, volume 471 of *Astronomical Society of the Pacific Conference Series*, page 49, April 2013.

[52] E. Elizalde. Reasons in Favor of a Hubble-Lemaître-Slipher's (HLS) Law. *Symmetry, Vol. 11, No. 1, article id. 15 (2019)*, 11:15, January 2019.

[53] M. J. Way. Dismantling Hubble's Legacy? In M. J. Way and D. Hunter, editors, *Origins of the Expanding Universe: 1912-1932*, volume 471 of *Astronomical Society of the Pacific Conference Series*, page 97, April 2013.

[54] S. Weinberg. The cosmological constant problem. *RvMP*, 61:1–23, January 1989.

[55] IAU. Iau 2018 general assembly: Resolution b4. Technical report, International Astronomical Union, 2018.

[56] E. A. Milne. World Structure and the Expansion of the Universe. *Nature*, 130:9–10, July 1932.

[57] E. A. Milne. *Kinematic relativity; a sequel to Relativity, gravitation and world structure.* Clarendon Press, Oxford, UK, 1948.

[58] H. P. Robertson. On E. A. Milne's Theory of World Structure. *ZAP*, 7:153, 1933.

[59] H. P. Robertson. Kinematics and World-Structure. *ApJ*, 82:284, November 1935.

[60] H. P. Robertson. Kinematics and World-Structure II. *ApJ*, 83:187, April 1936.

[61] H. P. Robertson. Kinematics and World-Structure III. *ApJ*, 83:257, May 1936.

[62] A. G. Walker. On Milne's theory of world-structure. *Proc. Lond. Math. Soc. (2)*, 42:90–127, 1936.

[63] W.H. McCrea. Observational relations in relativistic cosmology. *Zeitschrift fur Astrophysik*, 9:290–314, 1935.

[64] George Gale. Cosmology: Methodological debates in the 1930s and 1940s. In Edward N. Zalta, editor, *The Stanford Encyclopedia of Philosophy*. Metaphysics Research Lab, Stanford University, summer 2017 edition, 2017.

[65] P. J. E. Peebles. *Principles of Physical Cosmology*. Princeton University Press, 1993.

[66] H. Bondi and T. Gold. The Steady-State Theory of the Expanding Universe. *MNRAS*, 108:252, 1948.

[67] F. Hoyle. A New Model for the Expanding Universe. *MNRAS*, 108:372, 1948.

[68] F. Hoyle. *Steady-state cosmology re-visited.* University College Cardiff Press, 72 p., Cardiff, UK, 1980.

[69] S. Weinberg. *Cosmology*. Oxford University Press, UK, 2008.

[70] G. Gamow. Expanding Universe and the Origin of Elements. *Physical Review*, 70:572–573, October 1946.

[71] G. Gamow. The Evolution of the Universe. *Nature*, 162:680–682, October 1948.

[72] R. A. Alpher and R. Herman. Evolution of the Universe. *Nature*, 162:774–775, November 1948.

[73] R. A. Alpher and R. C. Herman. Theory of the Origin and Relative Abundance Distribution of the Elements. *Reviews of Modern Physics*, 22:153–212, April 1950.

[74] R. H. Dicke, P. J. E. Peebles, P. G. Roll, and D. T. Wilkinson. Cosmic Black-Body Radiation. *ApJ*, 142:414–419, July 1965.

[75] A. A. Penzias and R. W. Wilson. A Measurement of Excess Antenna Temperature at 4080 Mc/s. *ApJ*, 142:419–421, July 1965.

[76] A. McKellar. Molecular Lines from the Lowest States of Diatomic Molecules Composed of Atoms Probably Present in Interstellar Space. *Publications of the Dominion Astrophysical Observatory Victoria*, 7, 1941.

[77] B. Gumjudpai. Introductory Overview of Modern Cosmology. *arXiv Astrophysics e-prints*, May 2003.

[78] F. Hoyle and J. V. Narlikar. A Radical Departure from the 'Steady-State' Concept in Cosmology. *Proceedings of the Royal Society of London Series A*, 290:162–176, February 1966.

[79] F. Hoyle, G. Burbidge, and J. V. Narlikar. A quasi-steady state cosmological model with creation of matter. *ApJ*, 410:437–457, June 1993.

[80] J. V. Narlikar, R. G. Vishwakarma, A. Hajian, T. Souradeep, G. Burbidge, and F. Hoyle. Inhomogeneities in the Microwave Background Radiation Interpreted within the Framework of the Quasi-Steady State Cosmology. *Ap*, 585:1–11, March 2003.

[81] J. V. Narlikar, S. V. Dhurandhar, R. G. Vishwakarma, S. R. Valluri, and S. Auddy. Gravitational wave background in the quasi-steady state cosmology. *MNRAS*, 451:1390–1395, August 2015.

[82] S. V. Dhurandhar and J. V. Narlikar. Gravitational wave signature of a mini creation event (MCE). *Classical and Quantum Gravity*, 35(13):135003, July 2018.

[83] V. Trimble. Existence and nature of dark matter in the universe. *ARAA*, 25:425–472,

1987.

[84] S. M. Faber and J. S. Gallagher. Masses and mass-to-light ratios of galaxies. *ARAA*, 17:135–187, 1979.

[85] M. Davis, G. Efstathiou, C. S. Frenk, and S. D. M. White. The evolution of large-scale structure in a universe dominated by cold dark matter. *ApJ*, 292:371–394, May 1985.

[86] S. D. M. White, C. S. Frenk, M. Davis, and G. Efstathiou. Clusters, filaments, and voids in a universe dominated by cold dark matter. *ApJ*, 313:505–516, February 1987.

[87] G. W. Gibbons, S. W. Hawking, S. T. C. Siklos, and F. Wilczek. *The very early universe. Proceedings of the Nuffield Workshop, held at Cambridge, England, 21 June - 9 July, 1982.* Cambridge University Pres, Cambridge, UK, 1983.

[88] S. A. Bludman and M. A. Ruderman. Theoretical limits on interstellar magnetic poles set by nearby magnetic fields. *Physical Review Letters*, 36:840–843, April 1976.

[89] J. N. Fry. Gravitational correlations and the monopole problem. *ApJ*, 246:L93–L97, June 1981.

[90] P. J. E. Peebles. Large-scale background temperature and mass fluctuations due to scale-invariant primeval perturbations. *ApJ*, 263:L1–L5, December 1982.

[91] G. R. Blumenthal, H. Pagels, and J. R. Primack. Galaxy formation by dissipationless particles heavier than neutrinos. *Nature*, 299:37, September 1982.

[92] G. R. Blumenthal, S. M. Faber, J. R. Primack, and M. J. Rees. Formation of galaxies and large-scale structure with cold dark matter. *Nature*, 311:517–525, October 1984.

[93] A. H. Guth. Inflationary universe: A possible solution to the horizon and flatness

problems. *PhRvD*, 23:347–356, January 1981.

[94] A. D. Linde. A new inflationary universe scenario: A possible solution of the horizon, flatness, homogeneity, isotropy and primordial monopole problems. *PhLB*, 108:389–393, February 1982.

[95] A. H. Guth, D. I. Kaiser, and Y. Nomura. Inflationary paradigm after Planck 2013. *Physics Letters B*, 733:112–119, June 2014.

[96] A. Linde. Inflationary Cosmology after Planck 2013. *arXiv e-prints*, February 2014.

[97] A. Albrecht and P. J. Steinhardt. Cosmology for grand unified theories with radiatively induced symmetry breaking. *Physical Review Letters*, 48:1220–1223, April 1982.

[98] H. Weyl. Gravitation und Elektrizität. *Sitzungsberichte der Königlich Preußischen Akademie der Wissenschaften (Berlin), Seite 465-478*, 1918.

[99] H. Weyl. Republication of: 3. On the theory of gravitation. *General Relativity and Gravitation*, 44:779–810, March 2012.

[100] Mustapha Ishak. Testing general relativity in cosmology. *Living Reviews in Relativity*, 22(1):1, Dec 2019.

[101] C. W. Misner, K. S. Thorne, and J. A. Wheeler. *Gravitation*. W.H. Freeman and Co., 1973, San Francisco, 1973.

[102] H. Weyl. *Space-Time-Matter*. Dover Publications, London, 4 edition, 1952. Translated from the German by Henry L. Brose.

[103] C. O'Raifeartaigh, M. O'Keeffe, W. Nahm, and S. Mitton. One hundred years of the cosmological constant: from "superfluous stunt" to dark energy. *European Physical Journal H*, 43, April 2018.

[104] Y. B. Zel'dovich. Cosmological Constant and Elementary Particles. *Soviet Journal*

of Experimental and Theoretical Physics Letters, 6:316, November 1967.

[105] Ya B. Zel'dovich. Special Issue: the Cosmological Constant and the Theory of Elementary Particles. *Soviet Physics Uspekhi*, 11(3):381–393, Mar 1968.

[106] C. Sivaram. The Planck length as a cosmological constraint. *Apss*, 127:133–137, November 1986.

[107] Sean M. Carroll, William H. Press, and Edwin L. Turner. The cosmological constant. *Annual Review of Astronomy and Astrophysics*, 30(1):499–542, 1992.

[108] Balakrishna S. Haridasu, Vladimir V. Lukovi ć, Michele Moresco, and Nicola Vittorio. An improved model-independent assessment of the late-time cosmic expansion. *JCAP*, 2018(10):015, Oct 2018.

[109] Lawrence M. Krauss and Michael S. Turner. The cosmological constant is back. *General Relativity and Gravitation*, 27(11):1137–1144, Nov 1995.

[110] Shadab Alam et al. The clustering of galaxies in the completed SDSS-III Baryon Oscillation Spectroscopic Survey: cosmological analysis of the DR12 galaxy sample. *MNRAS*, 470(3):2617–2652, Sep 2017.

[111] Michael Blomqvist et al. Baryon acoustic oscillations from the cross-correlation of lyα absorption and quasars in eboss dr14. *A&A*, 629:A86, Sep 2019.

[112] S. W. Hawking. The development of irregularities in a single bubble inflationary universe. *Physics Letters B*, 115(4):295–297, Sep 1982.

[113] F. Hoyle. Stellar Evolution and the Expanding Universe. *Nature*, 163:196–198, February 1949.

[114] Joan Sola et al. Brans-Dicke gravity with a cosmological constant smoothes out ΛCDM tensions. *arXiv:1909.0255*, Sep 2019.

[115] Anatoly A. Svidzinsky. Vector theory of gravity: Universe without black holes and

solution of dark energy problem. *PhysScr*, 92(12):125001, Dec 2017.

[116] Anatoly A. Svidzinsky. Simplified equations for gravitational field in the vector theory of gravity and new insights into dark energy. *Physics of the Dark Universe*, 25:100321, Sep 2019.

[117] Sergei D. Odintsov, Diego Sáez-Chillón Gómez, and German S. Sharov. Is exponential gravity a viable description for the whole cosmological history? *European Physical Journal C*, 77(12):862, Dec 2017.

[118] Fabio Briscese, Gianluca Calcagni, and Leonardo Modesto. Nonlinear stability in nonlocal gravity. *PhRvD*, 99(8):084041, Apr 2019.

[119] Antonio Troisi. Higher-order gravity in higher dimensions: geometrical origins of four-dimensional cosmology? *European Physical Journal C*, 77(3):171, Mar 2017.

[120] S. Weinberg. *Gravitation and Cosmology*. John Wiley & Sons, Inc., USA, 1972.

[121] Sean M. Carroll. *Spacetime and geometry. An introduction to general relativity*. Addison Wesley, 2004.

[122] Wolfgang Rindler. *Relativity*. Oxford University Press, Inc., New York, USA, 2006.

[123] Norbert Straumann. *General Relativity*. Springer, Dordrecht, 2013.

[124] E. Hubble. A Relation between Distance and Radial Velocity among Extra-Galactic Nebulae. *Contributions from the Mount Wilson Observatory, vol. 3, pp.23-28*, 3:23–28, 1929.

[125] A. G. Walker. On Milne's Theory of World-Structure. *Proceedings of the London Mathematical Society, (Series 2) volume 42, p. 90-127*, 42:90–127, 1937.

[126] G. C. McVittie. The Problem of n Bodies and the Expansion of the Universe. *MNRAS*, 91:274, Jan 1931.

[127] G. C. McVittie. The mass-particle in an expanding universe. *MNRAS*, 93:325–339,

Mar 1933.

[128] Do Young Kim, Anthony N. Lasenby, and Michael P. Hobson. Spherically-symmetric solutions in general relativity using a tetrad-based approach. *General Relativity and Gravitation*, 50(3):29, Feb 2018.

[129] David R. Williams. Planetary fact sheet. *https://nssdc.gsfc.nasa.gov/planetary/factsheet/*, 2019.

[130] T. E. Strohmayer and et.al. NICER Discovers the Ultracompact Orbit of the Accreting Millisecond Pulsar IGR J17062-6143. *ApJL*, 858(2):L13, May 2018.

[131] F. K. Liu, Shuo Li, and S. Komossa. A Milliparsec Supermassive Black Hole Binary Candidate in the Galaxy SDSS J120136.02+300305.5. *ApJ*, 786(2):103, May 2014.

[132] W. Ishibashi and M. Gröbner. Evolution of binary black holes in AGN accretion discs: Disc-binary interaction and gravitational wave emission. *A&A*, 639:A108, July 2020.

[133] Gurtina Besla and et.al. Are the Magellanic Clouds on Their First Passage about the Milky Way? *ApJ*, 668(2):949–967, October 2007.

[134] Tolu Biressa and J. A. de Freitas Pacheco. The cosmological constant and the gravitational light bending. *General Relativity and Gravitation*, 43(10):2649–2659, 2011.

[135] Wolfgang Rindler and Mustapha Ishak. Contribution of the cosmological constant to the relativistic bending of light revisited. *Phys. Rev. D*, 76:043006, 2007.

[136] Oliver Piattella. On the Effect of the Cosmological Expansion on the Gravitational Lensing by a Point Mass. *Universe*, 2(4):25, 2016.

[137] Mustapha Ishak and Wolfgang Rindler. The relevance of the cosmological constant for lensing. *General Relativity and Gravitation*, 42(9):2247–2268, September 2010.

[138] Fan Zhao and Jianfeng Tang. Gravitational lensing effects of Schwarzschild-de Sitter

black hole. *PhRvD*, 92(8):083011, 2015.

[139] Volker Perlick, Oleg Yu. Tsupko, and Gennady S. Bisnovatyi-Kogan. Black hole shadow in an expanding universe with a cosmological constant. *PhRvD*, 97(10):104062, 2018.

[140] Javad T. Firouzjaee and Alireza Allahyari. Black hole shadow with a cosmological constant for cosmological observers. *EPJC*, 79(11):930, 2019.

[141] H. Goldstein, C. Poole, and J. Safko. *Classical mechanics*. Addison, Wesley, 2002.

[142] Subenoy Chakraborty. Treatise on Differential Geometry and its role in Relativity Theory. *arXiv:1908.10681*, 2019.

[143] Peter J. Redmond. Generalization of the Runge-Lenz Vector in the Presence of an Electric Field. *Physical Review*, 133(5B), 1964.

[144] Misha Feigin and Tigran Hakobyan. Algebra of Dunkl Laplace-Runge-Lenz vector. *arXiv:1907.06706*, 2019.

[145] Niall J. MacKay and Sam Salour. Kepler unbound: Some elegant curiosities of classical mechanics. *American Journal of Physics*, 83(1), 2015.

[146] A. G. Nikitin. Laplace-Runge-Lenz vector with spin in any dimension. *Journal of Physics A: Mathematical and Theoretical*, 47(37), 2014.

[147] Sean R. Dawson, Holger R. Dullin, and Diana M. H. Nguyen. Monodromy in Prolate Spheroidal Harmonics. *arXiv:2001.11270*, 2020.

[148] Andrew W Kerr, John C Hauck, and Bahram Mashhoon. Standard clocks, orbital precession and the cosmological constant. *Classical and Quantum Gravity*, 20(13), 2003.

[149] G. V. Kraniotis and S. B. Whitehouse. Compact calculation of the perihelion precession of Mercury in general relativity, the cosmological constant and Jacobi's inversion problem. *Classical and Quantum Gravity*, 20(22), November 2003.

[150] Philippe Jetzer and Mauro Sereno. Two-body problem with the cosmological constant and observational constraints. *Phys. Rev. D*, 73, 2006.

[151] Hideyoshi Arakida. Note on the Perihelion/Periastron Advance Due to Cosmological Constant. *International Journal of Theoretical Physics*, 52(5), 2013.

[152] G.-B. Zhao et al. The clustering of the SDSS-IV extended Baryon Oscillation Spectroscopic Survey DR14 quasar sample: a tomographic measurement of cosmic structure growth and expansion rate based on optimal redshift weights. *MNRAS*, 482:3497–3513, January 2019.

[153] Lev Davidovich Landau and E. M. Lifshitz. *The classical theory of fields*. Pergamon Press, 1975.

[154] A. P. Hatzes and et.al. Long-lived, long-period radial velocity variations in Aldebaran: A planetary companion and stellar activity. *A&A*, 580:A31, August 2015.

[155] J. M. Weisberg and Y. Huang. Relativistic Measurements from Timing the Binary Pulsar PSR B1913+16. *ApJ*, 829(1):55, September 2016.

[156] F. Eisenhauer and et.al. A Geometric Determination of the Distance to the Galactic Center. *ApJ*, 597(2):L121–L124, November 2003.

[157] S. Gillessen and et.al. A gas cloud on its way towards the supermassive black hole at the Galactic Centre. *Nature*, 481(7379):51–54, January 2012.

[158] Roeland P. van der Marel and Puragra Guhathakurta. M31 Transverse Velocity and Local Group Mass from Satellite Kinematics. *ApJ*, 678(1):187–199, May 2008.

[159] Frank J. Zerilli. Gravitational Field of a Particle Falling in a Schwarzschild Geometry Analyzed in Tensor Harmonics. *PhRvD*, 2(10):2141–2160, November 1970.

[160] D. K. Ross. Radiation from particles falling into black-holes. *Publications of the Astronomical Society of the Pacific*, 83:633, 1971.

[161] Antoine Folacci and Mohamed Ould El Hadj. Electromagnetic radiation generated by a charged particle falling radially into a Schwarzschild black hole: A complex angular momentum description. *PhRvD*, 102(2):024026, July 2020.

[162] Marlan O. Scully, Stephen Fulling, David M. Lee, Don N. Page, Wolfgang P. Schleich, and Anatoly A. Svidzinsky. Quantum optics approach to radiation from atoms falling into a black hole. *Proceedings of the National Academy of Sciences*, 115(32):8131–8136, 2018.

[163] Leandro A. Oliveira, Luís C. B. Crispino, and Atsushi Higuchi. Scalar radiation from a radially infalling source into a Schwarzschild black hole in the framework of quantum field theory. *European Physical Journal C*, 78(2):133, February 2018.